

Cross-Border Risk Assessment of Earthquake-induced Landslides in Central Asia

vorgelegt von

Master of Science

Annamaria Saponaro

geb. in Bari

von der Fakultät VI - Planen Bauen Umwelt

der Technischen Universität Berlin

zur Erlangung des akademischen Grades

Doktorin der Naturwissenschaften

- Dr.rer.nat. -

genehmigte Dissertation

Promotionsausschuss:

Vorsitzender: Prof. Dr.-Ing. Yuri Petryna

Gutachter: Prof. Dr.-Ing. Frank Rackwitz

Gutachter: Dr. Fausto Guzzetti

Gutachter: Prof. Dr. Stefano Parolai

Tag der wissenschaftlichen Aussprache: 11. September 2017

Berlin 2018

In memory of my father

ACKNOWLEDGEMENTS

This research could not have been undertaken without the generous contribution of some people I would like to acknowledge.

First of all, I would like to express my deepest gratitude to my supervisor Stefano Parolai for his trust and patient guidance throughout these years. His continuous encouragement and motivation is highly appreciated. Special thanks also to my colleagues Marco, Marc, Max, Dino, Kevin, Shahid for inspiring fruitful discussions and for making this work possible.

I would like to thank the colleagues of the Center of Early Warning and of the Section 2.1 for their friendship and the nice time spent together. Particularly thanks to Camilla for each shared scientific (and not) coffee break, to Kevin for the English language proof reading, to Dorina and Susanne for their constant and prompt help.

I am also grateful to people in CAIAG, for their warm hospitality during my trips in Central Asia. Special thanks go to Bolot Moldobekov, who inspired interesting landslide discussions.

I would also like to thank the reviewers for taking the time to read the dissertation.

Finally, my profound thanks go to my sister and my mum for their unconditional love and support. Words cannot express how thankful I am to you.

AUTHOR'S DECLARATION

I hereby declare that I have produced this thesis without the prohibited assistance of third parties and without making use of aids other than those specified; notions taken over directly or indirectly from other sources have been identified as such. This thesis has not previously been presented in identical or similar form to any other German or foreign examination board.

Potsdam, 08.09.2015

Annamaria Saponaro

ABSTRACT

Central Asia is one of the most challenging places in the world where various natural hazards can heavily injury populations and resources. Among these hazards, landslides pose a serious threat to human life and human facilities. The large variability of local geological materials, together with the difficulties in forecasting heavy precipitation locally and in quantifying the level of ground shaking, call for harmonized procedures to better quantify the hazard and the negative impact of slope failures across the Central Asian countries. Furthermore, the increase of population and the expansion of urban settlements towards landslide-prone slopes, exacerbate negative consequences associated to slope failures. Especially in less developed countries which are particularly suffering for appropriate resources, there is the urgent need to address landslide research in order to support disaster management and planning activities at the regional level.

Under conditions of data scarcity as well as of geographic remoteness – which are of particular concern to Central Asian countries - a sound statistical approach is presented that is able to quantify landslide hazard and risk, which also allows for the inference of information about landslide potential and expected damage for areas where no data coverage is available.

With these premises, the main objective of the work is to provide a cross-border risk map of earthquake-induced landslides in Central Asia. To this scope, the main components of risk are evaluated and two main questions are addressed: 1) where are earthquake-induced landslides more likely to occur in future, 2) how is it possible to quantify damages to exposed assets.

A first essential step of any landslide hazard and risk assessment is the preparation of a landslide susceptibility map with the objective to identify areas where the potential for landslide activation exists. For the purposes of this research, a landslide susceptibility analysis is performed by exploiting new advances in Geographic Information System (GIS) technology, together with concepts from Bayesian statistics, and promoting the use of open-source tools. Specifically, a range of conditioning factors and their potential impact on landslide occurrence are quantitatively assessed on the basis of the spatial distribution of landslides by applying weights-of-evidence modelling based on (1) a landslide inventory of past events, (2) terrain-derived variables of slope, aspect and

curvature, (3) a geological map, (4) a distance from faults map, and (5) a seismic intensity map. A spatial validation of the proposed method is performed, indicating sufficient measures of significance to predicted landslide susceptibility results, which present an overall level of accuracy greater than 70%.

Secondarily, the evaluation of expected damage to exposed population is achieved at a transnational level. A physically-based procedure, applicable over the entire Central Asian region, is adopted 1) to identify landslide source areas, 2) to define downhill trajectories of mass movements, and 3) to finally retrieve their impact velocities. By incorporating such dynamic concepts, a landslide hazard map is prepared allowing for a better quantification of the natural phenomenon. For the finally landslide risk task, the expected destructiveness due to landslide activation is calculated by integrating the distribution of population density with the hazard map. Results show that a relatively high level of risk is expected for large cities, i.e., those located in the Fergana Valley, in the proximity of Tashkent in Uzbekistan and Jalal-Abad in Kyrgyzstan, being highly dense populated areas. On the other hand, there is a general medium level of risk extensively expected over the entire Central Asia region, primarily due to the presence of small settlements (having a population density in the order of 1000 persons/km²) exposed to relatively high landslide hazard.

ZUSAMMENFASSUNG

Zentralasien ist einer der Orte der Welt, an dem verschiedenste Naturgefahren die Bevölkerung und die vorhandene Infrastruktur schwer treffen können. Unter diesen Gefahren stellen Hangrutsche eine bedeutende Bedrohung sowohl für menschliches Leben als auch die Wirtschaft und die zivile Infrastruktur dar. Starke räumliche Variationen unterschiedlicher geologischer Einheiten, zusammen mit nur schwer vorherzusagenden lokalen Starkregenereignissen und einer ebenso schwer abzuschätzenden Intensität der Bodenbewegung während eines Erdbebens, fordern eine harmonisierte Herangehensweise, um die Gefährdung und die daraus entstehenden negativen Folgen von Hangrutschen in Zentralasien in einem harmonisierten Ansatz zu quantifizieren. Neben der ohnehin schon hohen Gefährdung erhöhen ein starkes Bevölkerungswachstum und die daraus resultierende Ausdehnung von urbanen Siedlungen hin zu den von Hangrutschen bedrohten Talrändern die negativen Konsequenzen, die mit einem solchen Geländesturz einhergehen können. Insbesondere in weniger entwickelten Ländern, die besonders an einem Mangel an Ressourcen leiden, besteht der dringende Bedarf, die Vorsorge- und Nachsorgeaktivitäten auf regionaler Ebene für den Katastrophenfall zu verstärken.

Unter den nachteiligen Bedingungen eines vorherrschenden Datenmangels als auch von geographischer Abgelegenheit - welche besonders auf die zentralasiatischen Länder zutreffen - wird in dieser Arbeit ein fundierter statistischer Ansatz vorgestellt, der es ermöglicht, die Hangrutschungsgefährdung als auch das -risiko zu quantifizieren; darüberhinaus erlaubt es das vorgestellte Verfahren auch, Informationen über Hangrutschungspotential und erwartete Schäden für Gebiete ohne verfügbare Datenabdeckung abzuschätzen.

Unter diesen Prämissen besteht das Hauptziele dieser Arbeit in der Erstellung einer harmonisierten und grenzüberschreitenden Risikokarte für erdbeben-induzierte Hangrutsche in Zentralasien. Zu diesem Zweck werden die Hauptkomponenten des Risikos ausgewertet, und es werden zwei zentrale Fragen untersucht: 1) Wo befinden sich Gebiete, in denen eine hohe Wahrscheinlichkeit für das Auftreten zukünftiger durch Erdbeben induzierter Hangrutsche besteht? 2) Inwieweit ist es möglich, Schäden an exponierten Vermögensgütern zu quantifizieren?

Für eine angemessene Hangrutschungsgefährdungs- und Risikoanalyse wurde in einem ersten Schritt die Hangrutschsuszeptibilität kartiert mit dem Ziel, insbesondere jene Regionen zu identifizieren, die ein erhöhtes Potential für Hangrutsche aufweisen. Hierzu macht sich die vorgelegte Arbeit die Fortschritte bei den geographischen Informationssystemen (GIS) und Konzepte der Bayesschen Statistik zunutze. Es werden eine Vielzahl an Bedingungsfaktoren und deren potentieller Einfluss für das Auftreten von Hangrutschen quantitativ analysiert. Auf Basis der räumlichen Verteilung von Hangrutschen wird eine Weight-of-Evidence Modellierung durchgeführt mittels (1) einer Inventarisierung vergangener Hangrutschungsereignisse, (2) von der Topographie abgeleiteter Variablen der Hangneigung, Exposition und Krümmung, (3) einer geologischen Kartierung, (4) einer Karte mit der Entfernung zur nächstliegenden tektonischen Verwerfung, und (5) einer probabilistischen seismischen Gefährdungsanalyse in Einheiten der makroseismischen Intensität. Im Anschluss wird eine räumliche Validierung der vorgeschlagenen Methode durchgeführt, die insgesamt mit einem Genauigkeitsniveau von mehr als 70% ein ausreichendes Maß an Signifikanz zur Vorhersage der Hangrutschsuszeptibilität aufweist.

Darauf aufbauende werden in einem zweiten Schritt die erwarteten Verluste unter der gefährdeten Bevölkerung auf grenzüberschreitender Skala abgeschätzt. Dazu wird ein auf die gesamte zentralasiatische Region anwendbarer, physikalisch basierter Ansatz eingeführt, der 1) Ursprungsort von Hangrutschen, 2) Trajektorien der hangabwärts gerichteten Massenbewegung und 3) schließlich die Auftreffgeschwindigkeit der abwärts gleitenden Masse abschätzt. Durch die Überarbeitung der Hangrutschungsgefährdungskarte unter Berücksichtigung dieser dynamischen Konzepte ist es möglich, das natürliche Auftreten der Hangrutsche genauer zu quantifizieren. Für die letztliche Risikoabschätzung, d.h. die zu erwartende Zerstörungskraft aufgrund ausgelöster Hangrutsche, wird die Verteilung der Bevölkerungsdichte in die Gefährdungskarte integriert.

Die Ergebnisse zeigen, dass für große Städte in der Umgebung von Taschkent (Usbekistan) und Jalalabad (Kirgisistan) sowie für die dicht besiedelten Gebiete im Ferganatal ein relativ hohes Risiko gegenüber Hangrutschen besteht; die gesamte zentralasiatische Region weist ein mittleres Risikoniveau auf. Dafür ist hauptsächlich die große Anzahl kleiner Siedlungen (mit einer Bevölkerungsdichte in der Größenordnung von 1000 Personen/km²) verantwortlich, die einer relativ hohen Hangrutschungsgefährdung ausgesetzt sind.

CONTENTS

ACKNOWLEDGEMENTS	IV
AUTHOR'S DECLARATION	V
ABSTRACT	VI
ZUSAMMENFASSUNG	VIII
CONTENTS	X
LIST OF FIGURES.....	XII
1 INTRODUCTION	1
1.1 LANDSLIDE PHENOMENA IN CENTRAL ASIA.....	4
1.2 STATE OF THE ART	9
1.3 RELEVANCE OF THE WORK.....	12
1.4 OUTLINE OF THE THESIS	13
2 CONCEPTUAL LANDSLIDE RISK FRAMEWORK	15
2.1 INTRODUCTION	15
2.2 LANDSLIDE SUSCEPTIBILITY	17
2.3 LANDSLIDE HAZARD	20
2.4 LANDSLIDE EXPOSURE	22
2.5 LANDSLIDE VULNERABILITY	25
2.6 FINAL REMARKS ON LANDSLIDE RISK.....	28
3 METHODOLOGIES	32
3.1 WEIGHTS OF EVIDENCE THEORY	32
3.2 DYNAMIC SLOPE-STABILITY ANALYSIS	36
3.3 ADVANTAGES AND INNOVATIVE METHODOLOGICAL ASPECTS	39
4 DATA COLLECTION AND SPATIAL DATABASE	41

4.1 INTRODUCTION ON DATA COLLECTION.....	41
4.2 LANDSLIDE LOCATIONS	45
4.3 TOPOGRAPHIC FACTORS: SLOPE GRADIENT, SLOPE ASPECT, PROFILE CURVATURE .	46
4.4 GEO-TECTONIC FACTORS: GEOLOGY, DISTANCE FROM FAULTS	49
4.5 POPULATION DENSITY	51
4.6 TRIGGER MECHANISM: SEISMIC GROUND MOTION	52
5 APPLICATION OF WEIGHT-OF-EVIDENCE METHOD.....	55
5.1 TEST FOR CONDITIONAL INDEPENDENCY OF LANDSLIDE FACTORS	55
5.2 WEIGHTS' CALCULATION	56
5.3 LANDSLIDE SUSCEPTIBILITY MODEL	58
6 REGIONAL SLOPE-STABILITY ANALYSIS.....	59
6.1 IDENTIFICATION OF LANDSLIDE SOURCE AREAS: SEED-POINTS GENERATION.....	59
6.2 COMPUTATION OF DOWNHILL FLOW LINES.....	62
6.3 CALCULATION OF IMPACT VELOCITY	63
6.4 CREATION OF THE LANDSLIDE HAZARD INDEX (LHI)	65
7 RESULTS AND VALIDATION	68
7.1 LANDSLIDE SUSCEPTIBILITY RESULTS AND VALIDATION.....	68
7.2 LANDSLIDE SUSCEPTIBILITY MAP FOR CENTRAL ASIA	75
7.3 LANDSLIDE HAZARD INDEX (LHI) MAP FOR CENTRAL ASIA	76
7.4 LANDSLIDE RISK MAP FOR CENTRAL ASIA.....	77
8 DISCUSSION.....	81
9 CONCLUSIONS.....	88
10 REFERENCES	92
11 LIST OF PUBLICATIONS	105

LIST OF FIGURES

FIGURE 1: MAJOR TYPES OF LANDSLIDE MOVEMENTS AFTER VARNES (1978) (SOURCE: CROZIER, 2013).	2
FIGURE 2: DISTRIBUTION OF LANDSLIDE-INDUCED FATALITIES WORLDWIDE BETWEEN 1915 AND 2014 (CRED, 2015).	3
FIGURE 3: LOCATION MAP OF THE STUDY AREA AND SOME OF THE STRONGEST PAST EARTHQUAKES AND SEISMICALLY-INDUCED LANDSLIDES. IN PARTICULAR, THE 1911 SAREZ (TAJIKISTAN), THE 1911 KEMIN (KYRGYZSTAN), THE 1946 CHATKAL (KYRGYZSTAN), THE 1949 KHAIT (TAJIKISTAN), THE 1989 GISSAR (TAJIKISTAN), AND THE 1992 SUUSAMYR (KYRGYZSTAN) EARTHQUAKES ARE KNOWN TO HAVE TRIGGERED THE 1911 USOI (TAJIKISTAN), THE 1911 ANANIEVO AND KAINDY (KYRGYZSTAN), THE 1946 CHATKAL (KYRGYZSTAN), THE 1949 KHAIT (TAJIKISTAN), THE 1989 SHARORA AND OKULI-BOLO (TAJIKISTAN), THE 1992 BELALDY (KYRGYZSTAN) LANDSLIDES, RESPECTIVELY.	5
FIGURE 4: EXAMPLES OF SEISMICALLY-TRIGGERED LARGE SLOPE-FAILURES IN CENTRAL ASIA. TOP LEFT: THE ANANIEVO ROCKSLIDE (AFTER KEMIN EARTHQUAKE, 1911); TOP RIGHT: USOI ROCKSLIDE (AFTER SAREZ EARTHQUAKE, 1911); BOTTOM: KHAIT ROCK AVALANCHE (AFTER KHAIT EARTHQUAKE, 1949) (SOURCE: HAVENITH & BOURDEAU, 2010.)	7
FIGURE 5: TECTONIC MAP OF CENTRAL ASIA SHOWING THE ASIA-INDIA CONTINENTAL COLLISION ZONE, AFTER MOLNAR AND TAPPONNIER, (1975) (SOURCE: THOMAS ET AL., 2002).	8
FIGURE 6: OVERVIEW OF THE COMMON APPROACH APPLIED FOR LANDSLIDE HAZARD AND RISK EVALUATION (SOURCE: NADIM ET AL., 2006).	16
FIGURE 7: CONCEPTUAL FRAMEWORK TO CARRY OUT LANDSLIDE SUSCEPTIBILITY ANALYSIS. IN PARTICULAR, A NUMBER OF GEO-ENVIRONMENTAL PARAMETERS (SLOPE GRADIENT, SLOPE ASPECT, PROFILE CURVATURE, GEOLOGY, DISTANCE FROM FAULTS, AND SEISMIC INTENSITY) ARE COMBINED WITH LANDSLIDE OCCURRENCES TO MAP LANDSLIDE SUSCEPTIBILITY. DETAILS ON THE METHOD WILL BE OUTLINED IN CHAPTER THREE.	19
FIGURE 8: OVERVIEW OF THE STEPS FOLLOWED TO CARRY OUT THE LANDSLIDE HAZARD ANALYSIS. ON THE BASIS OF PRIOR-KNOWN LANDSLIDE SUSCEPTIBILITY, A PHYSICAL MODELING OF DOWNHILL SLOPE FAILURES IS PERFORMED TO RETRIEVE LANDSLIDE HAZARD INDEX.	22
FIGURE 9: EARTHQUAKE-INDUCED LANDSLIDES, SICHUAN PROVINCE, CHINA, 12 MAY 2008 (SOURCE: USGS).	24
FIGURE 10: FORCE DIAGRAM OF A LANDSLIDE IN DRY, COHESIONLESS SOIL THAT HAS A PLANAR SLIP SURFACE. W IS THE WEIGHT PER UNIT LENGTH OF THE LANDSLIDE, K IS THE PSEUDOSTATIC COEFFICIENT, S IS THE SHEAR RESISTANCE ALONG THE SLIP SURFACE, AND A IS THE ANGLE OF INCLINATION OF THE SLIP SURFACE (JIBSON, 2011).	37
FIGURE 11: DIGITIZATION OF GEOLOGICAL FEATURES FOR THE TERRITORY OF KYRGYZSTAN. IN THE TOP, THE ORIGINAL GEOLOGICAL MAP IS SHOWN; IN THE BOTTOM, DIGITIZED STRATIGRAPHIC UNITS ARE SHOWN: QUATERNARY (Q), NEOGENE-QUATERNARY (NQ), NEOGENE (N), PALEOGENE-NEOGENE (EN), PALEOGENE (E), CRETACEOUS (K), CRETACEOUS-PALEOGENE (KE), JURASSIC-CRETACEOUS (JK), JURASSIC (J), TRIASSIC-JURASSIC (TJ), TRIASSIC (T), PERMIAN-TRIASSIC (PT),	

PERMIAN (P), CARBONIFEROUS-PERMIAN (CP), CARBONIFEROUS (C), DEVONIAN-CARBONIFEROUS (DC), DEVONIAN (D), SILURIAN-DEVONIAN (SD), SILURIAN (S), ORDOVICIAN-SILURIAN (OS), ORDOVICIAN (O), CAMBRIAN-ORDOVICIAN (CAO), CAMBRIAN (CA), CAMBRIAN-PROTEROZOIC (PRCA), PROTEROZOIC (PR), ARCHEAN (AR), IGNEOUS ROCKS (IR).	43
FIGURE 12: FREQUENCY HISTOGRAMS RELATIVE TO CLASSIFIED LANDSLIDE POTENTIAL FACTORS IN JALAL-ABAD PROVINCE (LEFT) AND OVER ALL KYRGYZSTAN (RIGHT). IN PARTICULAR, THE DISTRIBUTION OF CLASSIFIED VALUES FOR SLOPE GRADIENT, SLOPE ASPECT, PROFILE CURVATURE, GEOLOGY, DISTANCE FROM FAULTS, AND SEISMIC INTENSITY IS SHOWN.	44
FIGURE 13: LOCATIONS OF PAST LANDSLIDES FOR THE TERRITORY OF KYRGYZSTAN (SOURCE: KALMETIEVA, ET AL., 2009). THE JALAL-ABAD STUDY AREA IS SHOWN IN BLUE.	45
FIGURE 14: SAMPLE OF LANDSLIDE LOCATIONS FOR THE JALAL-ABAD DISTRICT, SUBDIVIDED IN TRAINING (YELLOW POINTS) AND TEST (GREEN POINTS) DATASETS	46
FIGURE 15: DISTRIBUTION OF SLOPE GRADIENT FOR THE TERRITORIES OF KYRGYZSTAN, TAJIKISTAN AND UZBEKISTAN, RANGING FROM 0° TO 89° AND DIVIDED INTO FOUR BINS (QUANTILE CLASSIFICATION), 0°-6.6°, 6.6°-16.6°, 16.6°-27.5°, >27.5°.	47
FIGURE 16: DISTRIBUTION OF SLOPE ASPECT FOR THE TERRITORIES OF KYRGYZSTAN, TAJIKISTAN AND UZBEKISTAN, CLASSIFIED ACCORDING TO AZIMUTH AND CORRESPONDINGLY DIVIDED INTO EIGHT BINS, NORTH, NORTH-EAST, EAST, SOUTH-EST, SOUTH, SOUTH-WEST, WEST, NORTH-WEST.	48
FIGURE 17: DISTRIBUTION OF PROFILE CURVATURE FOR THE TERRITORIES OF KYRGYZSTAN, TAJIKISTAN AND UZBEKISTAN, CLASSIFIED (QUANTILE CLASSIFICATION) INTO FOUR BINS, -0.02507--0.00101, -0.00101--0.00005, -0.00005--0.00095, 0.00095 -0.01891.	49
FIGURE 18: GEOLOGY MAP FOR THE TERRITORIES OF KYRGYZSTAN, TAJIKISTAN AND UZBEKISTAN, BASED ON THE CLASSIFICATION OF STRATIGRAPHIC UNITS INTO CENOZOIC, MESOZOIC, AND PALEOZOIC ERAS.	50
FIGURE 19: DISTANCE FROM FAULTS MAP FOR THE TERRITORIES OF KYRGYZSTAN, TAJIKISTAN, AND UZBEKISTAN, PRESENTED THROUGH FOUR-BUFFER ZONE MAPS (< 1KM, 1 - 5KM, 5 - 10KM, > 10KM).	51
FIGURE 20: DISTRIBUTION OF POPULATION DENSITY FOR THE COUNTRIES OF KYRGYZSTAN, TAJIKISTAN AND UZBEKISTAN. (SOURCE: LANDSCAN, 2012).THE MAP IS CLASSIFIED INTO FOUR BINS (QUANTILE CLASSIFICATION), 0-1059, 1059-2137, 2137-3846, > 3846 (PEOPLE/KM ²).	52
FIGURE 21: DISTRIBUTION OF SEISMIC INTENSITY VALUES FOR THE COUNTRIES OF KYRGYZSTAN, TAJIKISTAN, AND UZBEKISTAN, EXPRESSED THROUGH THE OBSERVED MACRO-SEISMIC INTENSITY (MSK 64), AND CLASSIFIED INTO THREE CLASSES: VII, VIII, IX.	54
FIGURE 22: OVERVIEW OF TASKS AND RELATED TOOLS USED TO CARRY OUT THE LANDSLIDE HAZARD ANALYSIS. IN BLUE, TOOLS WHICH WERE MADE AVAILABLE FROM THE SENSUM PROJECT, IN YELLOW SCRIPTING TOOLS WHICH WERE DEVELOPED EX-NOVO, IN RED SCRIPTING TOOLS WHICH WERE PREPARED TO ADAPT AVAILABLE QGIS TOOLS AND TO INTEGRATE R AND QGIS TOOLS, RESPECTIVELY.	60

FIGURE 23: THE QGIS PROCESSING TOOLBOX, SHOWING SEVERAL AVAILABLE SCRIPTS. IN PARTICULAR, THE SENSUM SET OF TOOLS WHICH ARE USED TO GENERATE SEED-POINTS FOR LANDSLIDE HAZARD ANALYSIS IS SHOWN.....	61
FIGURE 24: DISTRIBUTION OF SOURCE-LOCATION POINTS FOR THE COUNTRIES OF KYRGYZSTAN, TAJIKISTAN, AND UZBEKISTAN. DARK AREAS INDICATE HIGH DENSITY OF POINTS, IN AGREEMENT WITH HIGH LANDSLIDE SUSCEPTIBLE AREAS. ON THE CONTRARY, LIGHT AREAS REPRESENT LOW DENSITY OF POINTS, IN AGREEMENT WITH LOW LANDSLIDE SUSCEPTIBILITY LEVELS.	62
FIGURE 25: EXEMPLIFICATION OF PUNCTUAL MODELING OF DOWNHILL VELOCITY. DETAILS ON THE VALUES ASSUMED BY THE VARIABLES ARE PROVIDED IN THE TEXT.	64
FIGURE 26: EXTRACT OF R OBJECT DATA FRAME (FIRST 10 OBSERVATIONS). “CAT” ATTRIBUTE (STANDING FOR CATEGORY) IDENTIFIES THE POINTS BELONGING TO THE SAME FLOW LINE; “X” AND “Y” COLUMNS CORRESPOND TO LONGITUDE AND LATITUDE, RESPECTIVELY; THE “SLOPE” ATTRIBUTE IS EXPRESSED IN RADIANS; “ACC” AND “VEL” ARE IN M/S^2 AND M/S , RESPECTIVELY; “DS” AND “DT” REPRESENT THE DISTANCE AND TRAVEL TIME BETWEEN CONSECUTIVE POINTS OF THE SAME FLOW LINE, IN METERS AND SECONDS, RESPECTIVELY.	65
FIGURE 27: DISTRIBUTION OF IMPACT VELOCITY VALUES FOR KYRGYZSTAN, TAJIKISTAN, AND UZBEKISTAN, AFTER THE INTERPOLATION AND THE APPLICATION OF THE SLOPE THRESHOLD.....	67
FIGURE 28: LANDSLIDE SUSCEPTIBILITY INDEX (LSI) MAPS FOR THE JALAL-ABAD STUDY AREA, KYRGYZSTAN, BASED ON THE COMBINATIONS OF CONDITIONAL INDEPENDENT FACTORS (MODEL A, B, C, D), AND A COMBINATION OF ALL FACTORS (MODEL E, AS OUTLINED IN TABLE5).SPECIFICALLY, MODEL A IS DERIVED FROM THE COMBINATION OF SLOPE, ASPECT, PROFILE CURVATURE, GEOLOGY, AND DISTANCE FROM FAULTS FACTORS, WHILE MODEL B IS FROM THE COMBINATION OF ASPECT, PROFILE CURVATURE, GEOLOGY, AND DISTANCE FROM FAULTS FACTORS. NORMALIZED SUSCEPTIBILITY VALUES ARE SHOWN. THE YELLOW CIRCLES INDICATE PREVIOUS LANDSLIDE LOCATIONS (TRAINING DATASET IN FIGURE 14).	69
FIGURE 29: ACCURACY ASSESSMENT OF LANDSLIDE SUSCEPTIBILITY MODELS FOR TRAINING (A) AND TEST (B) DATABASES, RESPECTIVELY. RECEIVING OPERATING CHARACTERISTIC CURVES (ROC) ARE USED TO CHECK THE VALIDITY AND ACCURACY OF LANDSLIDE SUSCEPTIBILITY MODELS.	74
FIGURE 30: LANDSLIDE SUSCEPTIBILITY INDEX (LSI) MAP FOR KYRGYZSTAN, TAJIKISTAN AND UZBEKISTAN CALCULATED WITH RESPECT TO (MODEL E, TABLE 5) SLOPE GRADIENT, SLOPE ASPECT, PROFILE CURVATURE, GEOLOGY, DISTANCE FROM FAULTS, AND SEISMIC INTENSITY FACTORS. NORMALIZED SUSCEPTIBILITY VALUES ARE SHOWN.	75
FIGURE 31: LANDSLIDE HAZARD INDEX (LHI) MAP FOR THE COUNTRIES OF KYRGYZSTAN, TAJIKISTAN, AND UZBEKISTAN. THE MAP SHOWS HAZARD LEVEL DUE TO THE IMPACT VELOCITY OF SLOPE FAILURES ACROSS THE REGION. NORMALIZED VALUES ARE SHOWN.	77
FIGURE 32: POPULATION DENSITY MAP (TOP) AND LANDSLIDE HAZARD INDEX MAP (BOTTOM) FOR KYRGYZSTAN, TAJIKISTAN AND UZBEKISTAN. A QUANTILE CLASSIFICATION SCHEME HAS BEEN CHOSEN TO CATEGORIZE VALUES INTO 4 BINS, BEING 0 – 1059, 1059 – 2137, 2137 – 3846, > 3846 (PEOPLE/ KM^2), FOR POPULATION DENSITY, AND 0 – 18.39, 18.39 – 22.11, 22.11 – 24.24, 24.24 – 39.13 (M/S), FOR LANDSLIDE HAZARD INDEX MAP.	78

FIGURE 33: CLASS-BY-CLASS MULTIPLICATIVE APPROACH WHICH HAS BEEN APPLIED TO PREPARE THE LANDSLIDE RISK MAP. FIRST, EACH CLASS OF LANDSLIDE HAZARD MAP IS MULTIPLIED BY EACH CLASS OF DENSITY POPULATION MAP (RIGHT); AFTERWARDS, VALUES ARE CLASSIFIED INTO 'LOW', MEDIUM', 'HIGH', AND 'VERY HIGH' LEVEL (RIGHT).79

FIGURE 34: RISK MAP OF EARTHQUAKE-INDUCED LANDSLIDES FOR KYRGYZSTAN, TAJIKISTAN AND UZBEKISTAN. THE MAP SHOWS THE EXPECTED LEVEL OF DAMAGE DUE TO THE OCCURRENCE OF LANDSLIDES HAVING A CERTAIN IMPACT VELOCITY ACROSS THE REGION. SPECIFICALLY, 4 LEVELS OF RISK ARE SHOWN: LOW, MEDIUM, HIGH, AND VERY HIGH.80

FIGURE 35: KHANDIZA BLOCK SLIDE SITE (UZBEKISTAN), OCCURRED IN LOESS AND PROBABLY CAUSED BY AN EARTHQUAKE IN THE PAMIR-HINDU KUSH REGION (APRIL, 2008) (SOURCE: NIYAZOV & NURTAEV, 2013).83

1 INTRODUCTION

Landslides are mass movements occurring along slopes under the influence of gravity (Varnes, 1978). They are complex natural systems, involving different types of materials as well as diverse types of movements. Consequently, following the classification proposed by Varnes in 1978, but still widely accepted within the scientific community - landslides are described by using the criteria of the type of material and the type of movement. Specifically, the main divisions of materials are rock, debris and earth, while movements are divided into five types: falls, flows, slides, spreads and topples. An overview of the main types of mass movements based on both material and movement is shown in Figure 1. The shape and size of slope movements vary because of the combination of several factors, such as dissolution, deformation and rupture induced by a static or dynamic load. These factors are mainly controlled by the topography (inclination and shape of the slope), the lithology (physical and geomechanical properties of the geological materials), the geological structure (dip, faulting, and discontinuity of layers), the hillslope hydrology (pore pressures, water contents) or a combination of all these factors.

Although landslides can have several predisposing causes, including geological, morphological, physical and anthropic, they are characterized by a unique trigger mechanism (Varnes, 1978). The trigger mechanism is defined as the external input, such as earthquake shaking, intense or prolonged rainfall, or rapid stream erosion that causes a near-immediate response in the form of a dislocation by rapidly increasing the stresses or by reducing the strength of materials forming the slope surface (Wieczorek, 1996).

Chapter 1: Introduction

The consequence for the slopes is a reduction in the inter-particle forces and the associated friction throughout the length of the rupture surfaces.

Throughout this dissertation, notions of landslide susceptibility, hazard and risk will be constantly recalled: they deal with the landslide potential, the likelihood of occurrence, and associated impact on the socio-environmental domain.

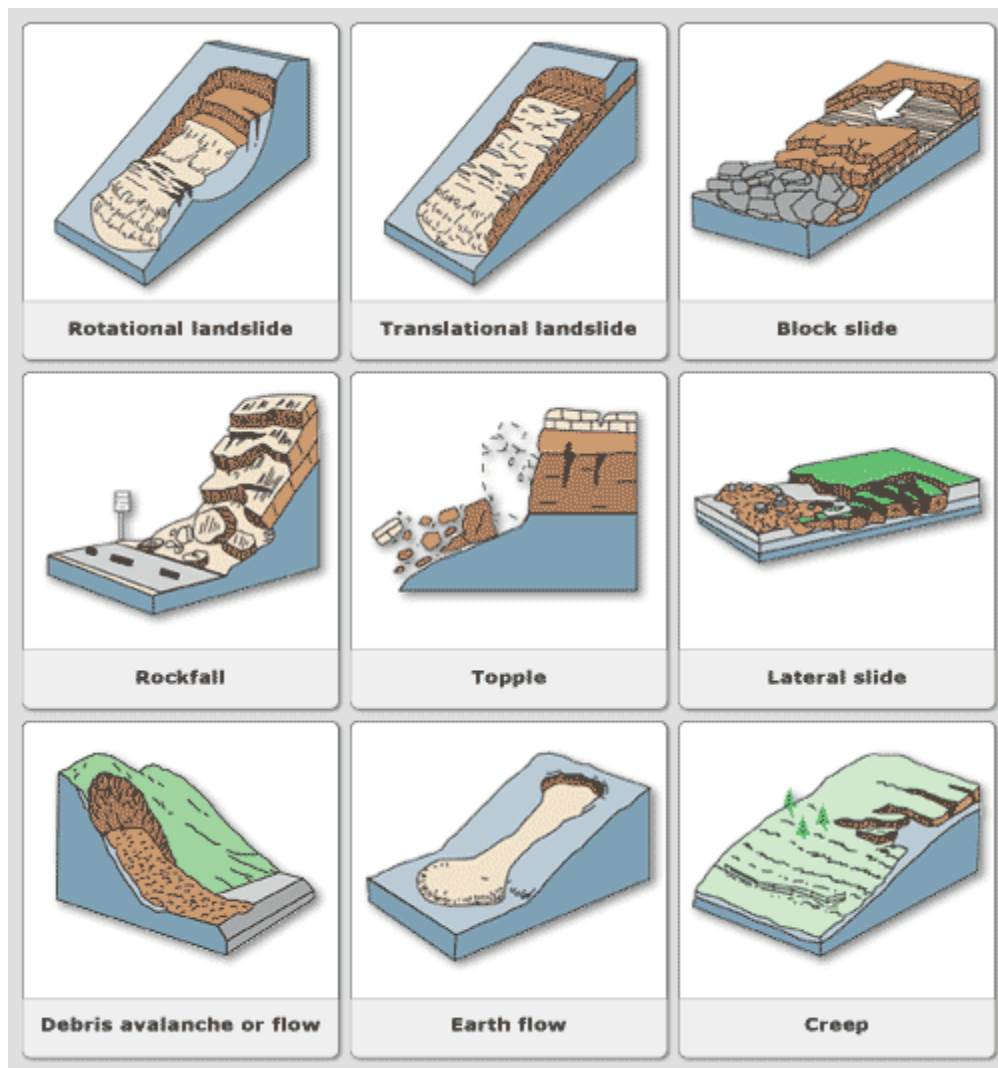


Figure 1: Major types of landslide movements after Varnes (1978) (Source: Crozier, 2013).

Landslides are well known for their devastating impact on human life, economy and environment. According to the Centre for Research on the Epidemiology of Disasters

(CRED) database (Guha-Sapir et al., 2015), landslides are responsible for the loss on average of 600 lives per year, considering the time span of the last 100 years (Figure 2), as well as associated enormous economic damages.

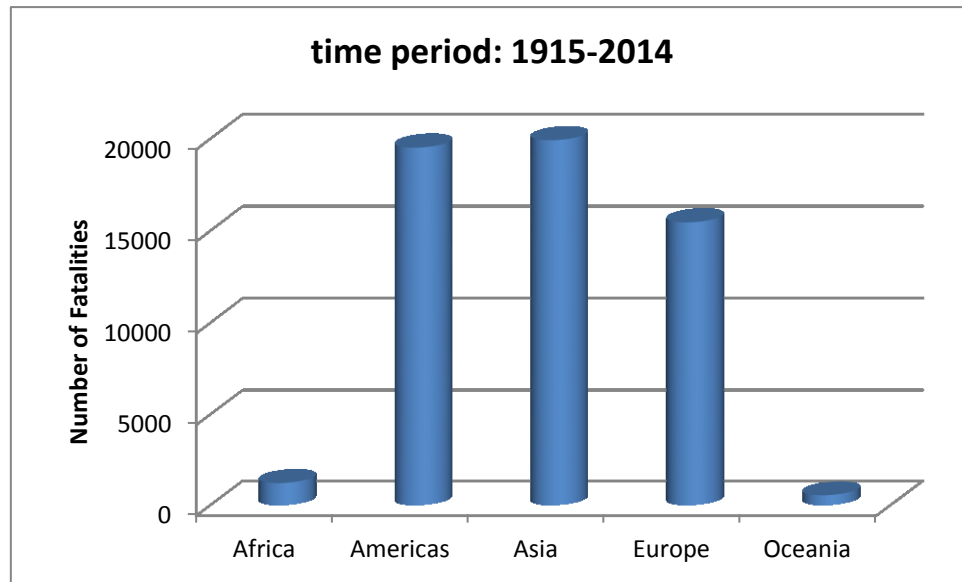


Figure 2: Distribution of landslide-induced fatalities worldwide between 1915 and 2014 (CRED, 2015).

In addition, it has been shown that economic losses associated with landslides have been rising over the past decades (Rosenfeld, 1994), mainly due to increased development and investment in landslide-prone areas. Particularly in developing countries, which have experienced rapid economic growth and population increase, the exposure of people and assets to natural hazards is growing at a faster rate than risk-reducing capacities are being strengthened, leading to increasing disaster risk (UNISDR, 2015).

Furthermore, it should be noted that the magnitude of human losses from landslides is poorly quantified and generally underestimated (Petley, 2012). This is due to the fact that most information related to landslide occurrences is systematically missing. In fact, for a natural phenomenon having an impact over inaccessible terrain, collecting data is not a trivial task; moreover, post-event databases usually classify information by trigger

mechanisms rather than cause of death. Thus, many landslide fatalities and damages are categorized as being the result of their primary trigger event (i.e., earthquake), resulting in the underestimation of human and economic losses associated with landslides. An example is the devastating Wenchuan earthquake (May 12, 2008), with around 70,000 fatalities, which in turn, triggered tens of thousands of landslides (Li et al., 2013). These mass movements obstructed the road system, and heavily impeded rescue actions by the Chinese Government, resulting in enormous numbers of losses.

Consequently, there is an overall lack of quantification and thus appreciation of the true impact of landslides, resulting in the poor prioritization of global-scale landslide research and mitigation.

1.1 Landslide phenomena in Central Asia

Within the framework of landslide risk research, this dissertation specifically deals with risk assessment of earthquake-triggered landslides in Central Asia. Central Asia is a large geographic region including the territory of Kyrgyzstan, Tajikistan, Uzbekistan, Turkmenistan, and Kazakhstan. However, for the purposes of this research, Central Asia is hereby referred to Kyrgyzstan, Tajikistan, and Uzbekistan.

Seismic-triggered landslides and their peculiarities have been described and analyzed by a number of researchers. In his pioneering work, Keefer (1984) showed that the number of landslides and their dimensions are strongly dependent upon the magnitude of the earthquake. Based on his investigations, the smallest earthquake magnitude that can cause landslides is about a magnitude of four. His work also revealed that, even in areas with abundant susceptible slopes, earthquakes with a magnitude of five typically produce only a few landslides, whereas events with a magnitude of 7.5 will produce thousands or tens of thousands of landslides.

It is well recognized that Central Asian countries (i.e., Kyrgyzstan, Tajikistan, Uzbekistan) constitute a worldwide hotspot in terms of natural hazard with a specific link between earthquakes and landslides (Nadim, 2006). Compelling evidence of the destructive power of secondary-triggered slope failures in Central Asia is readily

available (Figure 3), with landslides, mudslides and debris flows causing an extensive number of casualties (Table 1) during, e.g., the 1911 M=8.2 Kemin earthquake in the Kazakh/Kyrgyz border region, the 1949 M=7.4 Khait and the 1989 M=5.5 Gissar earthquakes in Tajikistan, and the 1946 M=7.5 Chatkal and the 1992 M=7.3 Suusamyr earthquakes in Kyrgyzstan. In addition, the 1911 M=7.6 Sarez earthquake in Tajikistan triggered a massive landslide, blocking the Murgab river and forming the tallest landslide river dam in the world.

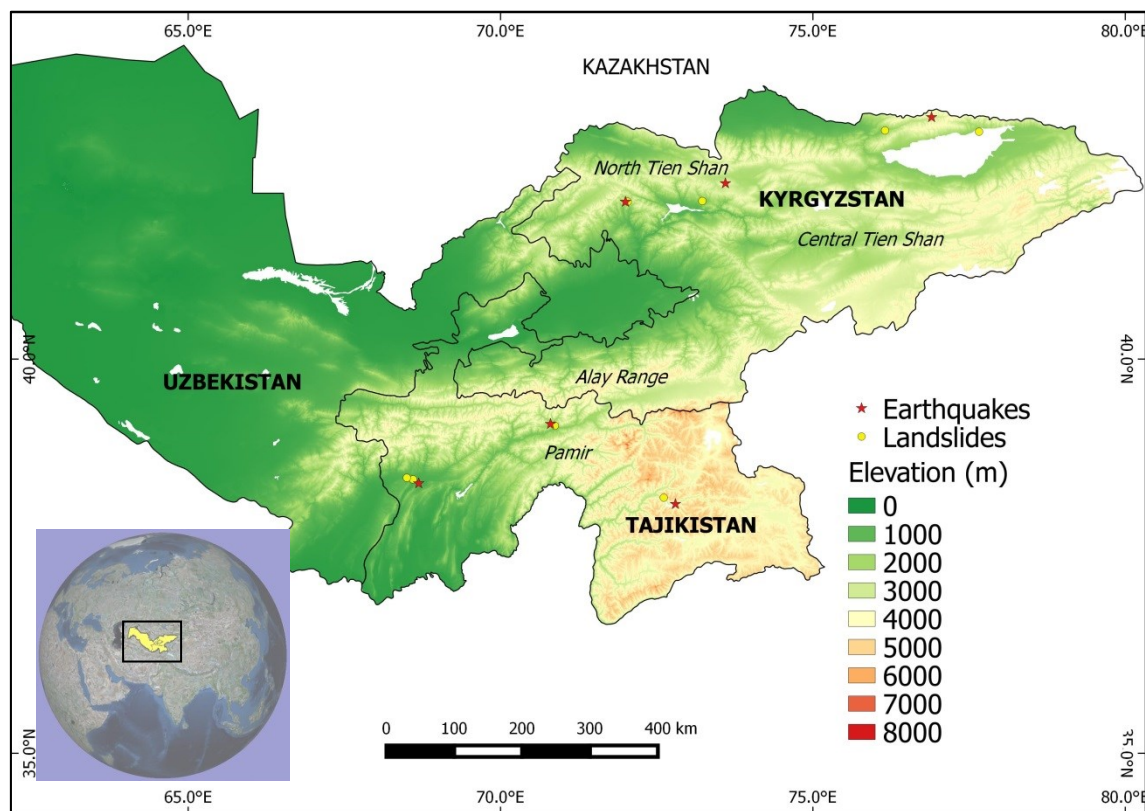


Figure 3: Location map of the study area and some of the strongest past earthquakes and seismically-induced landslides. In particular, the 1911 Sarez (Tajikistan), the 1911 Kemin (Kyrgyzstan), the 1946 Chatkal (Kyrgyzstan), the 1949 Khait (Tajikistan), the 1989 Gissar (Tajikistan), and the 1992 Suusamyr (Kyrgyzstan) earthquakes are known to have triggered the 1911 Usoi (Tajikistan), the 1911 Ananievo and Kaindy (Kyrgyzstan), the 1946 Chatkal (Kyrgyzstan), the 1949 Khait (Tajikistan), the 1989 Sharora and Okuli-bolo (Tajikistan), the 1992 Belaldy (Kyrgyzstan) landslides, respectively.

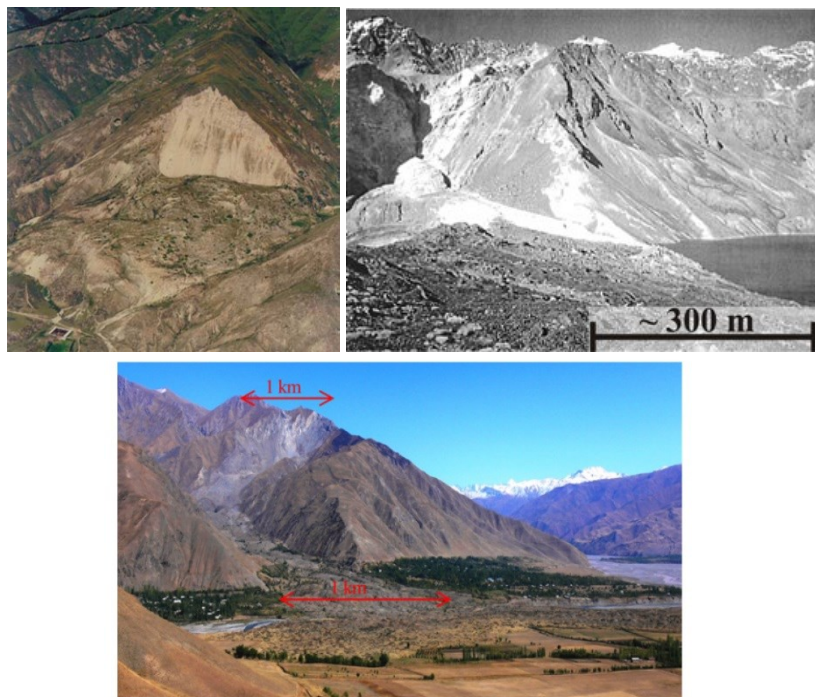
According to recent surveys for Kyrgyzstan and referring to the time period between 1988 and 2007 (CAC DRMI, 2009), 18 and 27% of yearly reported disasters in Kyrgyzstan are due to earthquakes and landslides, respectively. In particular, more than

Chapter 1: Introduction

300 large landslides occurred between 1993 and 2010, resulting in an average of 256 deaths per year (Torgoev et al., 2012) with substantial associated economic losses (an average of 2.5 million USD per year).

Table 1 : List of the largest historical earthquake-induced landslides in Central Asia.

Name	Location	Date	Volume	Trigger	Number of fatalities
Usoi landslide	Tajikistan	1911	2.2 billion m ³	Sarez earthquake	54 people
Kaindy, Ananevo rock avalanches	Kyrgyzstan	1911	15 million m ³ both	Kemin earthquake	38, 0 people
Chatkal	Kyrgyzstan	1946	15 million m ³	Chatkal Earthquake	NA
Khait rock avalanche	Tajikistan	1949	75 million m ³	Khait earthquake	7200 people
Sharora landslide, Okuli-bolo mudslide	Takijistan	1989	5 million m ³ , 40 milion m ³	Gissar earthquake	200, 70 people
Belaldy rockslide	Kyrgyzstan	1992	40 million m ³	Suusamyр earthquake	35 people



Chapter 1: Introduction

Figure 4: Examples of seismically-triggered large slope-failures in Central Asia. Top left: the Ananevo rockslide (after Kemin earthquake, 1911); top right: Usoi rockslide (after Sarez earthquake, 1911); bottom: Khait rock avalanche (after Khait earthquake, 1949) (Source: Havenith & Bourdeau, 2010.)

The root of the strong geological hazard component in the mountainous areas of Central Asia is related to a number of reasons. The region is located in the Asia-India continental collision zone (Figure 5), where the northward-moving Indian Plate indents the Eurasian Plate (Molnar & Tapponnier, 1975; Trifonov et al., 2002). The ongoing collision has resulted in high mountain topography which is subject to active deformation, contemporary faulting and frequent strong earthquakes (Gubin, 1962; Burtman & Molnar, 1993; Pavlis et al., 1997; Sidorova, 1997; Perov & Budarina, 2000), that combine to give rise to widespread landslide phenomena including massive rock slope failures in both the Pamir and Tien Shan Mountains (e.g., Gaziev, 1984; Havenith et al., 1999, 2006; Strom & Korup, 2006; Abdrakhmatov & Strom, 2006; Havenith & Bourdeau, 2010).

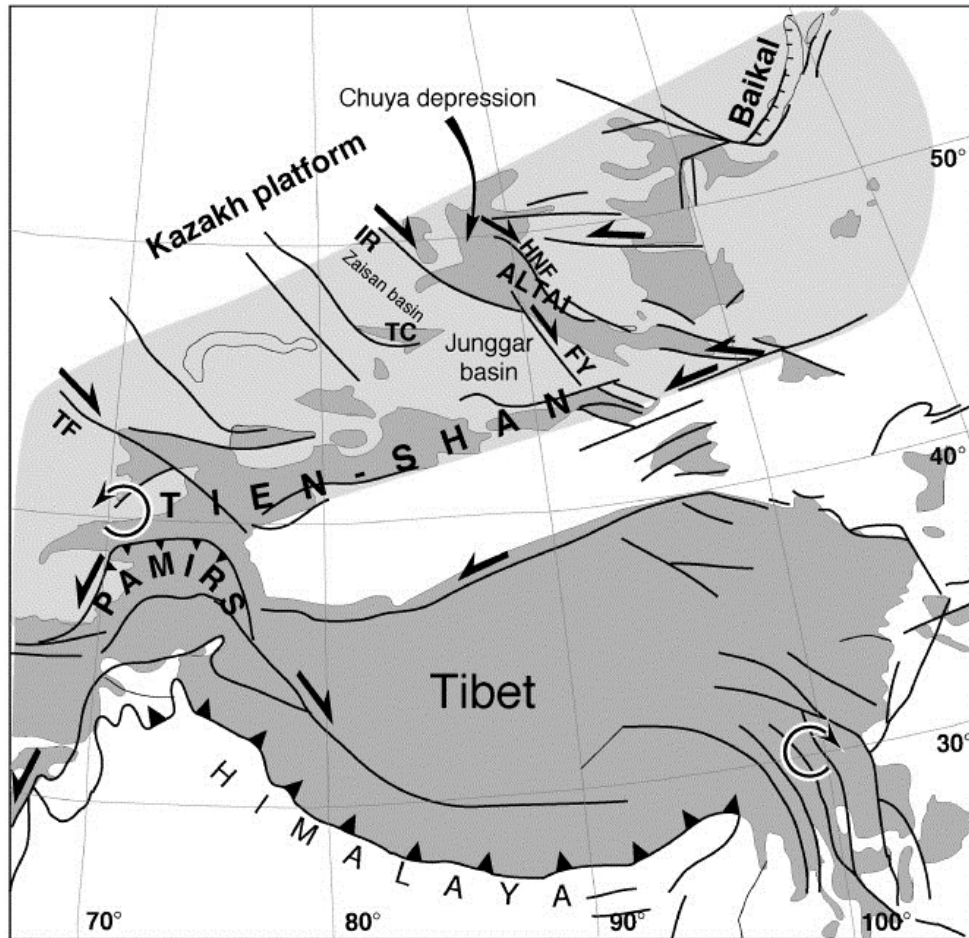


Figure 5: Tectonic map of central Asia showing the Asia-India continental collision zone, after Molnar and Tapponnier, (1975) (Source: Thomas et al., 2002).

In addition, much of the topography of the region is mantled by weakly consolidated sediments, being particularly prone to flowslides triggered by seismic shaking and/or heavy rainfall (Gubin, 1962; Ishihara, 1989, 2012).

The described strong natural landslide hazard component would not be matter of concern without considering the ubiquitous ability of landslide processes to impact upon exposed assets. In this context, it has to be noted that within the last 60 years, Central Asia has seen a growth in its population from 18 million in 1951 to more than 53 million in 2010 (Lutz, 2010). The increase of population, in combination with the expansion of urban settlements towards landslide-prone slopes, further contributes to the destructive impact of landslides due to relatively little investment in understanding the hazards and risks and an added lack of appropriate resources (Rosenfeld, 1994; Petley, 2012). The number of fatalities and damages related to landslides is hence

expected to increase over time, calling for the urgent need for risk assessment and mitigation initiatives.

1.2 State of the art

Actions with the aim of understanding and controlling slope instability phenomena are therefore necessary to implement appropriate landslide risk mitigation measures. Authorities and decision makers who are responsible for regional land use planning are in the constant need for maps that show areas that may be endangered by landslides. In order to be properly managed, landslide risk must first be quantified in an objective manner, so that results are comparable between regions.

In this context, over the last few decades, increasing attention has been paid by the international community to the topic of landslide risk, in order to find viable solutions to protecting hazard-prone targets (mainly population, buildings and infrastructures) against harmful slope failures phenomena. In particular, concepts of landslide susceptibility, hazard, and risk (which will be explained in detail in Chapter Two) have been addressed through a wide variety of methods, according to the scale of analysis and the aim of the investigation. Recently, several organizations and scientific institutions have proposed guidelines for the preparation of landslide hazard and risk maps (AGS, 2007; Fell et al., 2008; Corominas et al., 2014). In particular, a unified terminology together with identification of the fundamental data needed to prepare the necessary maps and guide practitioners in their analyses have been provided.

The foundations for landslide susceptibility and hazard analyses were laid by Varnes (1984). In his work, he clarified how it is possible to identify areas where a potential for landsliding exists by exploiting the uniformitarian principle, which states that “the past and the present are the keys for the future”: that is, slope failures in the future are more likely to happen under the same conditions that led to past and current instability. General overviews of research on the topic of landslide susceptibility can be found in the works of Soeters and van Westen (1996), Aleotti & Chowdhury (1999), Carrara et

al. (1999), Guzzetti et al. (1999), Dai et al. (2002), van Westen et al. (2006), and Fell et al. (2008).

The reliability of landslide susceptibility and hazard maps depends on the amount and the quality of input data. Geographical Information Systems (GIS) show great promise for meaningful and time-efficient landslide hazard and risk estimation over various scales and data quality, also allowing the coverage of large geographical areas.

To date, numerous studies have already shown that the spatial distribution of landslides at regional scales can be better understood through GIS-based assessments, and successful examples of regional scale susceptibility, hazard and risk analyses can be found in the works of Chung and Fabbri (2003), van Westen et al. (2003), Neuhäuser & Terhorst (2007), Oh & Lee (2010), Schicker & Moon (2012), Van den Eeckhaut et al., (2012), Holec et al. (2013), and Dahal et al. (2013). Furthermore, many works have already been carried out at a local scale in order to highlight the factors that control landslide activation as well as the expected damage to exposed assets. Some examples are Bell & Glade (2004) for Iceland, Remondo et al. (2005) for Spain, Sterlacchini et al. (2007) for Italy, Zezere et al. (2007) for Portugal, Cassidy et al. (2008) for Norway, Crovelli et al. (2009) for California, Jaiswal et al. (2011) for India, Mousavi et al. (2011) for Iran, Nefeslioglu et al. (2011) and Akgun et al. (2012) for Turkey, Andersson-Sköld et al. (2014) for Sweden. Due to difficulties in performing risk investigations for larger areas, the number of existent landslide risk studies at a regional-scale level is definitely lower than those achieved at local scales.

Focusing on the Central Asian region, several programs were developed during the Soviet Union times to deal with the high level of landslide activity. Already as early as 1924, the Soviet government set up a special commission to direct landslide control measures along the south coast of the Crimea (Sheko, 1983). Over the next 40 years, landslide observation stations were established in many parts of the Soviet Union. Regular monitoring of endangered areas was conducted from the 1960s until the collapse of the Soviet Union at the beginning of the 1990s. These activities also included extensive field-based mapping of single landslides, as well as detailed engineering-geological investigations and their relationships to ground water conditions and precipitation, resulting in a good understanding of local slope instabilities. The

main goal of these investigations had been the timely warning of the population and, if necessary, their evacuation and resettlement. Based on a 1978 decree of the Soviet Council of Ministers and coordinated by the State Committee on science and technology, homogeneous landslide hazard maps have been published for those areas of high landslide risk which had been of greatest importance for the Soviet economy. Unfortunately, most of this previous research has been published only in Russian, hence limiting the possibility to make it publicly available throughout the global scientific community. Furthermore, for state security reasons, most of the figures have been published without any related geographic location.

However, after the fall of the Soviet Union in 1991, the possibilities for landslide investigations and monitoring were drastically reduced. Even in Central Asian countries such as Kazakhstan, which have greater resources to devote to hazard analysis, landslide surveys remain underfunded and adequate observation posts are lacking. In addition, significant parts of the already existing data (e.g., maps and reports) are no longer available or their use is limited because of the loss of accompanying information related to methodology and data sources.

More recently, in Kyrgyzstan, landslide processes and their impacts have been again investigated, although at the local scale. Examples can be found for the Suusamyr (Havenith, 2006), the Mailuu-Suu (Schlögel et al., 2011; Torgoev & Havenith, 2013), and Toktogul (Khampilang & Whitworth, 2013) regions. On the other hand, for the Tajik territory, some relevant research has been conducted for Southeastern (Schuster & Alford, 2004) and Central Tajikistan (Evans et al., 2009).

Moreover, despite the systematic cataloguing activity that was initiated in the 1990s by the Ministries of Emergency Situations of Kyrgyzstan and Tajikistan (Havenith et al., 2015), the available landslide hazard and risk analyses across Central Asian countries are outdated and there is a serious need for updated analyses. In addition, a sound statistical analysis of country-wide and transboundary landslide susceptibility and hazard was not yet been achieved.

With these premises, the work presented in this thesis sets out to help fill this research gap by providing a harmonized and cross-border analysis with respect to landslide potential and related expected damage to exposed assets.

1.3 Relevance of the work

Based on the highlighted research gap which has been described in the previous paragraph, the principal aim of this dissertation is to develop state-of-the-art techniques to carry out statistically-based and harmonized analyses of landslide hazard and risk for Central Asian countries. In particular, new insights are provided regarding the following themes:

1. By harmonizing topographic, geological, tectonic and seismic data, this work provides a novel product, which highlights landslide potential at a cross-border level;
2. Under conditions of data scarcity as well as of geographic remoteness – which are of particular concern to Central Asian countries - an innovative approach is presented that is able to run a quantitative analysis of landslide hazard and risk, which also allows for the inference of information about landslide potential and expected damage for areas where no data coverage is available; moreover, the presented approach promotes the implementation of open source software (QGIS, GRASS, R)¹, and takes advantage of their ease of distribution, an aspect

¹ Quantum GIS Development Team. Quantum GIS Geographic Information System. Open Source Geospatial Foundation Project. <http://qgis.osgeo.org>.

GRASS Development Team. Geographic Resources Analysis Support System (GRASS) Software. Open Source Geospatial Foundation Project. <http://grass.osgeo.org>.

R Development Core Team. R: A language and environment for statistical computing. R Foundation for Statistical Computing, Vienna, Austria. ISBN 3-900051-07-0, URL <http://www.R-project.org>.

that is particularly desirable in developing countries such as those in Central Asia;

3. Considering that damage resulting from seismic-induced landslides is sometimes greater than damage due to the ground motion and rupture of the earthquake itself (Hasegawa et al., 2009), this dissertation contributes to the topic of landslide exposure and presents a statistically-based tool to estimate the expected destructiveness of landslide occurrences to exposed assets;
4. As will be explained in Chapter Two, interest within the scientific community to properly address concepts related to landslide risk has recently grown in order to enhance a constructive interaction with land-use planners and governmental bodies. For this specific reason, this work tests the applicability of integrating known standard statistical tools (e.g., Bayesian statistics) with a physically-based approach to carry out landslide hazard and risk assessments;
5. Finally, considering the overall lack of appreciation of the true impact of landslides upon society, the research hereby presented aims at filling this gap by providing natural authorities with landslide hazard and risk products, allowing for a better quantification of the global disaster burden associated with landslides.

1.4 Outline of the Thesis

The thesis is organized in the following way. After the first Chapter introducing the topic, Chapters Two and Three are dedicated to presenting the necessary theoretical background in order to understand the conceptual and methodological framework, respectively, in which the work is undertaken. Chapter Four provides an overview of the data which are used to conduct the analysis. Specifically, landslide locations, predisposing factors and related trigger mechanism, as well as exposed elements are described. In Chapters Five and Six, the application of the statistical and physically-based methodological frameworks in Central Asia is described. In Chapters Seven and Eight, landslide susceptibility, landslide hazard and landslide risk maps are presented

Chapter 1: Introduction

and discussed, including a detailed explanation of the applied validation procedure, as well as a discussion about the advantages and limitations related to this research work. Finally, in Chapter Nine, the conclusions and elements related to the outlook for future research are drawn.

2 CONCEPTUAL LANDSLIDE RISK FRAMEWORK

2.1 Introduction

The research presented in this thesis was developed within the framework of landslide risk assessment. From a general perspective, risk assessments represent a crucial basis for decision making and mitigation purposes. When applied to the context of landslide analysis, they are particularly supportive across a wide range of sectors, for example construction, land-use and urban planning.

The topic of landslide risk analysis calls for a specific methodological framework where a number of well-defined components are addressed. The objective of this Chapter is to summarize the most relevant landslide risk components, by providing definitions, explaining their conceptual development over the past decades, and by explaining the existing challenges related to those concepts, as well as to provide an appropriate context for those highlighted concepts.

Following the terminology of landslide risk assessment provided by Varnes & the International Association of Engineering Geology Commission (1984), a landslide risk evaluation aims to determine the “expected degree of loss due to a landslide (namely referred to as specific risk) and the expected number of lives lost, people injured, damage to property and disruption of economic activity (referred to as total risk)”. Specifically, the landslide risk (R) framework is composed of hazard (H), exposure (E) and vulnerability (V) components, which are mathematically combined as follows:

$$R = H \times E \times V, \quad 1)$$

where \times indicates multiplication. Based on this, a more inclusive overview highlighting elements which are singularly addressed for quantifying landslide risk is presented in Figure 6.

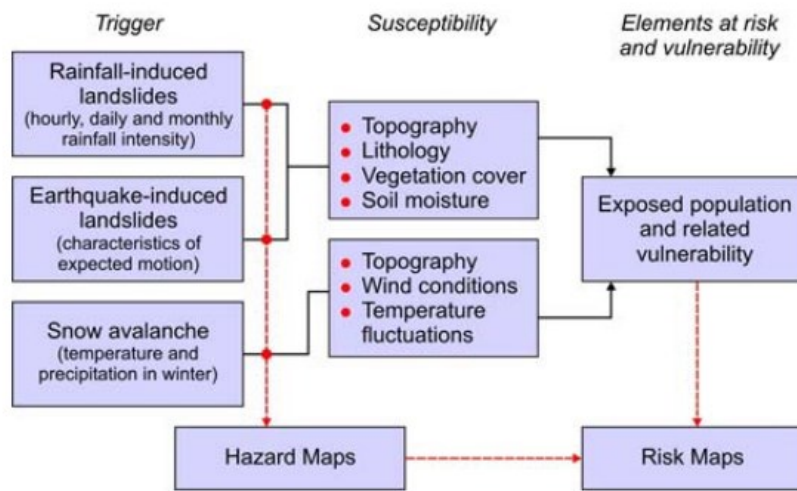


Figure 6: Overview of the common approach applied for landslide hazard and risk evaluation (Source: Nadim et al., 2006).

As can be seen from the scheme (Figure 6), from one side it is possible to recognize a component of landslide risk (hereby referred to as the *natural* component), which mainly relates to the concepts of landslide susceptibility and triggers as a basis for the hazard. The natural component of landslide risk is specifically linked to the spatial and temporal probability of landslide occurrence. In the most common cases, landslide susceptibility and, subsequently, hazard analyses, are carried out by including information about topography, geology, vegetation cover and soil, as well as considering climate-related parameters. Also, information on trigger mechanisms – e.g., rainfall, earthquakes – is required to allow the characterization of rainfall intensity, or of expected seismic shaking. On the other hand, the occurrence of a landslide would not be a matter of concern if there were not a number of assets (environment, society,

infrastructures), being potentially affected and threatened by its impact. This latter component (hereby referred to as the *impact* component) is typically addressed by means of landslide exposure and vulnerability concepts, and refers to the analysis of the exposed assets together with their propensity to suffer due to the occurrence of the natural hazardous phenomenon of concern, in our case landslides.

2.2 Landslide susceptibility

Landslide susceptibility is defined as the probability of the spatial occurrence of known slope failures, given a set of geo-environmental conditions (Guzzetti et al., 2005). Through their pioneering work concerning landslide susceptibility and hazard analyses, Varnes and the International Association of Engineering Geology Commission (1984) demonstrated that the potential for mass movements has not a random root, but slope failures in the future are more likely to happen under the same conditions that led to past and current instability, in line with the uniformitarian principle. Many landslide susceptibility analyses have been conducted worldwide. Of particular relevance for their comprehensive nature in addressing topics of landslide susceptibility and hazard are the works of Soeters and van Westen (1996), Aleotti & Chowdhury (1999), Carrara et al. (1999), Guzzetti et al. (1999), Dai et al. (2002), van Westen et al. (2006), and Fell et al. (2008). These works explain how deterministic, heuristic and statistical approaches can be adopted to assess the potential of mass movement activation. Deterministic approaches are based on detailed slope stability analyses to assess landslide probability at large scales. For medium and small scale analysis, heuristic and statistical approaches are mainly applied by considering expert opinions for estimating landslide potential from data on preparatory variables and by developing statistical analyses of the relationships among variables that led to slope instability in the past.

A number of challenges exist when addressing landslide susceptibility. As already stated in the beginning of the Chapter, landslide susceptibility concerns the potential of spatial probability of slope failures, based on the analysis of topographic, geological, and environmental factors. The availability of information related to these specific factors, together with knowledge about past landslide occurrences, is therefore crucial.

However, complete data sets concerning geological, tectonic, land use and cover are not easily obtainable, especially when needed for large areas. In most cases, detailed investigations are initiated for single sites, where more insight is necessary for engineering purposes, allowing for geological and geotechnical data to become available at a later stage. Additionally, compiling a landslide database represents a difficult task, requiring slope failures to be mapped and described one by one, and distinguishing each different characteristic. Even in situations where landslide inventories exist, their maintenance is not always attainable, due to the limited nature of scientific research projects. Moreover, public works agencies or infrastructure departments will take care of mapping in detail only those slope failures which have affected, for instance, a specific segment of a road network. As an additional difficulty, historical archives often record information concerning only major slope failures, causing, therefore, a significant underestimation of the number of observations. Due to these reasons, a landslide database most likely will be incomplete.

It has to be noted that, in conditions of geographical remoteness and data limitation, like those existing for the region here targeted, the challenge of data acquisition is even more exacerbated. Therefore, much care should be taken in order to properly collect and prepare data sets and making a landslide susceptibility analysis realistic.

Another aspect to be considered in landslide susceptibility analyses is the fact that an area might be subjected to more than one type of slope failure, e.g., rock falls and debris flows. For these specific situations, a statistical analysis which develops distinctive susceptibility models, for different landslide types, should be carried out (Fell et al., 2008). In this context, including information concerning the triggering mechanism of different landslide types into a landslide susceptibility analysis through a probabilistic-based approach is a very challenging task.

Based on highlighted significant challenges in the topic of landslide susceptibility, a procedure is hereby presented to cope with these difficulties. In particular, this research conveys a statistically-based landslide susceptibility assessment for the investigated region. For this purpose, a comprehensive database of past landslide locations is compiled in order to identify areas affected by past slope instability. A GIS archive is established in order to harmonize data regarding landslide locations, topographic

attributes, geological and tectonic factors, as well as the seismic input responsible for landslide activation (Figure 7). Specifically, a number of geo-environmental factors (slope gradient, slope aspect, profile curvature, geology, distance from faults), and information concerning seismic intensity, are combined with landslide occurrences to identify areas having a potential for landslide activation. One specific landslide type is considered for the purposes of the analysis, allowing a distinctive susceptibility model to be carried out. Details concerning landslide factors, landslide locations and the applied statistical method will be outlined in Chapters Three and Four.

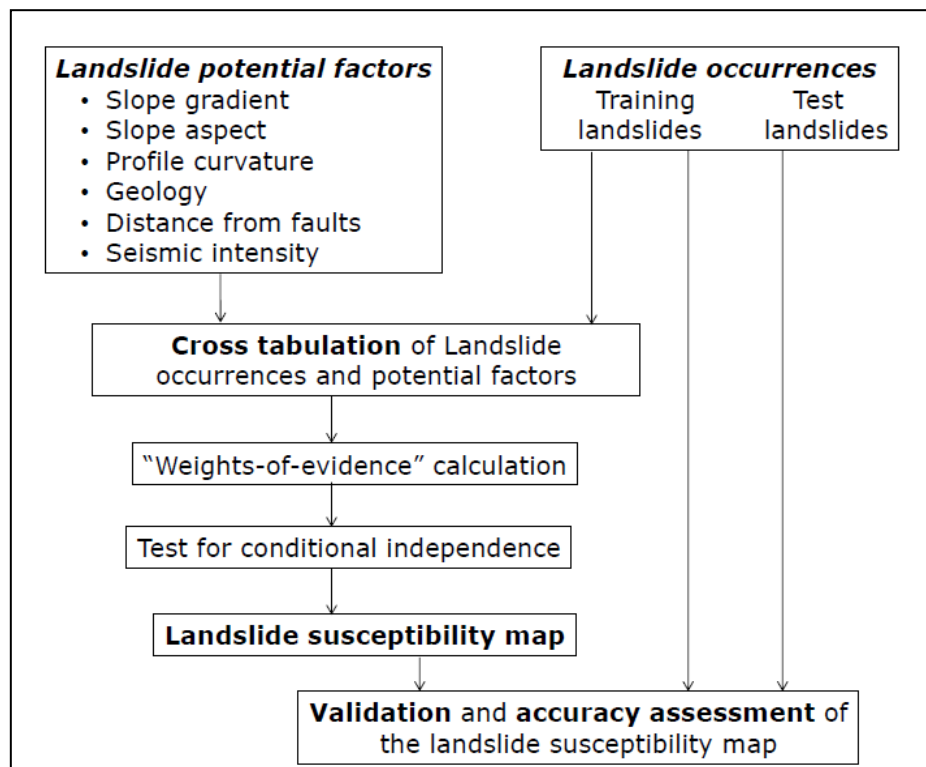


Figure 7: Conceptual framework to carry out landslide susceptibility analysis. In particular, a number of geo-environmental parameters (slope gradient, slope aspect, profile curvature, geology, distance from faults, and seismic intensity) are combined with landslide occurrences to map landslide susceptibility. Details on the method will be outlined in Chapter Three.

2.3 Landslide hazard

Landslide hazard represents the probability of occurrence over an area within a specified period of time of a potentially damaging phenomenon (Varnes & IAEG, 1984). It could be regarded as a temporal extension of susceptibility. Landslide hazard is sometimes confused with landslide susceptibility, although the temporal dimension makes a clear distinction. In other words, landslide susceptibility might be thought as a special case of landslide hazard, having one single temporal perspective instead of a time series (Lee & Jones, 2004).

The definition of landslide hazard has undergone some modifications over time. Guzzetti et al. (1999) revised the definition provided by Varnes and the IAEG Commission to include the magnitude of the landslide, with a specific link to the area, volume and velocity of the expected slope failure.

Nowadays, this definition of landslide hazard is widely accepted throughout the scientific community. In spite of this, there are a number of challenges related to landslide hazard analyses. First of all, it should be remarked that compared to other natural hazards, like earthquakes, landslides have different characteristics which make the hazard evaluation more complex. One of the major problems in landslide hazard assessment is the incompleteness of landslide observations. Also, establishing a clear magnitude-frequency relation for a given landslide location is normally hampered. Indeed, after a landslide occurs, topographic conditions are changed, and the occurrence of the same slope failure in the same location is not likely to happen. An additional difficulty is that, unlike for other natural hazards, for landslides no unique measure of landslide magnitude is available (Hungr et al., 2005). For example, while for earthquakes, magnitude is a measure of the energy released during an event, in the case of landslides, a measure of the energy released during the failure is difficult to obtain.

Despite these difficulties, landslide hazard analyses are widely performed (in Iceland: Bell & Glade, 2004; in Japan: Uchida et al., 2006; in Turkey: Akgun et al., 2012), and statistically-based methods for local landslide hazard assessments, for modeling seismically triggered shallow landslides and related run-out (travel distance)

calculations, are presented. On the other hand, landslide hazard analyses at the regional scale are quite rare. Run-out calculations are time consuming: they require huge data collection and integration efforts, as well as high computation times.

With these premises, this work tries to overcome the difficulty of achieving a landslide hazard analysis over a large region, when only a limited number of landslide observations are available. By properly integrating GIS and programming tools, slope failures are simulated and a slope stability analysis is performed for the entire Central Asian region.

Downhill movements of masses belong to a family of phenomena whose behavior is too complex to accurately predict. For this reason, the use of a limited number of downhill movements is not recommended for a reliable estimation of the overall slope stability conditions. Instead, running a large number of simulations provides information about the average most-likely physically possible paths along slopes. In this work, this limitation has been overcome with the adoption of an R package, which includes a function allowing for the generation of a high number of sampling points, based on an inhomogeneous Poisson Point Process (e.g., Pittore, 2014).

Finally, it should be noted that unlike susceptibility, landslide hazard intrinsically contains more elements, allowing for the incorporation of dynamic concepts directly linked to the loss of life, injury, property damage, loss of livelihoods and services, social and economic disruption, or environmental damage (UNISDR, 2015). Therefore, in line with this, among the objectives of this work is the preparation of landslide hazard maps on the basis of previously computed susceptibility maps, in order to retrieve impact velocities of simulated slope failures, hence, deriving the hazard for exposed assets (Figure 8). Additional details concerning the method and data used for are provided in Chapters Three and Four, respectively.

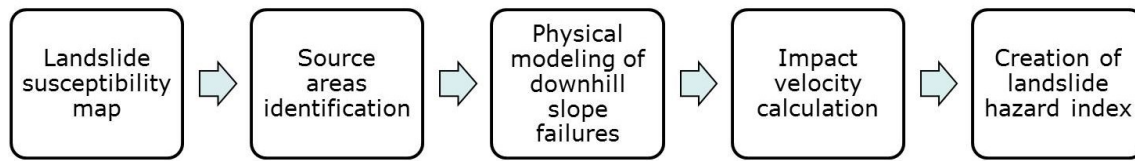


Figure 8: Overview of the steps followed to carry out the landslide hazard analysis. On the basis of prior-known landslide susceptibility, a physical modeling of downhill slope failures is performed to retrieve landslide hazard index.

2.4 Landslide exposure

Landslide exposure refers to the locations and characteristics of assets having a social or economic value, such as people, buildings, engineering structures, infrastructure areas and life lines, public service utilities and economic activities, that may be threatened by landslide occurrences.

The purpose of exposure analysis is to identify elements at risk in areas that could potentially be affected by natural hazard events. In other words, if a natural hazardous event occurs in an area with no exposure, there is no risk. Exposure analysis plays a critical role in risk assessment, also considering that the greatest influence on the output of loss estimates from risk models arises from exposure data (UNISDR, 2015).

Practically speaking, evaluating the exposure of elements at risk means evaluating the proportion of the assets that are located in the potential hazardous area. Although exposure analysis is widely carried out for other natural hazard, especially earthquakes and floods, very few studies have been devoted so far to the development of approaches for landslide exposure.

Following the classification provided by Lee & Jones (2004), the elements at risk are divided into these major groups:

1. *Populations*. This identifies the number of people which are located in the area likely to suffer a negative impact. More detailed analysis could include age-sex

distributions, as well as an indication of the state-of-health, as these aspects influence death rates and the nature of injuries within a population (see Section Vulnerability in this Chapter);

2. *Buildings, structures, services and infrastructures*. The value of these physical assets is usually determined from local authority tax bands;
3. *Property*. This includes the contents of houses, businesses and retailers, machinery, vehicles, and personal property. Information related to the value of these may be obtained from trade organizations and the insurance industry;
4. *Activities*. This group includes all activities having both a financial or social basis, such as those linked to business, commerce, retailing, entertainment, transportation, agriculture, manufacturing and industry, minerals, cultural, social and recreation. Losses related to landslide occurrences are mainly linked to the temporary or permanent disruption of these activities and, expressed in terms of loss of revenue.

One difficulty related to exposure analysis is that the total value of the elements at risk does not remain constant over time, and inflation, developmental growth, decline and depreciation have to be taken into consideration (Lee & Jones, 2004). Vulnerability itself also changes over time, due to increased initiatives for improvements in health and safety, standards of living, housing quality, technological development.

Estimates of exposure have to take into account the following two distinct components:

1. *Permanent*, where fixed assets, such as buildings or pipelines, could be damaged, irrespective of the timing of the landslide event. Assuming that these assets are always present in the zone of impact, the adverse consequences for a particular magnitude of event can be approximated to remain constant;
2. *Temporary*, where the degree of risk can vary with the timing of the event, being it night or day, week-day or weekend, tourist season or off-season. In these specific circumstances, the consequences will reflect the chance of the event occurring at a time when mobile assets are either within the zone of impact or at

Chapter 2: Conceptual landslide risk framework

a relatively high level of concentration (i.e., occupancy rates for housing are higher at night).

The effects of landslides can be very significant and vary according to geographic location. For example, landslides in Europe can cause significant economic losses, while in Asia, they can cause significant loss of life (Alexander, 2005).

Addressing the exposure of people when they represent a mobile asset is very challenging. The principal difficulties are related to the assessment of the temporal and spatial distribution of people in an urban center, together with the ethical dilemma in quantifying the economic value of human injuries or deaths.



Figure 9: Earthquake-induced landslides, Sichuan Province, China, 12 May 2008 (Source: USGS).

Despite these difficulties, fortunately, a catastrophic disaster is not the inevitable consequence of hazardous event, and much can be done to reduce the exposure of populations living in areas where natural hazards occur, irrespective of frequency.

For the purpose of this work, a procedure to assess the exposure for people at the regional scale is presented, although no temporal information on past slope failures is available for the study-area. However, the quantification of the value of the elements at risk is not achieved in monetary terms, given the lack of this specific information. Nevertheless, a quantitative analysis of population exposure is achieved by expressing the proportion of persons in the zone of impact. By combining landslide hazard maps with the distribution of population over the entire Central Asian region, it is possible to retrieve population exposure, and subsequently identify high-exposed areas, which may require more attention and, if specifically needed, detailed risk analyses.

2.5 Landslide vulnerability

Landslide vulnerability identifies the reaction of the assets when exposed to the spatially variable forces produced by the hazardous event (Lee & Jones, 2004). It can be mathematically expressed as (Einstein, 1988):

$$V_L = P[D_L \geq 0|L] \quad (0 \leq D_L \leq 1) \quad 2)$$

where D_L is the assessed or expected damage to an element given the occurrence of a hazardous landslide (L). It is expressed on a scale from 0 (no loss) to 1 (total loss), and is a function of the intensity of the phenomenon.

Measuring vulnerability to hazards of natural origins has been addressed in the past over different scales and for different purposes (Birkmann, 2007). Compared to other components of risk assessment (e.g., susceptibility, hazard), a literature review reveals that a relatively low number of available methodologies which have been developed for the analytical analysis of vulnerability.

Of particular concern is vulnerability analysis of exposed assets to slope instabilities, for which a more profound research gap exists. The reason for this is linked to the intrinsic complexity of landslide vulnerability, which depends on the landslide typology and mechanism, as well as on the intensity of the landslide movement. Additionally, based

on a literature review, it is evident that there is no common approach used for the assessment of vulnerability for communities prone to landslide. In particular, in situations where landslide vulnerability has to be determined over large areas, there is the problem of a lack of accepted standards among different investigators that can be used for effective emergency and disaster management (Galli & Guzzetti, 2007).

Landslide vulnerability can be expressed using economic (monetary, quantitative) or heuristic (qualitative) scales (Alexander, 2005). When using economic measurements, vulnerability is most commonly expressed in terms of the element value, which can be expressed by its monetary value, or by its intrinsic value, or by its utilitarian value. The intrinsic value of human life is incalculable; however, several measures are used in actuarial work to put a monetary value on death or injury, including the “private value” of a statistical life (Alexander, 2005).

Most of the work on landslide vulnerability has focused on buildings, structures and infrastructures. Some examples are the works of Hollenstein (2005), Galli & Guzzetti (2007), Kaynia et al. (2008), Uzielli et al. (2008), Papathoma-Köhle et al. (2011), Mavrouli et al. (2014).

When addressed heuristically, landslide vulnerability describes in qualitative terms expected or definite damage to an element at risk. Landslides can cause not only the loss of human lives, but they can also cause damage and temporary or permanent malfunctioning of economic and productive activities. With reference to instability phenomena, vulnerability typically expresses the level of loss produced in a given element or group of elements exposed to risk resulting from the occurrence of the natural phenomenon of a given intensity.

Damage to structures and infrastructures can be classified as (Lee & Jones, 2004):

- *Superficial* (minor damage), where the functionality of buildings and infrastructures is not compromised, and the damage can be repaired, quickly and at a relatively low cost;
- *Functional* (medium damage), where the functionality of structures or infrastructures is compromised, with repairs taking time and significant effort;

- *Structural* (total damage), where buildings, life lines and transportation routes are severely damaged or destroyed, and extensive costly repairs or demolition and reconstruction operations are needed.

While in the 1970s and early 1980s vulnerability was solely linked to physical fragility (e.g., the likelihood of a building collapsing due to the impact of an earthquake), nowadays the concepts of vulnerability describe the conditions of a society or element at risk that also determine the potential or revealed hazard's impact in terms of losses and disruption (Birkmann, 2007).

Recently, the concept of vulnerability has been broadened towards a more comprehensive approach including susceptibility, exposure, as well as different thematic areas, such as physical, social, economic, and environmental vulnerability (Li et al., 2010; Papathoma-Köhle et al., 2011; Yang et al., 2015).

Pascale et al. (2010) address landslide vulnerability of territorial systems through a novel conceptual approach. At the first place, the following subcategories are defined: physical, functional and systemic vulnerability. Physical vulnerability represents the extent to which an element suffers damage from a natural phenomenon of a given intensity; functional vulnerability represents the tendency of an element to suffer impaired functioning due to external pressure; finally, systemic vulnerability considers the system or territory as a whole, that is considering together people, infrastructures, industrial plant, natural elements, etc., and their interconnections. In particular, the concept of systemic vulnerability measures the tendency of a territorial system to suffer damage (usually functional) due to its interconnections with other elements of the same system. Unlike physical and functional vulnerability, the effects of systemic vulnerability on a territorial system are not linked to the particular disaster typology in question, but they are related to the level of interconnections between the various elements in the system (Pascale et al., 2010). In this way, areas with greater vulnerability within the urban fabric are identifiable, and programming strategies against landslide risk can be better defined.

As an additional consideration, it should be noted that similarly to landslide exposure, assessing landslide vulnerability involves a certain degree of temporal variation. In fact,

landslide vulnerability is expected to change over time, due to increased initiatives for improvements in health and safety, standards of living, housing quality, technological development, or the reverse due to, for example, economic problems.

In general, the risk to human life is considerably greater in developing countries, especially in Central Asia and South America. In both regions, high levels of tectonic activity, steep and unstable slopes, and populations concentrated in deep valleys where rockfalls, debris slides and rock avalanches can occur suddenly and with great devastation, emphasize the dangers involved. An additional distinction concerning landslide vulnerability should be made with respect to fast and slow landslides. Extremely rapid landslides may threaten life, as there is little time to react to them; in contrast, slow and extremely slow landslide rarely threaten life, although they can destroy structures leading to exorbitant economic costs (Alexander, 2005).

Based on the highlighted challenges and difficulties, this work tries to carry out a vulnerability analysis of exposed assets to landslide phenomena. Considering the high impact on population which results from mass movements in developing countries like those in Central Asia, an approach aimed at identifying the expected level of social damage is defined, including a link to the expected impact velocity of slope failures. Specifically, the concept of territorial vulnerability is adapted to the study area, and proportional dependency between population density and expected human vulnerability is assumed. Thus, landslide vulnerability analysis is tailored to landslide occurrence, by considering the proximity of a population to the most landslide-prone geographic areas.

2.6 Final remarks on landslide risk

Landslide risk assessments represent the first step of the landslide risk management chain, from risk identification to risk reduction and preparedness activities. With the objective of defining actions to reduce the negative consequences of slope failures, landslide risk has to be at the first place identified, in a quantitative and objective manner.

As previously explained in this Chapter, landslide hazard and risk analysis are intrinsically complex. Like for any other natural hazard, for a comprehensive understanding of landslide-related disasters and risk, the natural environment, together with the social, political and economic environments, must be considered.

Although the landslide risk formula – as defined in Eq. 1 – appears relatively simple, applying this formulation to practical situations (for example, a specific exposed element or a given trigger mechanism), gives rise to a number of complications. In particular, specific characteristics of the natural phenomenon causing damages and fatalities – i.e., the spatial probability, the temporal probability, the frequency and the intensity of landslide occurrences - have to be defined. In situations where the incidence of more than one natural hazard is expected, a potentially substantial increase in the system complexity also arises. In these circumstances, the definition of characteristics related to each single natural hazard is fundamental.

In past decades, assessments of landslide risk have generally relied on the judgement and skills of experienced geologists, engineers, and geomorphologists. Based on their knowledge, a range of topics have been addressed, covering the recognition of the hazard, mapping of areas having a potential for slope instability, the creation of a terrain model and the development of approaches for the assessment of the main contributing factors and principal causal-mechanism of failure. However, their works are mainly related to particular areas or specific sites, and therefore a certain degree of subjectivity in addressing landslide risk is implied. Furthermore, a consensus among different perspectives is difficult to achieve. There is, hence, the need to introduce more rigorous and systematic procedures to better formalize the evaluation process towards a more ‘opened’, ‘objective’ and ‘consistent’ assessment of landslide risk.

Furthermore, a certain degree of complexity arises also in relation to the definition of the exposed assets and their vulnerability. Especially within contexts where an impact to multiple-assets is expected, the proper characterization of each exposed element is necessary for a reliable and unbiased risk assessment. To this respect, one should take care of properly defining the individual elements at risk, which are typically linked to exposed buildings, people and business infrastructures. In parallel, for these exposed

assets, the evaluation of physical, social and economic vulnerability has to be undertaken.

An additional complexity is that risk zoning depends on the elements at risk, and hence on their temporal-spatial probability and vulnerability. In regions where a future urban development is expected, it should be clarified that the associated risk will change over time.

Therefore, considering these premises, necessary criteria and issues related to the general complexity and associated gaps in knowledge, which have been highlighted in previous sections, the principal task of this dissertation is to accomplish a quantitative risk assessment of earthquake-induced landslides and its components for Central Asia. In particular, given the scope of performing a trans-border analysis, the number of landslide risk indicators is kept relatively low and the whole system relatively simple. In this way, it is possible to achieve a quantitatively-based analysis of landslide hazard and risk over a large area, where only the most relevant parameters involved in landslide processes are taken into consideration, without diminishing the significance of the results. In addition, it has to be remarked that an assumption has been made concerning the adopted landslide triggering mechanism. Being among the worldwide hotspots in seismicity, the wide threat of earthquakes is recognized over the entire Central Asian region; on the contrary, the influence of heavy or prolonged precipitations has only a local effect. Given the final objective of providing a cross-border product, the seismic input as the principal mechanism of landslide activation is adopted.

A quantitative transnational analysis may be a very challenging and time-consuming task. This research work takes advantage of procedures for data sets harmonization – with a specific link to seismic and geo-technical data - which have been conducted during the period covering these research activities.

In the following Chapters, methodologies and data which have been adopted to undertake the analysis for the countries of Kyrgyzstan, Tajikistan, and Uzbekistan, will be outlined in detail. Specifically, the theoretical background to the Weights-of-Evidence method, and of dynamic slope-stability analysis, combined with an overview

Chapter 2: Conceptual landslide risk framework

of landslide factors, triggering mechanisms and the distribution of population, will be presented.

3 METHODOLOGIES

3.1 Weights of Evidence Theory

In this study, the Weights-of-Evidence method is used for generating a landslide susceptibility map for the entire Central Asian region. The Weights-of-Evidence method is a data-driven quantitative method used to combine evidences in support of a hypothesis (Bonham-Carter, 1994). The method was originally developed for medical studies and subsequently has been applied to other disciplines, e.g., identifying mineral deposit potential (Bonham-Carter et al., 1989).

With respect to other methods, the Weights-of-Evidence method has been successfully used in previous landslide susceptibility studies for examining the distribution and spatial relationships of particular features. The method offers a flexible way of testing the importance of various input factors to the potential of slope failure, providing a simple statistical and straightforward tool that allows the calculated weights to be interpreted. Although already carried out in large scale contexts, the method has not been previously tested in data-scarce regions.

Within the context of landslide susceptibility analysis, the influence of landslide potential factors (evidence) on the occurrence of landslides themselves (hypothesis) is assessed. Weights for each landslide causative factor are calculated based on the presence or absence of landslides within the study area.

Considering a given number of cells affected by landslide phenomena ($N\{L\}$), then the prior probability of landslide occurrence $P\{L\}$ within the studied area T is expressed as (Bonham-Carter, 1994):

$$P\{L\} = \frac{N\{L\}}{N\{T\}}, \quad 3)$$

where $N\{T\}$ is the total number of cells in the studied area. This initial estimate can be increased or decreased based on the relationships between landslide potential factors and the occurrence of landslides. In particular, the probability of finding a landslide potential factor within the studied area is given by: $P\{F\} = N\{F\} / N\{T\}$, where $N\{F\}$ is the number of cells in which the landslide factor is present, and $N\{T\}$ is the total number of cells in the studied area.

Suppose that a landslide potential factor occurs in the studied area, and that a number of known landslides occur preferentially within the factor, it is possible to indicate the probability of finding a landslide given the presence (F) or the absence (\bar{F}) of a factor, through the definition of conditional probabilities:

$$P\{L | F\} = \frac{P\{L \cap F\}}{P\{F\}} = P\{L\} \frac{P\{F | L\}}{P\{F\}} \quad 4)$$

$$P\{L | \bar{F}\} = \frac{P\{L \cap \bar{F}\}}{P\{\bar{F}\}} = P\{L\} \frac{P\{\bar{F} | L\}}{P\{\bar{F}\}}, \quad 5)$$

where $P\{F | L\}$ and $P\{\bar{F} | L\}$ are the conditional probabilities of being and not being within the factor, given the presence of a landslide.

Equations 3) and 4) can be expressed in an odds-type formulation, where the odds, O , are defined as: $O = P / (1 - P)$.

The weights for a landslide potential factor are, hence, defined as:

$$W^+ = \ln \frac{P\{F | L\}}{P\{F | \bar{L}\}} \quad 5)$$

$$W^- = \ln \frac{P\{\bar{F} | L\}}{P\{\bar{F} | \bar{L}\}}, \quad 6)$$

being W^+ and W^- the positive and the negative weight, respectively.

In the Weights-of-Evidence method, the natural logarithms of both sides of the equations are taken, resulting in:

$$\ln O\{L | F\} = W^+ + \ln O\{L\} \quad 7)$$

$$\ln O\{L | \bar{F}\} = W^- + \ln O\{L\}. \quad 8)$$

In case the influence of several factors on the distribution of landslides is taken into consideration, the summation of the weights of each factor is then used, provided that these factors are mutually conditional independent. The general expression for combining $i = 1, 2, 3, \dots, n$ landslide factors is therefore:

$$\ln O\{L | F_1 \cap F_2 \cap F_3 \cap \dots \cap F_n\} = \sum_{i=1}^n W^+ + \ln O\{L\}. \quad 9)$$

If the i^{th} factor is absent, then W^+ becomes W^- . The difference between positive and negative weights is known as the weight contrast ($C = W^+ - W^-$) and provides a useful measure of the overall spatial correlation between a certain class of factor and the occurrence of landslides (Bonham-Carter, 1994). A positive C indicates that the causative factor is present at the landslide location, and its magnitude is a measure of the positive correlation between the presence of the causative factor and landslides. On the other hand, a negative C is used to assess the importance of the absence of the factor in landslide occurrence. Factors with contrast values around 0 have no significant

connection with the occurrence of landslides. The statistical significance of the weights can be verified by calculating their variances (S^2) together with the studentized contrasts ($C / S(C)$) by means of the following equations:

$$S^2(W^+) = [1 / N\{F \cap L\} + 1 / N\{F \cap \bar{L}\}] \quad 10)$$

$$S^2(W^-) = [1 / N\{\bar{F} \cap L\} + 1 / N\{\bar{F} \cap \bar{L}\}] \quad 11)$$

$$S^2(C) = S^2(W^+) + S^2(W^-) \quad 12)$$

A script code in R has been prepared to perform the necessary calculations.

In Weights-of-Evidence modelling, it is typically assumed that factors, which are outlined in Chapter Four, are conditionally independent with respect to landslide occurrences.

It can be shown that equation 9) is equivalent to:

$$N\{F_1 \cap F_2 \cap L\} = \frac{N\{F_1 \cap L\} N\{F_2 \cap L\}}{N\{L\}} \quad 13)$$

The left side of equation 13) indicates the observed number of occurrences in the overlap zone where both F_1 and F_2 are present, while the right side represents the expected number of occurrences in this overlap zone. $N\{L\}$ is the number of cells affected by landslides. A contingency table can be prepared based on this relationship for testing the conditional independency of two factors (Table 2). Outcomes in the table which are greater than a reference value (for this specific case, the 99% significance level is adopted), suggest that the tested pair is not significantly different, and should not be used together in the analysis. Details concerning the test for conditional independence applied to each pair of landslide factors are provided in Chapter Five.

Table 2 Contingency table for testing conditional independence between Factor 1 (F_1) and Factor 2 (F_2)

	Factor 1 Present	Factor 1 Absent	Totals
Factor 2 Present	$N\{F_1 \cap F_2 \cap L\}$	$N\{\bar{F}_1 \cap F_2 \cap L\}$	$N\{F_2 \cap L\}$
Factor 2 Absent	$N\{F_1 \cap \bar{F}_2 \cap L\}$	$N\{\bar{F}_1 \cap \bar{F}_2 \cap L\}$	$N\{\bar{F}_2 \cap L\}$
	$N\{F_1 \cap L\}$	$N\{\bar{F}_1 \cap L\}$	$N\{L\}$

3.2 Dynamic slope-stability analysis

This research work, far from providing a detailed slope characterization analysis, aims at achieving a regional scale assessment of the overall stability conditions over Central Asia slopes, part of the landslide hazard analysis. In particular, trajectories corresponding to downhill movements over geospatial environments are modeled, and expected run-out extensions of downhill sliding movements of predicted slope failures are then quantified.

The first attempts at modeling the effects of seismic shaking on slopes were developed in the early 20th century (Bell, 1900). Later formalized by Terzaghi in 1950, these efforts mainly led to the definition of three different approach: 1) Pseudostatic analysis, 2) Stress-deformation analysis, and 3) Permanent displacement analysis.

Pseudostatic analysis typically assumes seismic shaking as a permanent body force, which is added to a conventional static limit-equilibrium analysis, for a dry, cohesionless slope material (Figure 10). In particular, only the horizontal component of seismic acceleration is considered, assuming null the vertical one, to determine the factor of safety (FS), defined as the ratio between the shear strength of the soil and the shear stress induced on the potential surface. The pseudostatic factor-of-safety equation is given by:

$$FS = [(W \cos \alpha - k W \sin \alpha) \tan \phi] / (W \sin \alpha + k W \cos \alpha) \quad 14)$$

where FS is the pseudostatic factor of safety, W is the weight per unit length of slope, α is the slope angle, ϕ is the friction angle of the slope material, and k is the pseudostatic coefficient.

Due to its simplicity and easy of use, this method has been widely applied (Stewart et al., 2003; Bray & Travasarou, 2009), although the assumption that the force due to seismic shaking being constant and acting only in one direction, promoting instability, may lead to conservative estimates (Kramer, 1996).

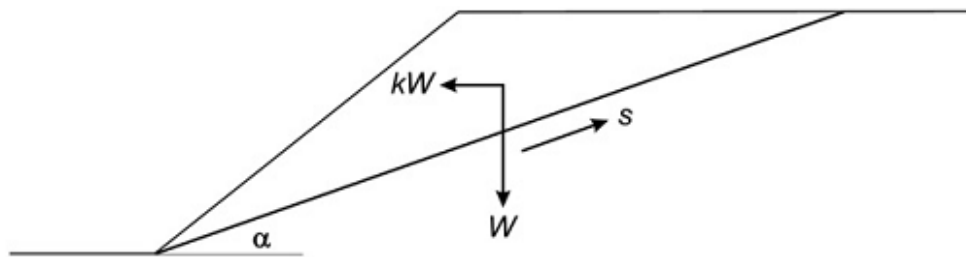


Figure 10: Force diagram of a landslide in dry, cohesionless soil that has a planar slip surface. W is the weight per unit length of the landslide, k is the pseudostatic coefficient, s is the shear resistance along the slip surface, and α is the angle of inclination of the slip surface (Jibson, 2011).

The objective of Stress-deformation analysis is to model the static and dynamic deformation of soil, providing the most accurate picture of what actually happens in the slope during the occurrence of an earthquake (Kramer, 1996). Over time, it has been applied to solve site-specific problems (Clough & Chopra, 1966), although not over regional scales.

Finally, permanent displacement methods allow for the determination of displacement related to the sliding of a rigid block on an inclined plane, when a critical value of acceleration is exceeded. This family of methods – which is based on the work of Newmark (1965) – has been broadly applied in the past (Newmark, 1965; Jibson, 2011), provided that slope geometry, soil properties and earthquake strong motion records are available. Since the effect of dynamic pore pressure is neglected, permanent displacement methods are considered valid in case of compacted or overconsolidated materials (Kramer, 1996).

The application of one of the above described methodologies within the context of the landslide research in this thesis was not attainable, for the following two main reasons. Given the focus of determining the main conditions for slope instability over a large geographic region, the inclusion of several parameters in the modeling procedure is not recommended. In addition, information concerning the expected seismic acceleration involved in the stability analysis was not available, nor was that of soil properties, leading to the necessity of adopting a simplified model procedure.

Considering that seismic stability of a slope is highly influenced by its static stability (Terzaghi, 1950), the limit equilibrium model is assumed to approximate slope stability conditions of earthquake-induced landslides across Central Asia. In particular, based on the type of slope materials that can be approached at best by the model, the choice was for disrupted and unconsolidated Quaternary and Mesozoic materials, which are typical of the foothill areas of the study region. These slope failures are relatively small in size, and can be thought to be characterized by conditions of dried friction as well as null cohesion.

The limit equilibrium model (Kramer, 1996) allows the analysis of total forces acting on a mass of rigid soil, above a potential failure surface. The main assumptions are that 1) the soil above the failure surface is rigid, and 2) the Factor of Safety (FS) is constant along the failure surface.

For the dynamic stability analysis, it is considered a system consisting of a sliding punctual mass, under the action of F_n - the normal force, F_s - the sliding force, being α the slope angle, g the gravity acceleration, and μ the coefficient of friction.

It is assumed that the rapid downhill motion of a relatively small mass is governed by the laws of dry friction (Scheidegger, 1973; Scheidegger, 1975). Friction and slope control the acceleration of the sliding mass and this is physically described by the following equation:

$$ma = mg \sin \alpha - \mu mg \cos \alpha \quad 15)$$

Consequently, observed mass acceleration take on values of:

$$a = g(\sin \alpha - \mu \cos \alpha) \quad 16)$$

With these premises, the downhill movement of punctual masses is modeled. At first, a number of sources (seed points) are generated, and some flow lines corresponding to the expected traces of each sliding mass are subsequently retrieved. The farthest points reached by the sliding masses, identify the run-out zones.

Based on the type of studied slope failures, a proper value for the angle of friction is chosen, in relation to common adopted values. Previous geotechnical studies (i.e., Hungr et al., 2005; Geotechdata.info, 2013) suggest a value of 30 degrees for a loos sand soil, hence this value for angle of friction is selected for this work.

It has to be underlined that the approach which has been described above is developed under a number of assumptions. Those assumptions were necessary to favor the application of a relatively simple approach over a large area. With regard to the type of slope failure which has been modeled, a particular case of disrupted soil slides is hereby addressed, given their known connection with seismic triggering (Keefer, 1984). Based on data availability, only landslides occurring in soft materials are addressed in this work, which are a particular case of disrupted soil slides.

3.3 Advantages and innovative methodological aspects

Associated with the above methods, GIS are very powerful known tools for time-efficient processing of multi-source data covering large areas. This work hereby takes advantage of GIS tools, by performing a spatial analysis of landslide hazard and risk. In particular, the presented approach promotes the implementation of open source software (QGIS, GRASS, R), and take advantage of their ease of distribution, an aspect that is particularly desirable in developing countries such as those in Central Asia.

The Weight-of-Evidence method offers a uniquely flexible way of testing the importance of various input factors to the potential of landslides, providing a simple statistical tool to interpret weights for each questioned landslide factor. On the other

hand, dynamic slope-stability analysis allows for identifying areas subjected to landslide movement on the basis of a physically modeled parameter (i.e., impact velocity). In this way, a cross-border physically-based analysis of slope-failure conditions is achievable, which in turn allows for identifying exposed assets to landslide runout.

Although landslide processes and their impacts have already been investigated in Central Asia at local scales, a robust statistical analysis of country-wide landslide hazard and risk has been achieved yet. Additionally, the Weight-of-Evidence method has not been applied before over large areas: data which are usually adopted for regional scale analyses are typically coarsely defined, an aspect which prevents the application of statistically-based procedures. By properly collecting and processing geospatial data, this work hence succeeds in applying a statistically-based framework for landslide susceptibility analysis across Central Asia.

While achieving a statistically-based analysis at the regional scale is a very challenging task, however, performing a physically-based analysis might be even harder. The most innovative part of this research is the integration of statically-based analyses with a physically-based approach, with the objective of identifying the hazard and risk associated with the occurrence of earthquake-induced landslides across Central Asian countries.

4 DATA COLLECTION AND SPATIAL DATABASE

4.1 Introduction on data collection

Among the primary steps in any kind of landslide susceptibility or hazard assessment are data collection and construction of a spatial database. Usually, the identification of factors correlated with slope instability is based on the choice of physically-based indicators (Guzzetti et al., 1999). For the present research work, data relevant to a number of known parameters are collected, which will be described in detail throughout this Chapter: slope gradient, slope aspect, profile curvature, geology, distance from faults and seismic intensity are selected to perform the landslide susceptibility analysis, while population density is subsequently used for the exposure and risk assessment (Table 3).

An inventory of landslides in the region is compiled and used as a reference dataset. The NASA released Shuttle Radar Topographic Mission digital elevation model, with a spatial resolution of around 90m (SRTM, 2004), has been used to derive topographic attributes over the entire Central Asian territory. Specifically, slope gradient, slope aspect, and profile curvature are calculated through the terrain analysis tool in QGIS.

Chapter 4: Data collection and spatial database

Table 3: Overview of data sets and corresponding sources, which are used for the landslide analysis.

Data type	Source
Location of past landslides	Atlas of earthquakes in Kyrgyzstan (Kalmetieva et al., 2009)
Slope gradient	STRM Digital Elevation Model (2004)
Slope aspect	STRM Digital Elevation Model (2004)
Profile curvature	STRM Digital Elevation Model (2004)
Geology	Geological Map of Central Asian and Adjacent Areas” (Tingdong et al., 2008)
Distance from faults	Geological Map of Central Asian and Adjacent Areas” (Tingdong et al., 2008)
Population density	LandScan population density (Bright et al., 2012)
Seismic intensity	Probabilistic seismic hazard analysis (Bindi et al., 2012)

With respect to geology and distance from faults, features of interest have been extracted from the “Geological Map of Central Asian and Adjacent Areas” (Tingdong et al., 2008), by means of digitization (Figure 11).

In particular, the Jalad-Abad province, in Kyrgyzstan, has been selected as a study area, given the wide variability of landslide factors in the area. Additionally, as can be seen from the frequency histograms (Figure 12), the distribution of landslide factors in Jalal-Abad area is comparable to the one concerning the entire Kyrgyz territory. For this reason, this area is considered to be representative of the existing relationships among landslide factors in Kyrgyzstan.

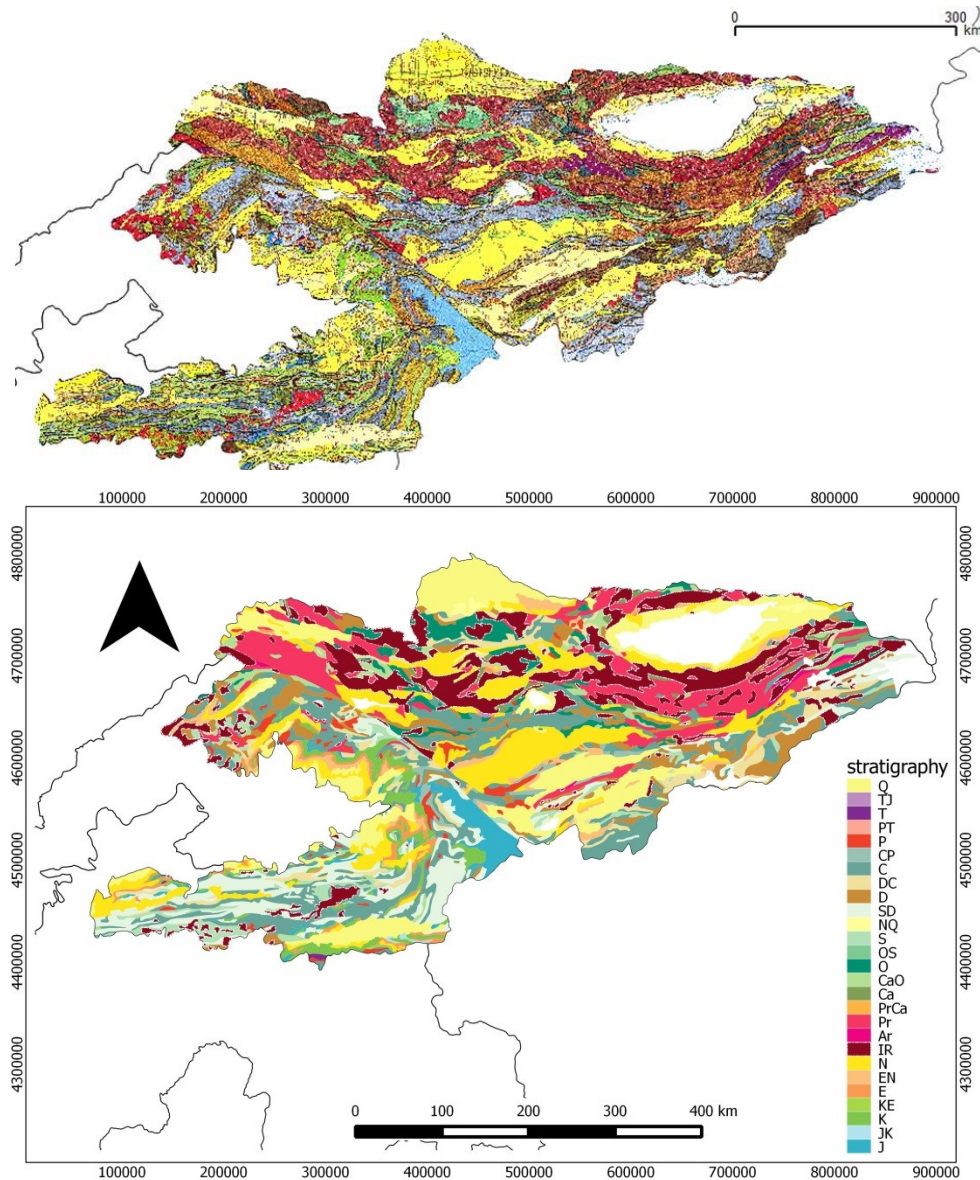


Figure 11: Digitization of geological features for the territory of Kyrgyzstan. In the top, the original geological map is shown; in the bottom, digitized stratigraphic units are shown: Quaternary (Q), Neogene-Quaternary (NQ), Neogene (N), Paleogene-Neogene (EN), Paleogene (E), Cretaceous (K), Cretaceous-Paleogene (KE), Jurassic-Cretaceous (JK), Jurassic (J), Triassic-Jurassic (TJ), Triassic (T), Permian-Triassic (PT), Permian (P), Carboniferous-Permian (CP), Carboniferous (C), Devonian-Carboniferous (DC), Devonian (D), Silurian-Devonian (SD), Silurian (S), Ordovician-Silurian (OS), Ordovician (O), Cambrian-Ordovician (CaO), Cambrian (Ca), Cambrian-Proterozoic (PrCa), Proterozoic (Pr), Archean (Ar), Igneous Rocks (IR).

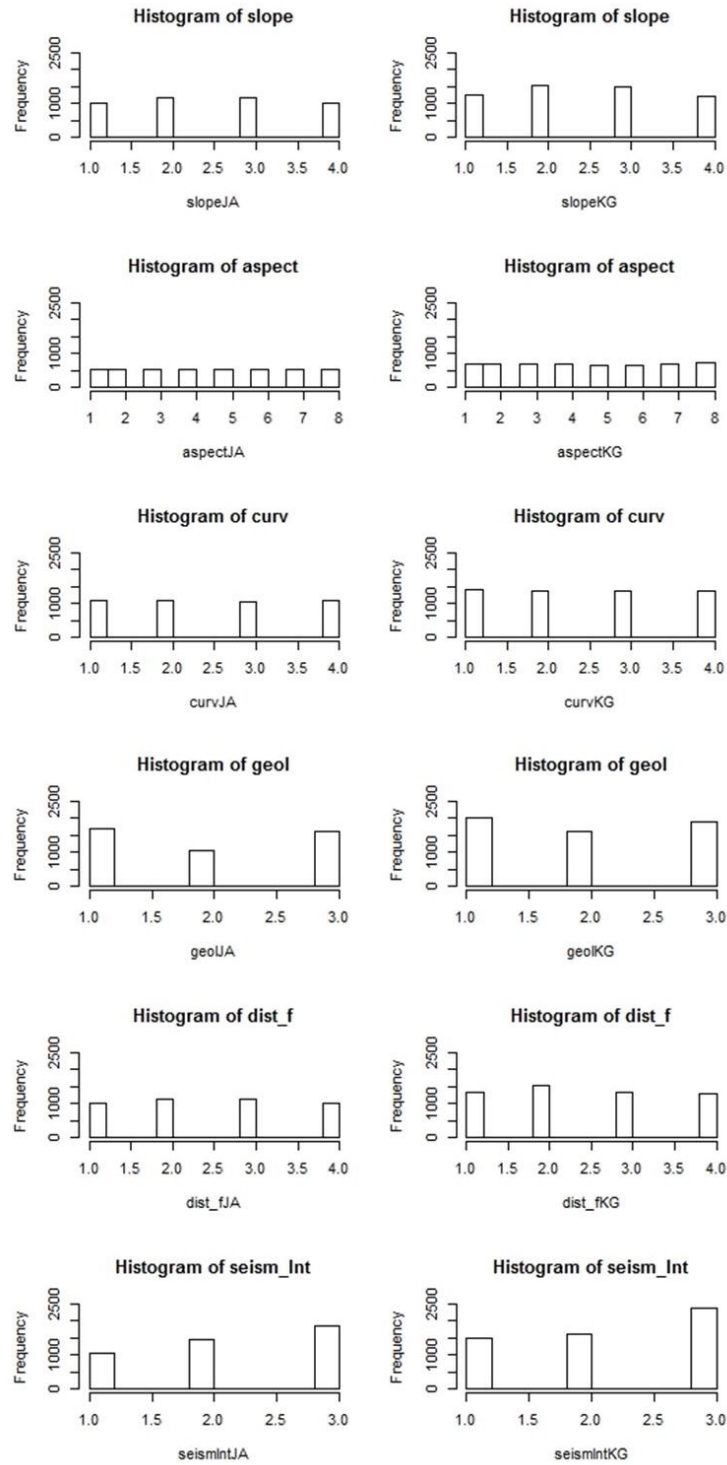


Figure 12: Frequency histograms relative to classified landslide potential factors in Jalal-Abad province (left) and over all Kyrgyzstan (right). In particular, the distribution of classified values for slope gradient, slope aspect, profile curvature, geology, distance from faults, and seismic intensity is shown.

4.2 Landslide locations

A landslide inventory represents an essential ingredient in order to carry out landslide hazard analysis at the regional scale (Guzzetti et al., 1999). This helps to identify the locations of previous landslides in order to be able to predict future slope failures.

There is no agreement within the scientific community on the best technique for the preparation of landslide inventory maps; researchers usually adopt different inventory maps where landslides are shown as points, scarps, and seed cells (Yilmaz, 2010). Small-scale maps may only show landslide locations (point strategy), as due to the scale of the map, it is not possible to outline the landslide's extent. On the other hand, large-scale maps may distinguish between source and deposit areas (Yilmaz, 2010).

As mentioned, for the purposes of this study, we considered only one type of mass movement, i.e., landslides occurring in soft materials, which are a particular case of disrupted soil slide type. A selection of landslide sites is defined on the basis of published information (Kalmetieva et al., 2009), and their distribution is mapped as point locations (Figure 13).

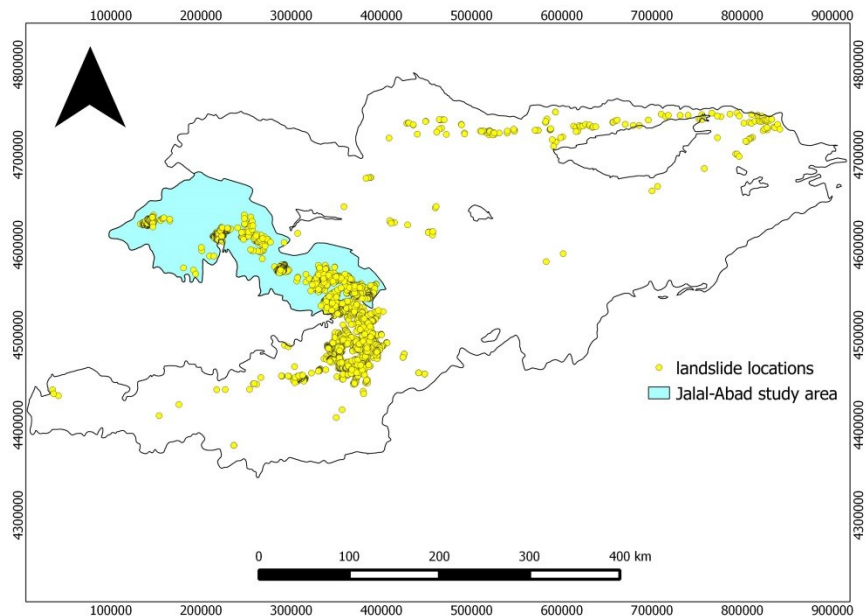


Figure 13: Locations of past landslides for the territory of Kyrgyzstan (Source: Kalmetieva, et al., 2009). The Jalal-Abad study area is shown in blue.

The landslide susceptibility analysis was initially conducted for the Jalal-Abad region over a landslide sample consisting of 1,347 landslide locations (Figure 14). Specifically, 50% of the total number of locations were randomly selected, and then used as the “training dataset”. The remaining 50% were then used as the “test dataset” for validating results.

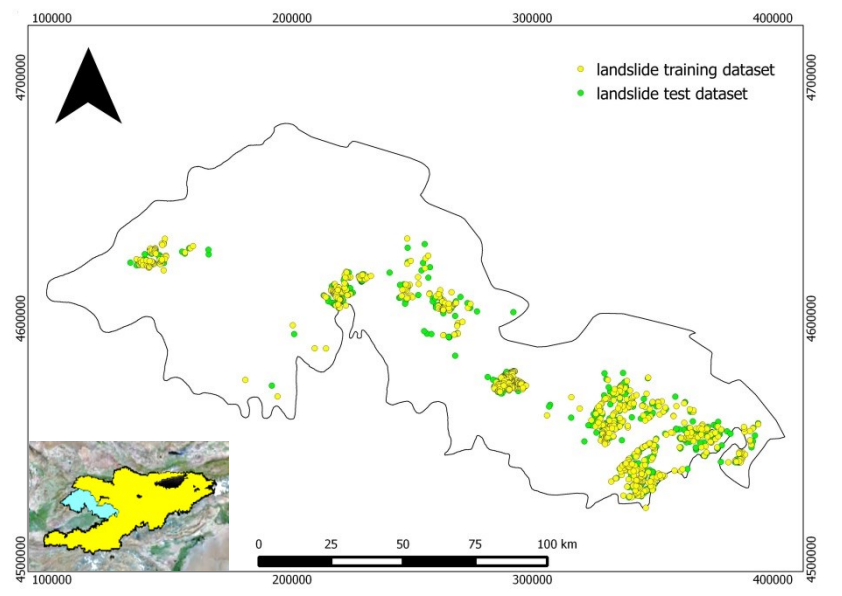


Figure 14: Sample of landslide locations for the Jalal-Abad district, subdivided in training (yellow points) and test (green points) datasets

4.3 Topographic factors: slope gradient, slope aspect, profile curvature

The stability of a slope is known to be highly dependent upon the slope gradient (angle) and its material properties (Terzaghi & Peck, 1967). The slope (Figure 15) is presented in degrees ranging from 0° to 89° and is divided into four bins with approximately the same number of features (quantile classification), 0° - 6.6° , 6.6° - 16.6° , 16.6° - 27.5° , $>27.5^{\circ}$.

Defined as the direction of maximum slope of the terrain surface, slope aspect is typically taken into consideration, although in some cases its importance has been questioned (Guzzetti et al., 1999). For the selected areas, a classification based on

azimuth being divided into eight bins, North, North-East, East, South-East, South, South-West, West, North-West, has been carried out (Figure 16).

Curvature represents one of the topographic attributes which is also commonly included in landslide susceptibility analysis (Ayalew et al., 2004). In particular, the profile curvature - defined as the second derivative of the slope with respect to the maximum steepness direction – may help in understanding patterns of the flows' acceleration and deceleration, and therefore, erosion and deposition. For the selected area, profile curvature values have been classified (quantile classification) into four bins, -0.02507--0.00101, -0.00101--0.00005, -0.00005--0.00095, 0.00095 -0.01891 (Figure 17).

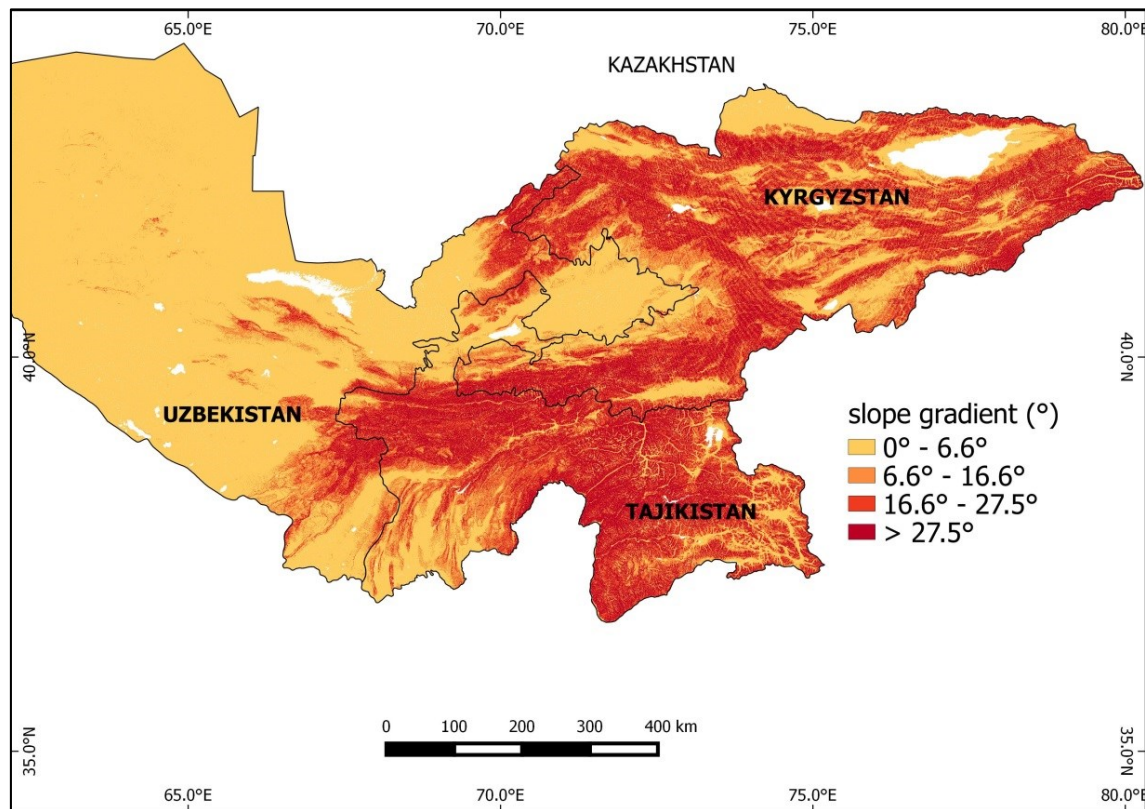


Figure 15: Distribution of slope gradient for the territories of Kyrgyzstan, Tajikistan and Uzbekistan, ranging from 0° to 89° and divided into four bins (quantile classification), 0°-6.6°, 6.6°-16.6°, 16.6°-27.5°, >27.5°.

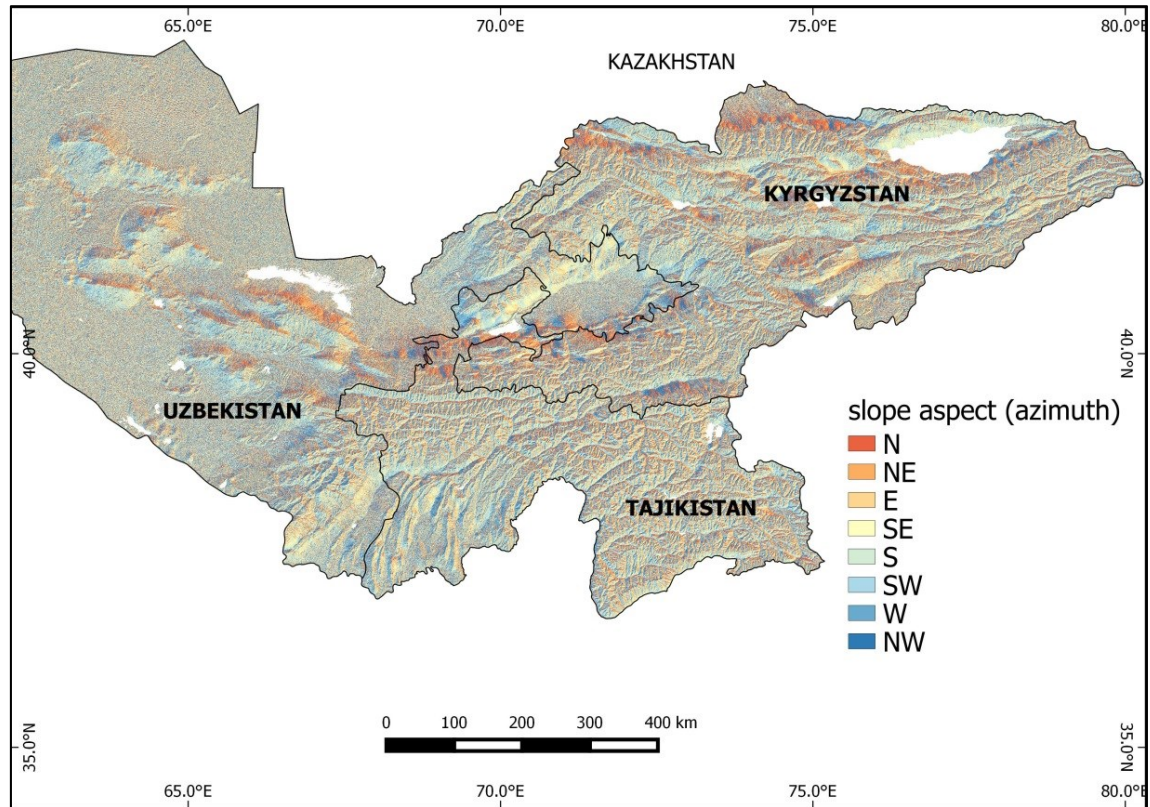


Figure 16: Distribution of slope aspect for the territories of Kyrgyzstan, Tajikistan and Uzbekistan, classified according to azimuth and correspondingly divided into eight bins, North, North-East, East, South-East, South, South-West, West, North-West.

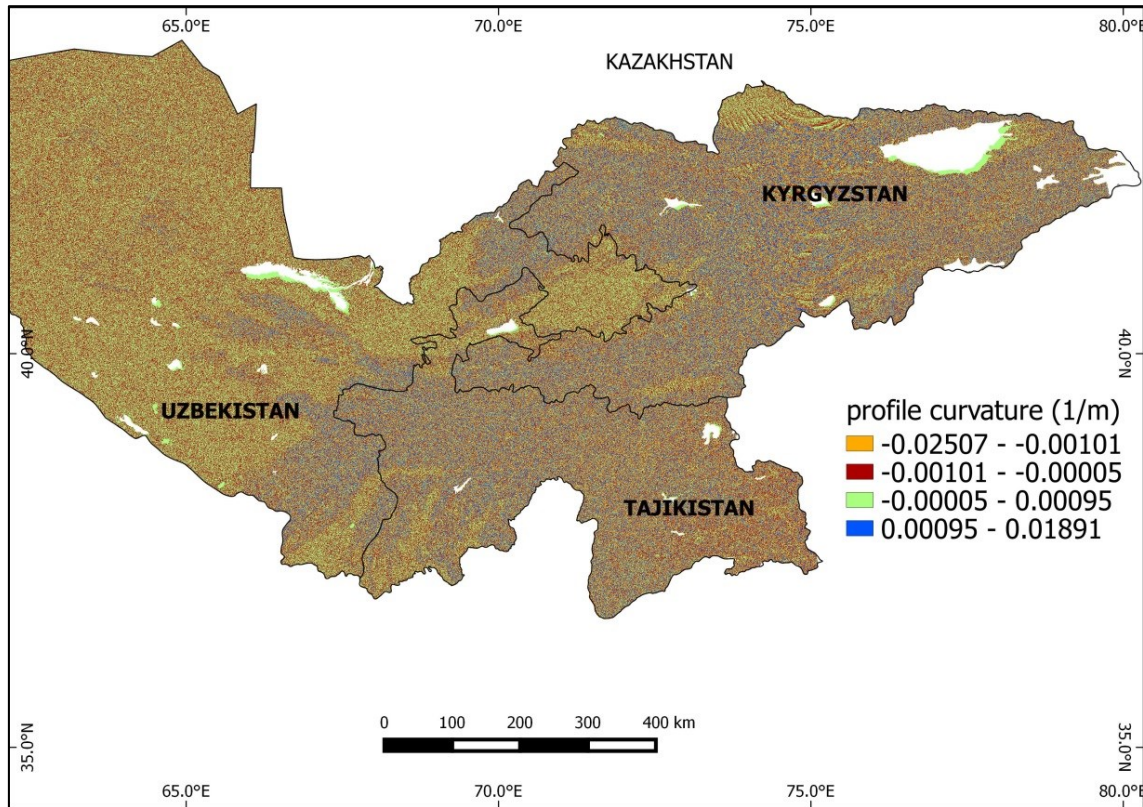


Figure 17: Distribution of profile curvature for the territories of Kyrgyzstan, Tajikistan and Uzbekistan, classified (quantile classification) into four bins, -0.02507--0.00101, -0.00101--0.00005, -0.00005--0.00095, 0.00095 -0.01891.

4.4 Geo-tectonic factors: geology, distance from faults

Lithology plays an important role in landslide susceptibility studies because different geological units have different slope failure behaviours. For example, landslides in loess materials have occurred in Uzbekistan, while landslide-prone slopes in Cretaceous rocks may be found in Kyrgyzstan. For our study, geological information is obtained from “The Geological Map of Central Asia and Adjacent Areas” (Tingdong et al., 2008), scaled 1:2,500,000. Overall, the region is covered by a range of different sedimentary formations, mostly dated to the Quaternary, Neogene, Paleogene, Cretaceous, Jurassic, and Triassic. Igneous rocks related to the Palaeozoic epoch are also present.

Based on this information, stratigraphic units have been digitised from Tingdong et al. (2008) and accordingly classified into Paleozoic, Mesozoic and Cenozoic units (Figure 18).

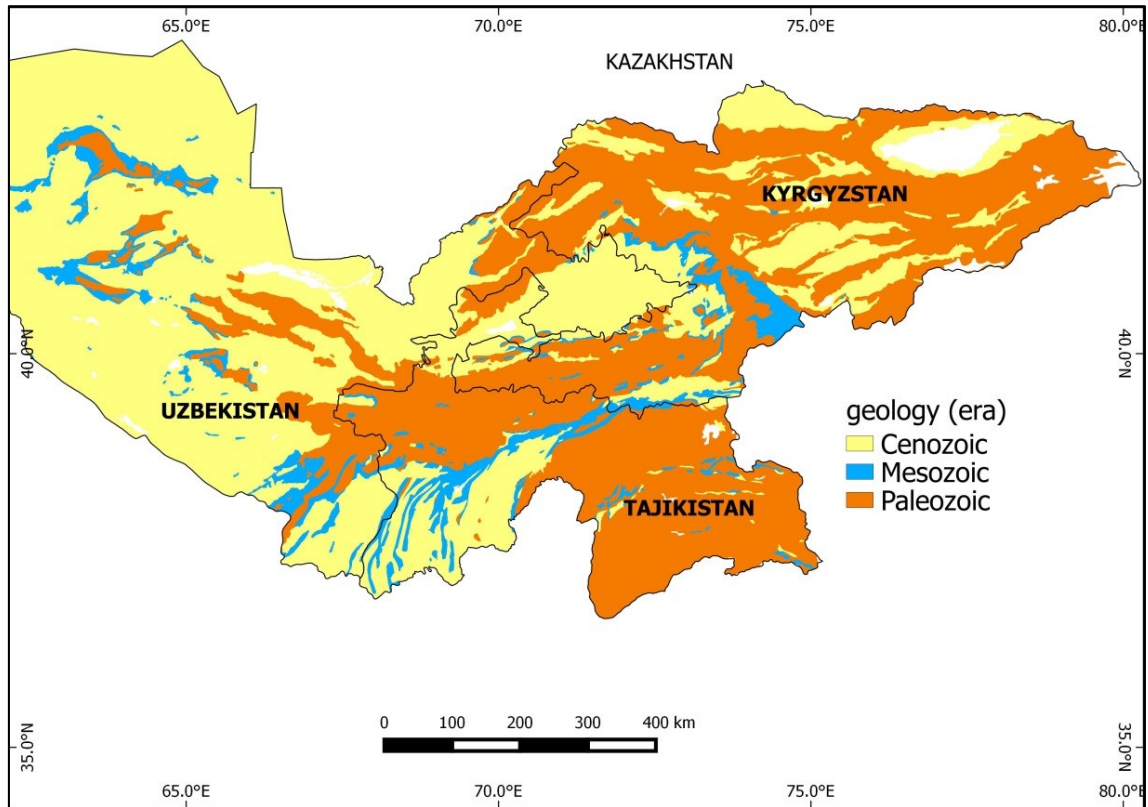


Figure 18: Geology map for the territories of Kyrgyzstan, Tajikistan and Uzbekistan, based on the classification of stratigraphic units into Cenozoic, Mesozoic, and Paleozoic eras.

The presence of major lineaments is among the important factors governing the stability of slopes (Varnes & IAEG, 1984). Tectonic structures form zones of weakness in rocks and might accelerate the process of slope failures. In landslide susceptibility studies, distance from lineament features (i.e., faults) is typically used to investigate any cause-effect relationships between lineaments and landslide occurrence (Gemitzi et al., 2011; Pradhan et al., 2010). Central Asia is covered by a large number of active faults (e.g., the Talas-Fergana fault). For the actual analysis, fault lines were derived from the 1:2,500,000 scale geology map and four-buffer zone maps (< 1km, 1 - 5km, 5 - 10km, > 10km) were prepared in GIS (Figure 19).

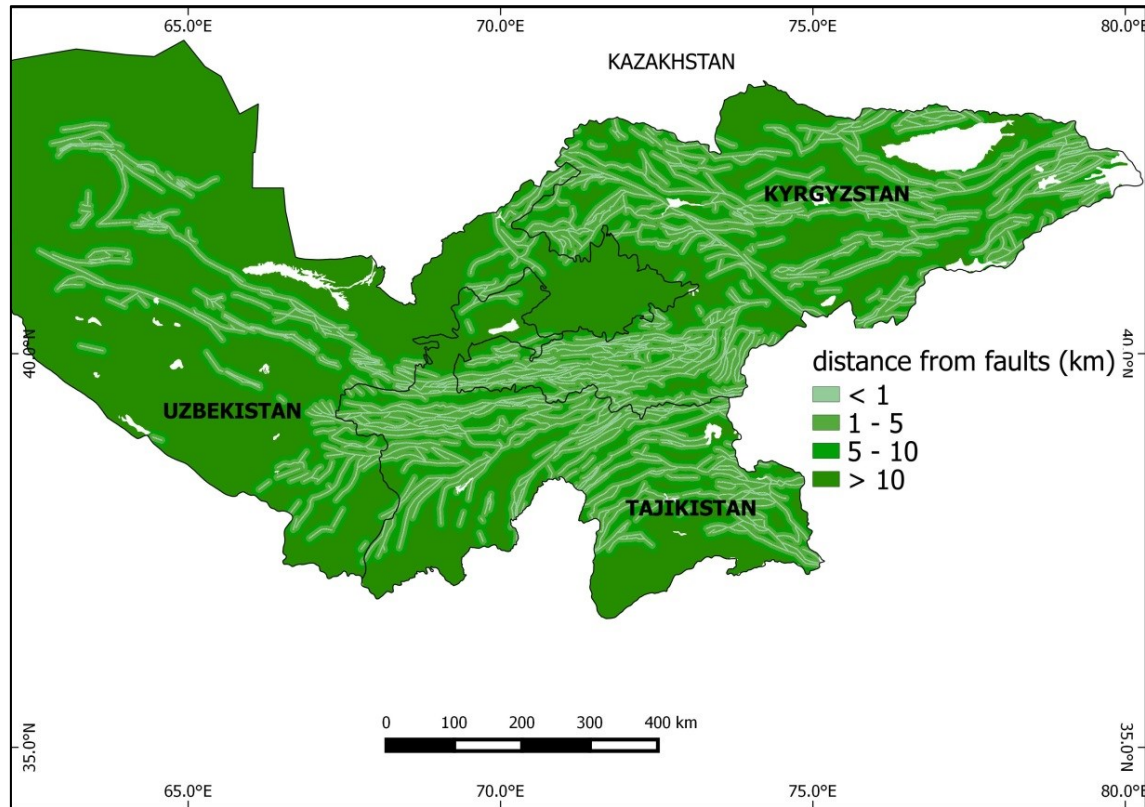


Figure 19: Distance from faults map for the territories of Kyrgyzstan, Tajikistan, and Uzbekistan, presented through four-buffer zone maps (< 1km, 1 - 5km, 5 - 10km, > 10km).

4.5 Population density

Population density is known to represent an appropriate measure to assess the exposure and vulnerability related to earthquakes occurrences. For landslide tailored studies, the analysis of exposure and vulnerability in small cities as well as rural communities – which by definition have a lower population density – is particularly relevant. While large cities often have considerable resources for dealing with natural disaster, smaller settlements are usually more vulnerable (Cross, 2001).

In this work, the LandScan population density dataset (Bright et al., 2012) is adopted, given that it provides the finest resolution global population distribution data available (approximately 1 km resolution) and represents an ambient population (average over 24 hours).

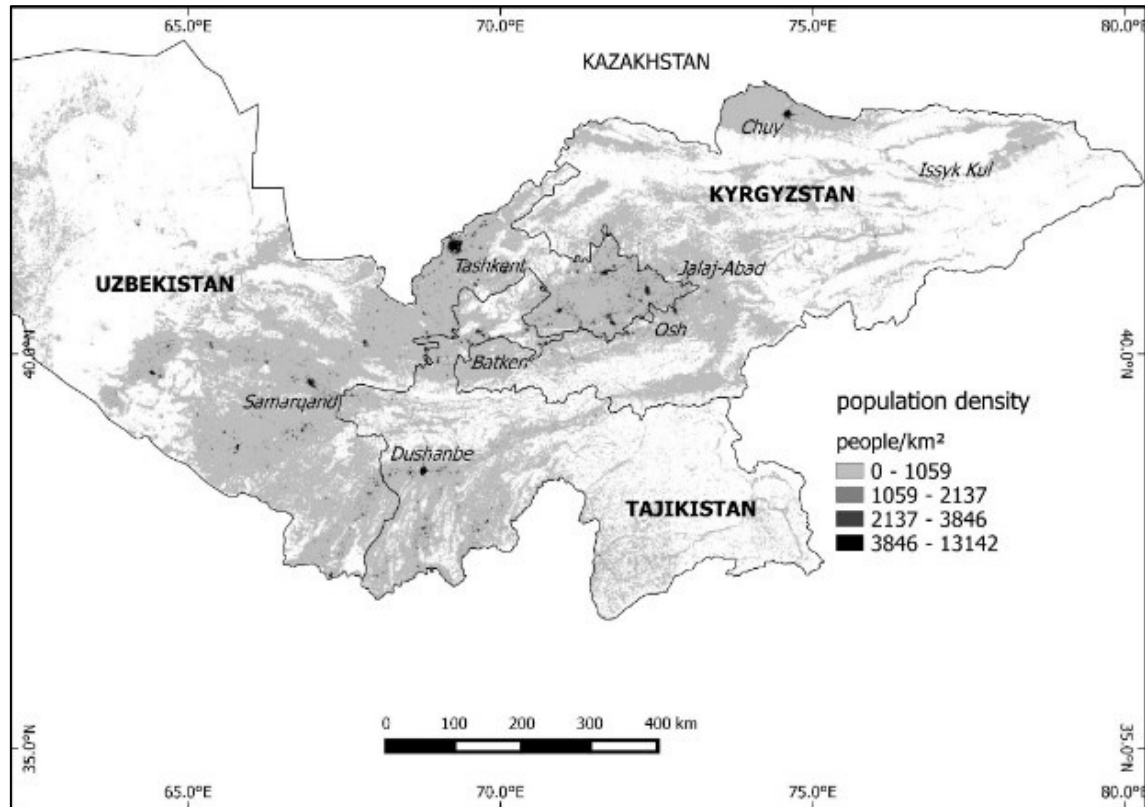


Figure 20: Distribution of population density for the countries of Kyrgyzstan, Tajikistan and Uzbekistan. (Source: LANDSCAN, 2012). The map is classified into four bins (quantile classification), 0-1059, 1059-2137, 2137-3846, > 3846 (people/km²).

From this data set, population density map for the territories of Kyrgyzstan, Tajikistan, and Uzbekistan was prepared (Figure 20). The map is presented in values ranging from 0 to 13172 persons/km², and divided into four bins with approximately the same number of features (quantile classification), 0-1059, 1059-2137, 2137-3846, > 3846 (persons/km²).

4.6 Trigger mechanism: seismic ground motion

As the study area is widely and strongly affected by earthquakes, it is necessary to take seismic ground shaking, expressed through the observed macro-seismic intensity (MSK 64), into account as a triggering factor for landslides. Within the Earthquake Model Central Asia (EMCA) project, Bindi et al. (2012) carried out an uniform assessment of the seismic hazard in Central Asia, mainly guided by the observed seismic histories

without any a-priori assumption on seismic zonation or model of time recurrence. The application of such an approach to cross-border catalogues and considering intensity prediction equations developed for the investigated area (Bindi et al., 2011), allowed a systematic and homogeneous evaluation of the hazard to be obtained, as well as the evaluation of the probability of exceedance of any given intensity value over a fixed exposure time (50 years) over the entire region of interest.

For the territory of Kyrgyzstan and Tajikistan, these studies returned intensities of IX to be expected in the future (over 50 years), while for Uzbekistan, lower intensities of VII and VIII are expected. The main advantage of the approach followed is that it serves as a step towards a homogenized and updated seismic input.

After importing values to GIS, a raster map was created and the resulting intensities categorized into 3 classes: I = VII, I = VIII, and I = IX (Figure 21). Although intensity values have not been provided at each individual landslide location, such a map provides an overall suggestion of future intensities, and hence the potential for landslide triggering.

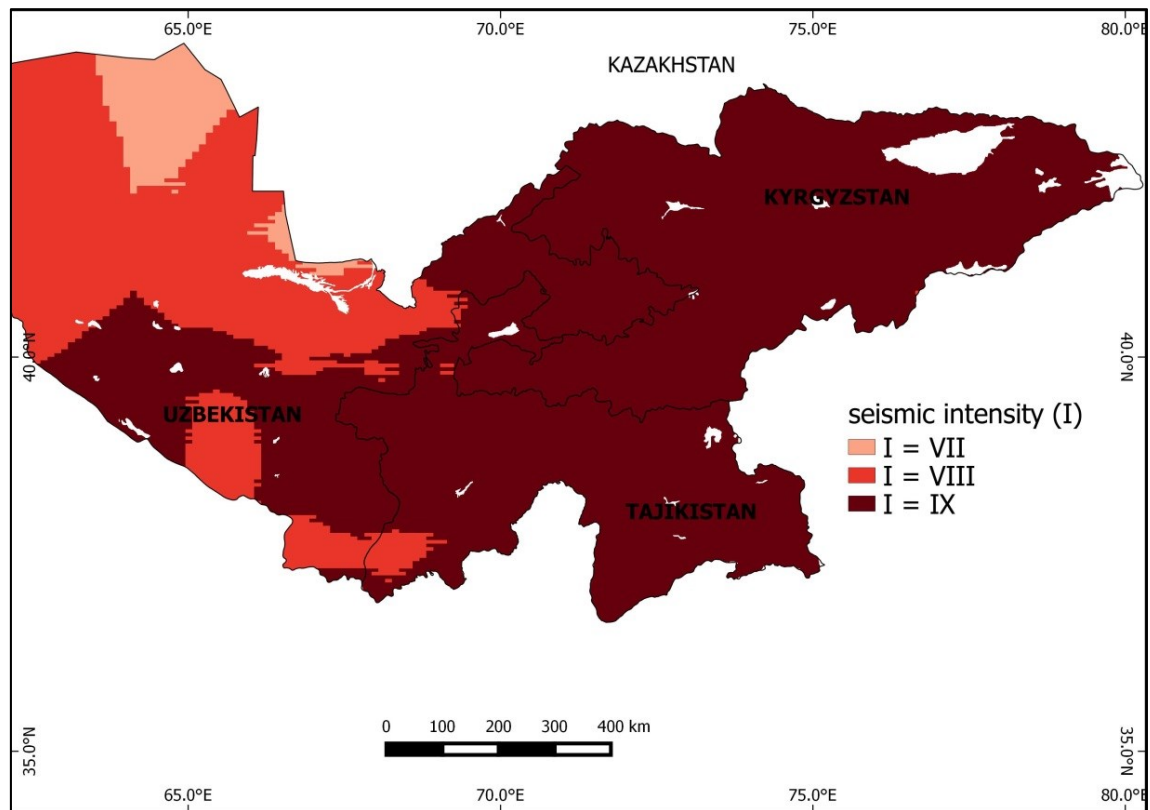


Figure 21: Distribution of seismic intensity values for the countries of Kyrgyzstan, Tajikistan, and Uzbekistan, expressed through the observed macro-seismic intensity (MSK 64), and classified into three classes: VII, VIII, IX.

5 APPLICATION OF WEIGHT-OF-EVIDENCE METHOD

5.1 Test for Conditional Independency of landslide factors

As already explained in Chapter Three, the application of the Weight-of-Evidence method requires landslide factors to be conditional independent of each other. Hence, a chi-square test for checking the conditional independency for each possible pair of landslide factor is performed. In particular, equation 13) is adopted to calculate the number of cells following criteria expressed in Table 2. The chi-square values are calculated at the 99% significance level and 1 degree of freedom, and compared with tabulated values, where calculated chi-square values greater than 6.64 suggest that the pairs are not significantly different. In our study, conditional dependency exists between distance from faults and seismic intensity ($\chi^2 = 9.579$), while geology and distance from faults are conditional independent of each other ($\chi^2 = 0.320$). This means, for example, that the pair distance from faults-seismic intensity should not be used together to map landslide susceptibility. On the contrary, the pair geology-distance from faults could be combined. The whole overview of chi-square outcomes in relation to each pair of landslide factor is provided in Table 4.

Chapter 5: Application of Weight-of-Evidence method

Table 4: Chi-square values for testing pair-wise conditional independency of all factors (99% significance level). Those pairs where conditional dependency is found are highlighted in bold.

	Slope	Aspect	Prof. Curv.	Geology	Dist. Faults	Seismic Intensity
Slope	-	2.943	0.064	6.310	0.600	12.756
Aspect		-	3.115	1.008	1.801	0.741
Prof. Curv.			-	1.466	0.003	0.817
Geology				-	0.320	176.823
Dist. Faults					-	9.579
Seismic Intensity						-

5.2 Weights' calculation

Following the statistical approach described in Chapter Three, the landslide susceptibility analysis is conducted for the Jalal-Abad district in Kyrgyzstan. The choice of this test area is primarily due to the need to find a region where the distribution of landslide factor values is representative of existing relationships for the entire country, while preserving enough variability in these values.

The landslide susceptibility analysis is carried out over a landslide sample consisting of 1,347 landslide locations. Specifically, 50% of the total number of locations is randomly selected from the sample, and then used as the “training dataset”. The remaining 50% is used as the “test dataset” for validating results.

The “training dataset” of landslides is overlaid with each landslide potential factor to calculate weights and the statistical parameters representative of existent spatial relationships (Table 5) by applying equations 5, 6, 9, 10, 11 and 12. As can be seen, the most noteworthy classes of parameters with a positive impact on slope instability are: slope gradient 6° - 16.6° , north-facing slope aspect, profile curvature $-0.00101(1/m)$ – $-0.00005(1/m)$, Mesozoic-aged lithologies, distance from faults greater than 10km, and seismic intensity values (MSK 64) equal to IX. Furthermore, the highest contrasts ($C/S(C)$) values are found for the geology factor, while lowest ones are for profile curvature.

Chapter 5: Application of Weight-of-Evidence method

Table 5: Class, computed weights, variances and contrast values obtained from the application of the Weights-of-Evidence method to the Jalal-Abad study area, Kyrgyzstan.

Factor / Class	total cells	landslide cells	free from landslides cells	W^+	$S^2(W^+)$	W^-	$S^2(W^-)$	C	$C / S(C)$
<i>Slope gradient (°)</i>									
0-6.6	560,923	36	560,887	-0.970	0.028	0.098	0.002	-1.069	-6.235
6.6-16.6	1,144,613	356	1,144,257	0.608	0.003	-0.420	0.003	1.028	13.240
16.6-27.5	1,193,560	250	1,193,310	0.213	0.004	-0.109	0.002	0.321	4.017
> 27.5	1,025,605	25	1,025,580	-1.938	0.040	0.263	0.002	-2.202	-10.801
<i>Slope aspect (°)</i>									
N (337.5 – 22.5)	353,555	84	353,471	0.339	0.012	-0.041	0.002	0.379	3.249
NE (22.5 – 67.5)	364,992	57	364,935	-0.081	0.018	0.008	0.002	-0.089	-0.642
E (67.5 – 112.5)	523,164	84	523,080	-0.053	0.012	0.008	0.002	-0.061	-0.524
SE (112.5 – 157.5)	535,069	84	534,985	-0.076	0.012	0.011	0.002	-0.087	-0.747
S (157.5 – 202.5)	561,148	67	561,081	-0.350	0.015	0.048	0.002	-0.397	-3.085
SW (202.5 – 247.5)	552,571	91	552,480	-0.028	0.011	0.004	0.002	-0.032	-0.287
W (247.5 – 292.5)	602,707	112	602,595	0.093	0.009	-0.018	0.002	0.111	1.068
NW (292.5 – 337.5)	426,817	88	426,729	0.197	0.011	-0.027	0.002	0.224	1.954
<i>Profile curvature (1/m)</i>									
-0.02507 – -0.00101	1,028,255	189	1,028,066	0.082	0.005	-0.031	0.002	0.113	1.310
-0.00101 – -0.00005	934,311	176	934,135	0.107	0.006	-0.036	0.002	0.142	1.617
-0.00005 – 0.00095	947,914	130	947,784	-0.211	0.008	0.059	0.002	-0.269	-2.757
0.00095 – 0.01891	1,028,232	172	1,028,060	-0.012	0.006	0.004	0.002	-0.017	-0.187
<i>Geology(era)</i>									
Cenozoic	1,161,722	203	1,161,519	0.031	0.005	-0.013	0.002	0.045	0.532
Mesozoic	391,100	351	390,749	1.668	0.003	-0.643	0.003	2.311	29.793
Paleozoic	2,382,883	113	2,382,770	-1.273	0.009	0.743	0.002	-2.016	-19.534
<i>Distance from faults(km)</i>									
< 1	522,534	31	522,503	-1.049	0.032	0.095	0.002	-1.144	-6.218
1 – 5	1,586,752	200	1,586,552	-0.295	0.005	0.159	0.002	-0.455	-5.378
5 – 10	970,330	205	970,125	0.221	0.005	-0.084	0.002	0.306	3.642
> 10	834,883	230	834,653	0.487	0.004	-0.185	0.002	0.671	8.241
<i>Seismic Intensity (I)</i>									
I = VII	1,145,958	55	1,145,903	-1.261	0.018	0.258	0.002	-1.519	-10.789
I = VIII	973,285	84	973,201	-0.674	0.012	0.149	0.002	-0.823	-7.055
I = IX	1,816,462	528	1,815,934	0.540	0.002	-0.950	0.007	1.490	15.633

5.3 Landslide susceptibility model

After the weights and statistical parameters of relevance are calculated, landslide factors maps are re-classified according to their positive or negative correlation with landslide locations. A landslide susceptibility zonation map is, hence, obtained by combining previously calculated contrast values with re-classified factors maps based on:

$$LSI = \sum_{j=1}^n C_{ij}, \quad 17)$$

where LSI indicates a Landslide Susceptibility Index and C_{ij} represents the contrast for the i^{th} bin of the j^{th} factor.

6 REGIONAL SLOPE-STABILITY ANALYSIS

6.1 Identification of landslide source areas: seed-points generation

The procedure for the analysis of slope-stability for the entire Central Asian region has the ultimate objective to create an index denoting expected earthquake-induced landslides' destructiveness across the region. Hence, a number of statistical and spatial analysis tools available in the R programming language, in combination with Quantum GIS (QGIS) and GRASS tools, are adopted in order to develop a computational routine and, subsequently, create the landslide hazard index for the whole region (Figure 23).

The first step for the slope-stability analysis is the identification of potential source areas, meaning those areas where slope failures are more likely to originate. This operation is conducted on the basis of previously computed landslide susceptibility values. Specifically, for each investigated country, the landslide susceptibility map is used as the input for the automatized generation of source-locations (points) samples.

The generation of seed points is achieved thanks to the adoption of a collection of QGIS scripts and models developed within the FP-7 SENSUM Project to implement algorithms for generating Focus Maps (SENSUM project, 2014). A focus map is a representation of the spatial “relevancy” with respect to the set of available information, and constraints (SENSUM project, 2014). Based on spatial landslide susceptibility, it is possible to obtain a map defining the spatial density of probability of sampling a location given the level of susceptibility.

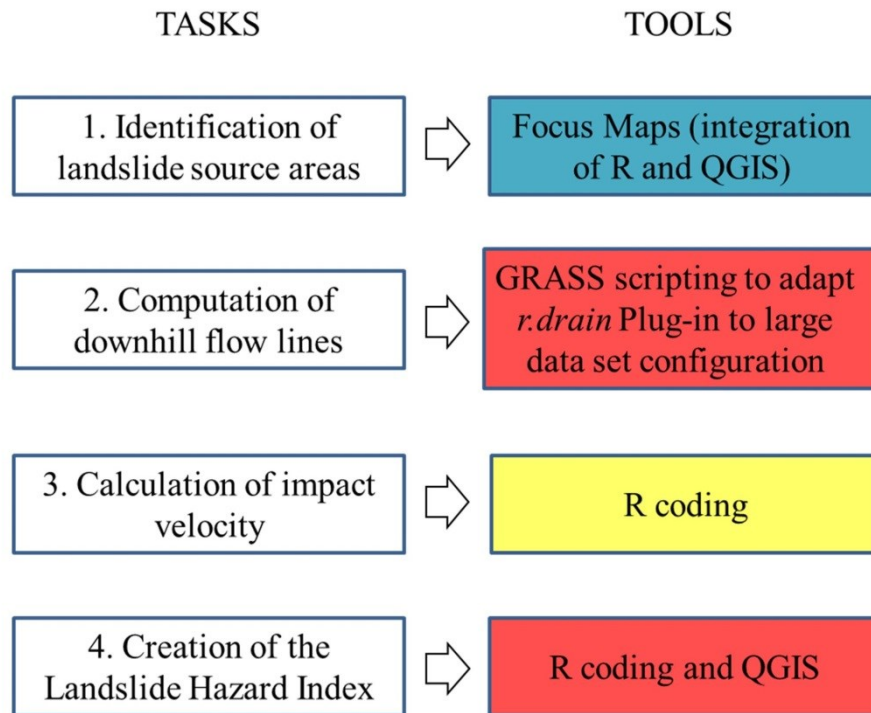


Figure 22: Overview of tasks and related tools used to carry out the landslide hazard analysis. In blue, tools which were made available from the SENSUM project, in yellow scripting tools which were developed ex-novo, in red scripting tools which were prepared to adapt available QGIS tools and to integrate R and QGIS tools, respectively.

In QGIS, the Processing Toolbox environment is used to call native and third-party algorithms by means of a simple graphical interface. In such a geoprocessing environment (Figure 23), tools are subdivided into scripts and models, each referring to a specific scripting type, which are automatically loaded when starting QGIS. In this case, the body of the script is composed of R code. A detailed overview about the installation and use of Focus Maps utilities is provided throughout the SENSUM document Deliverable 3.4.

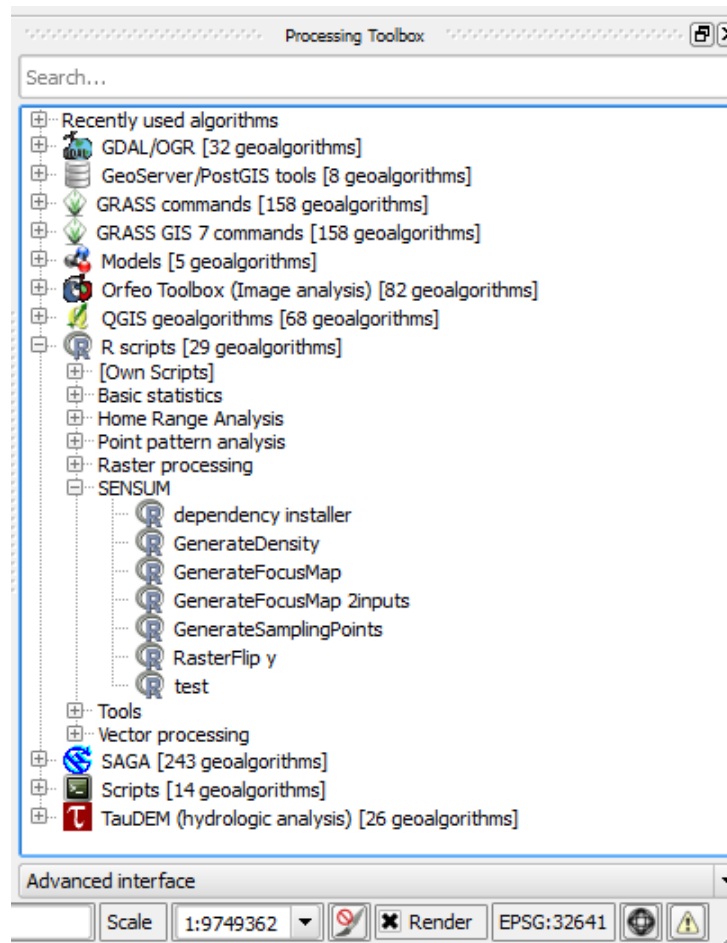


Figure 23: The QGIS Processing Toolbox, showing several available scripts. In particular, the SENSUM set of tools which are used to generate seed-points for landslide hazard analysis is shown.

In particular, the raster map corresponding to the landslide susceptibility map is used as the spatial density distribution layer, and a scaling coefficient is adopted to control the final number of seed points. Due to computational constraints, the scaling factor is set equal to 0.1, allowing for the generation of a total of 1675156, 879899, and 3713918 points for Kyrgyzstan, Tajikistan and Uzbekistan, respectively (Figure 24). In the end, a specific function calling for an inhomogeneous Poisson Point Process, allows for the generation of points, based on input prior landslide susceptibility.

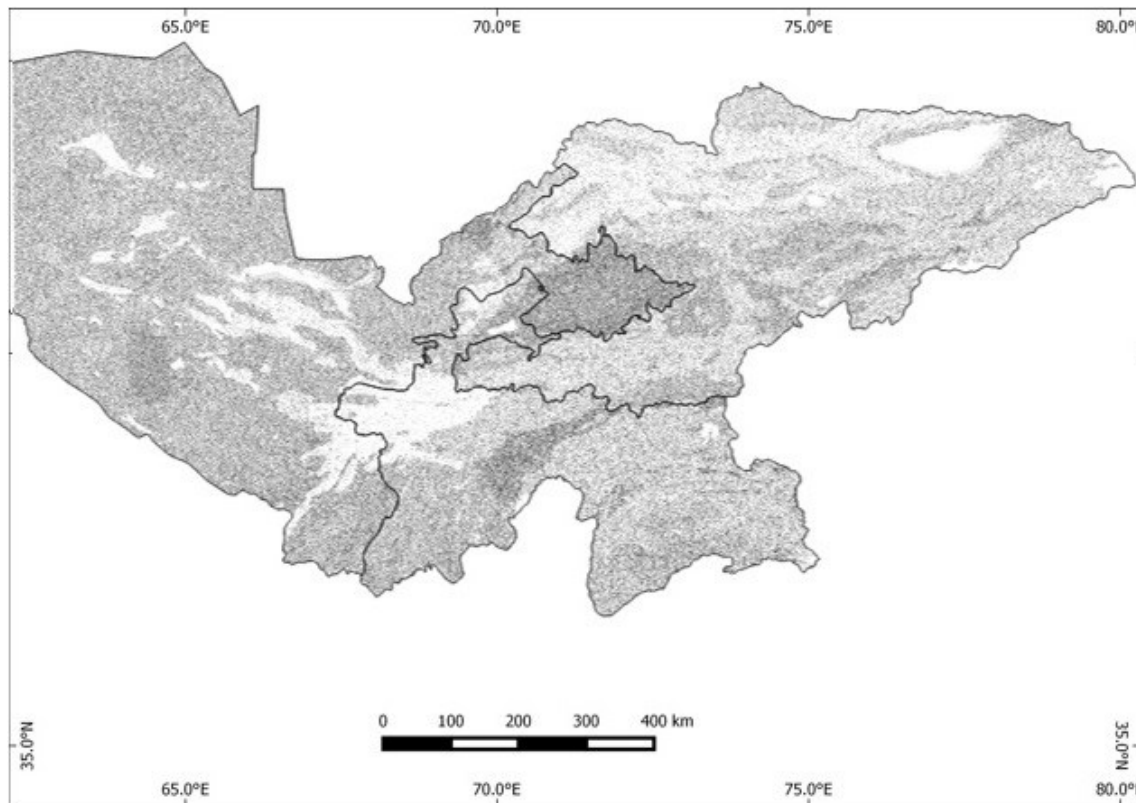


Figure 24: Distribution of source-location points for the countries of Kyrgyzstan, Tajikistan, and Uzbekistan. Dark areas indicate high density of points, in agreement with high landslide susceptible areas. On the contrary, light areas represent low density of points, in agreement with low landslide susceptibility levels.

6.2 Computation of downhill flow lines

Next, source points are used to calculate surface trajectories of hypothetical punctual masses during their downhill movements across mountain slopes. This task is achieved by means of the *r.drain* GRASS plug-in combined with R coding. By taking an elevation model as the input raster layer, *r.drain* is iteratively used to calculate flows corresponding to least-cost paths at user-provided locations (a coordinate parameter is specified). Each path is computed by choosing the steeper slope between adjacent cells. It should be noted that *r.drain* currently finds only the lowest point in the input file that can be reached through directly adjacent cells that are less than or equal in value to the cell reached immediately prior to it; therefore, it will not necessarily reach the lowest point in the input file.

Although multiple starting points can be provided, a maximum of 1024 starting points can be used as input to *r.drain*. Therefore, for each country, the large seed-points sample is initially split into smaller subsamples, each having 900 points. Flow lines are subsequently obtained by means of an automatized procedure through GRASS command line scripting. Specifically, the procedure includes the following steps:

- Importing the elevation model (raster format) together with sub-samples of starting points (vector format) as the needed input to *r.drain*;
- Saving *r.drain* output flow lines, including the assignment of an identifier (ID) to each output;
- Extracting nodes from computed flow lines (being the row format of “line” type);
- Adding geometric attributes to each retrieved node, maintaining the consistency with the original projected reference system of elevation model.

6.3 Calculation of impact velocity

After having retrieved coordinates of points delineating downhill surface trajectories, the associated impact velocity is determined, starting from observed mass acceleration (eq. 15). It is assumed a friction angle (ϕ) equal to 30° , a value which is commonly found for loose sand materials, and friction coefficient (μ) equal to $\tan(\phi)$. For the calculation of mass acceleration, α represents the slope angle and g the acceleration due to the gravity. For each trajectory, the distance between adjacent points is computed (ds), based on the corresponding cell sizes defined from the projected reference system: 72.921m, 77.668m, 74.574m, for Kyrgyzstan, Tajikistan, and Uzbekistan, respectively.

Let's consider the case of a 4-point trajectory (Figure 25), calculated in Kyrgyzstan. At point $[x_1, y_1]$, mass acceleration is equal to $a_1 = g(\sin\alpha_1 - \mu\cos\alpha_1)$, while its initial velocity is null ($v_1 = 0$). Once downhill movement of the point mass starts, its mass acceleration and velocity values will correspondingly change, following Newton's laws of motion. At point $[x_2, y_2]$, the point mass will hence have acceleration $a_2 =$

$g(\sin\alpha_2 - \mu\cos\alpha_2)$, and velocity $v_2 = v_1 + a_1 dt_1$ (given that $v = v_0 + at$), dt_1 being the time to cover the distance ds_1 (known from the Digital Elevation Model's resolution: $\sim 103\text{m}$). Since $ds_1 = v_1 dt_1 + 0.5a_1(dt_1)^2$ (given that $ds_1 = v_1 dt_1 + 0.5a_1(dt_1)^2$), it turns out that $dt_1 = \sqrt{2ds_1/a_1}$. Similarly, in order to reach the point $[x_3, y_3]$, the point mass will cover ds_2 (known from the Digital Elevation Model's resolution: $\sim 73\text{m}$), with a velocity $v_3 = v_2 + a_2 dt_2$, and a travel time $dt_2 = (-v_2 + \sqrt{(v_2)^2 + 2ds_2a_2})/a_2$.

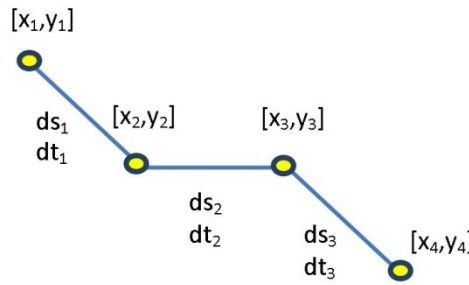


Figure 25: Exemplification of punctual modeling of downhill velocity. Details on the values assumed by the variables are provided in the text.

Under this physical framework, the impact velocity of sliding point masses is then calculated for each single point of the downhill retrieved flow lines. R coding has shown a better time computation efficiency, the reason why it is used to perform all necessary calculations. Specifically, for the entire territory of Kyrgyzstan, Tajikistan, and Uzbekistan, a data frame spatial object including attributes for each point is constructed, with a total number of 275876, 258779, and 933810 points, for Kyrgyzstan, Tajikistan, and Uzbekistan, respectively. Each velocity value is calculated between consecutive points belonging to the same trajectory (hence having, the same identifier field).

Figure 26 shows an example of the calculations for the country of Kyrgyzstan. In this figure, each observation refers to a prior modeled flow line identified by means of “cat” column name, where the “cat” label stands for category. “x” and “y” attributes indicate

the longitude and latitude for each observation, while the “slope” attribute is converted from degrees to radians, in order to make practicable the calculations in R; mass acceleration (“acc”) of rapid moving materials is sub-sequentially calculated as a function of slope angle, gravity acceleration, and coefficient of friction values. Distances (“ds”) and expected travel times (“dt”) between consecutive points, are then used to retrieve velocities values (“vel”). “ds” attribute field can take on a value either equal to 72.921 m (vertical or horizontal path) or to 103.126 m (diagonal path), in agreement with the Digital Elevation Model’s resolution in Kyrgyzstan. It should be noted that, at the source-location point corresponding to the first point in flow line, the impact velocity is null.

	cat	x	y	slope	acc	ds	dt	vel
1	1	809793.8	4644723	0.47529885	2.8806417	0.00000	0.00000	0.00000
2	1	809720.8	4644796	0.31910103	1.3598773	103.12583	12.31541	16.74745
3	1	809720.8	4644869	0.24292245	0.6038443	72.92098	15.54099	9.38434
4	2	603281.6	4482838	0.45741526	2.7093944	0.00000	0.00000	0.00000
5	2	603281.6	4482911	0.30131021	1.1838578	72.92098	11.09919	13.13987
6	2	603354.5	4482984	0.11501789	0.6711771	103.12583	17.52993	11.76569
7	2	603427.4	4483057	0.04816967	1.3345088	103.12583	12.43191	16.59050
8	3	278637.4	4618107	0.50843926	3.1955066	0.00000	0.00000	0.00000
9	3	278710.3	4618107	0.36470297	1.8089580	72.92098	8.97898	16.24260
10	3	278783.2	4618107	0.28549483	1.0270666	72.92098	11.91631	12.23885

Figure 26: Extract of R object data frame (first 10 observations). “cat” attribute (standing for category) identifies the points belonging to the same flow line; “x” and “y” columns correspond to longitude and latitude, respectively; the “slope” attribute is expressed in radians; “acc” and “vel” are in m/s^2 and m/s , respectively; “ds” and “dt” represent the distance and travel time between consecutive points of the same flow line, in meters and seconds, respectively.

6.4 Creation of the Landslide Hazard Index (LHI)

The creation of the Landslide Hazard Index (LHI) map is accomplished by means of the following steps:

- Interpolation of velocity values over the entire region;
- Application of a slope threshold to results;
- Quantile classification of velocity values.

It has to be remarked that, due to computation constraints, information concerning the impact velocities of potential slope failures relate only to 10% of maximum achievable sampling points (see section 6.1 for more details). For this reason, a point-by-point physical modeling of the expected impact velocities is not obtained. However, seed-point samples adopted for the physical modeling are properly scaled to the national landslide susceptibility input information, and are hence considered representative of the overall relationships between landslide potential and geometrical slope configuration.

In order to retrieve the distribution of the impact velocities of the modeled landslides over a regular grid of points adjusted to the Digital Elevation Model's resolution, a spatial interpolation over the entire region covering Kyrgyzstan, Tajikistan and Uzbekistan is carried out. The Interpolation plugin in QGIS is used to generate an Inverse Distance Weighted (IDW) interpolation of the impact velocity vector layer, together with a raster layer preserving spatial extent and resolution of the map. The computation is performed by averaging the values of data points in the neighborhood of each processing cell, being a 10km-sized cell. The outcomes of the interpolation in raster format show an overall distribution of impact velocities, with values ranging between 11.692.–39.128 m/s, for the entire Central Asian region.

Afterwards, a slope threshold is applied over the entire region in order to limit velocity values to areas where slope is greater than 6 degrees, under the assumption that slope failures do not occur for slope gradient values lower than 6 degrees. For this specific step, the Raster Calculation tool in GIS is adopted to multiply the output raster map of interpolation velocity values by a user-defined raster map accounting for the slope threshold. The distribution of impact velocity values can be visualized in Figure 27. Finally, impact velocity values are classified into 4 sub-classes, based on the quantile scheme.

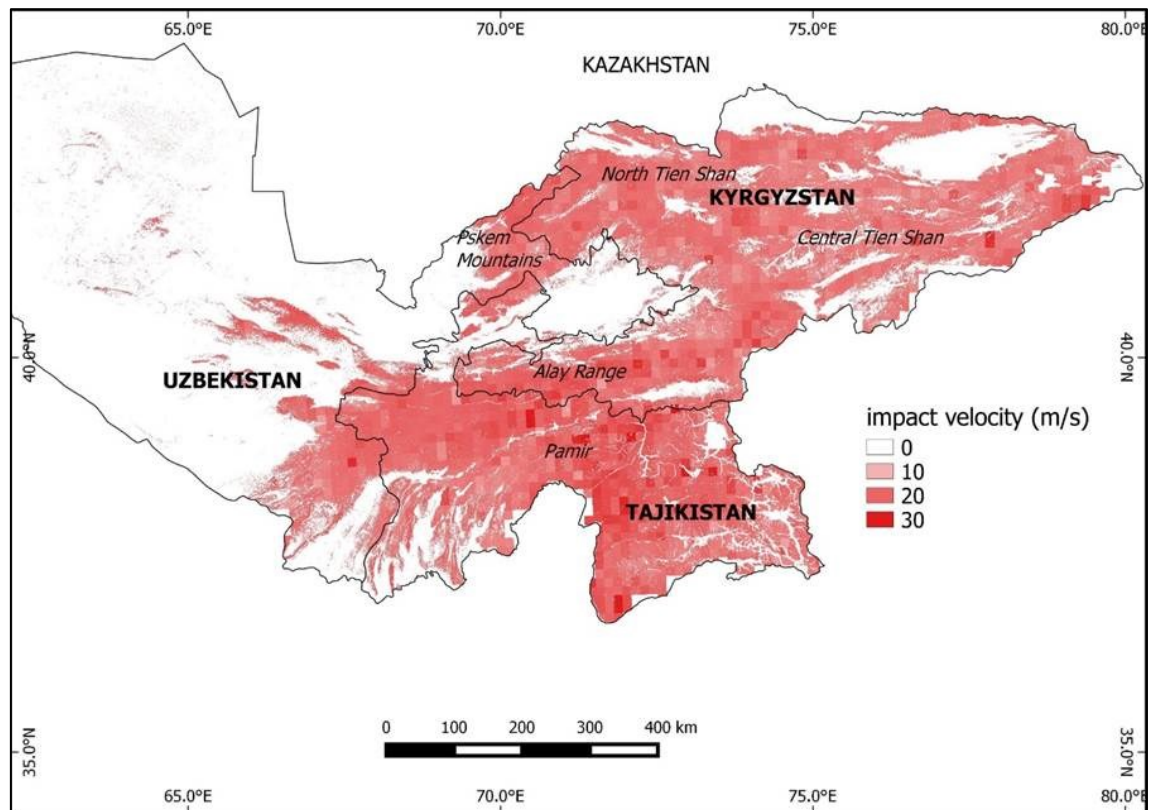


Figure 27: Distribution of impact velocity values for Kyrgyzstan, Tajikistan, and Uzbekistan, after the interpolation and the application of the slope threshold.

7 RESULTS AND VALIDATION

7.1 Landslide susceptibility results and validation

Following the approach explained in Chapter Five, landslide susceptibility maps are created by combining weighted landslide factors maps. Specifically, maps are prepared by combining those landslide factors which are found to exhibit conditional independency of each other (Table 6). In this way, the influence of choosing a certain combination of landslide factors to map susceptibility can be investigated. Additionally, the susceptibility model obtained by considering all factors together is considered (Table 6).

Table 6 : Four possible landslide susceptibility models of independent factors, based on the outcomes of the chi-square test, which has been described in Chapter 5. Additionally, the model resulting by the combination of all factors is considered.

Model A	Model B	Model C	Model D	Model E
Slope	Aspect	Prof. curvature	Aspect	Slope
Aspect	Prof. curvature	Geology	Prof. curvature	Aspect
Prof. curvature	Geology	Distance from faults	Seismic Intensity	Prof. curvature
Geology	Distance from faults			Geology
Distance from faults				Distance from Faults
				Seismic Intensity

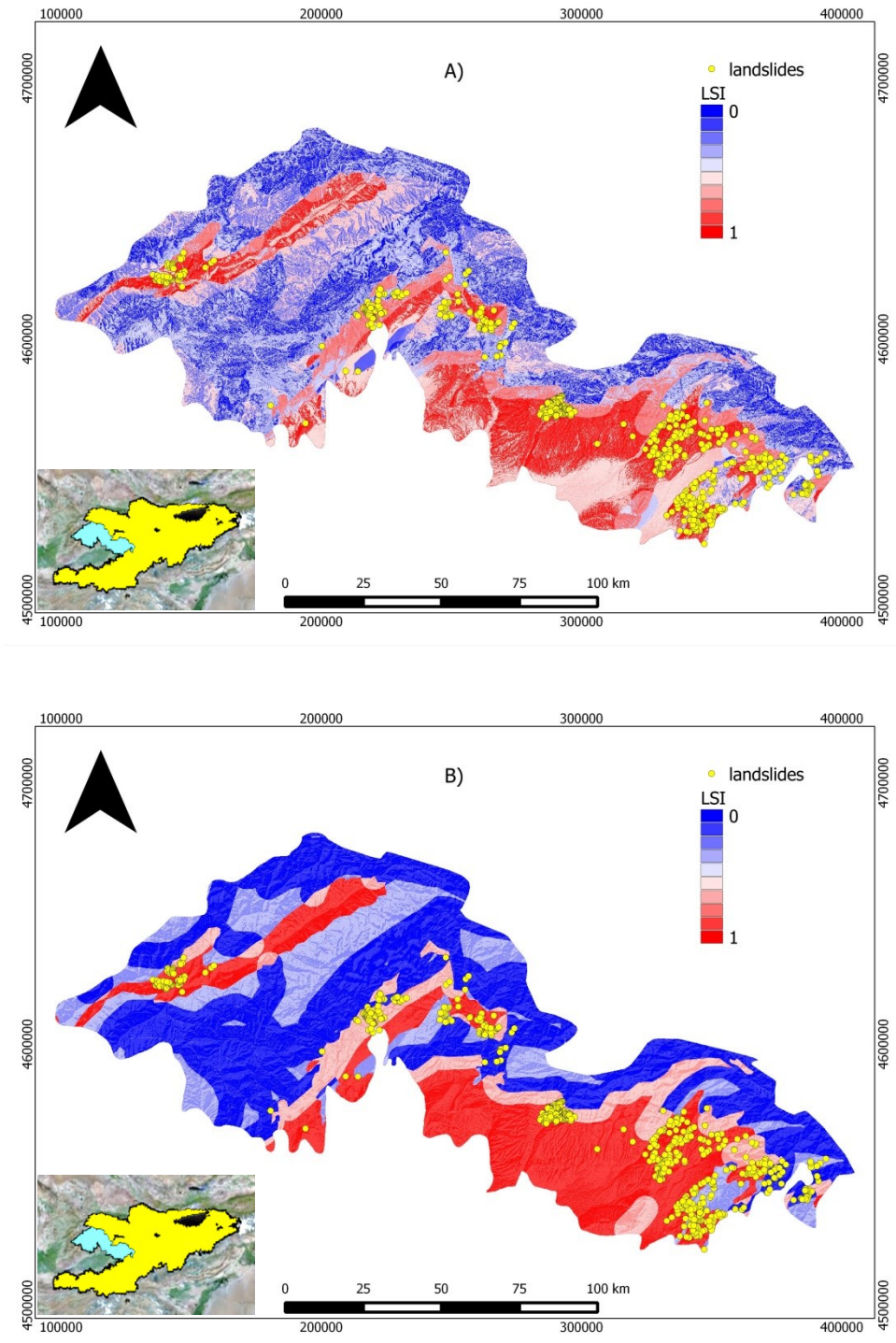


Figure 28: Landslide Susceptibility Index (LSI) maps for the Jalal-Abad study area, Kyrgyzstan, based on the combinations of conditional independent factors (Model A, B, C, D), and a combination of all factors (Model E, as outlined in Table5). Specifically, Model A is derived from the combination of slope, aspect, profile curvature, geology, and distance from faults factors, while Model B is from the combination of aspect, profile curvature, geology, and distance from faults factors. Normalized susceptibility values are shown. The yellow circles indicate previous landslide locations (training dataset in Figure 14).

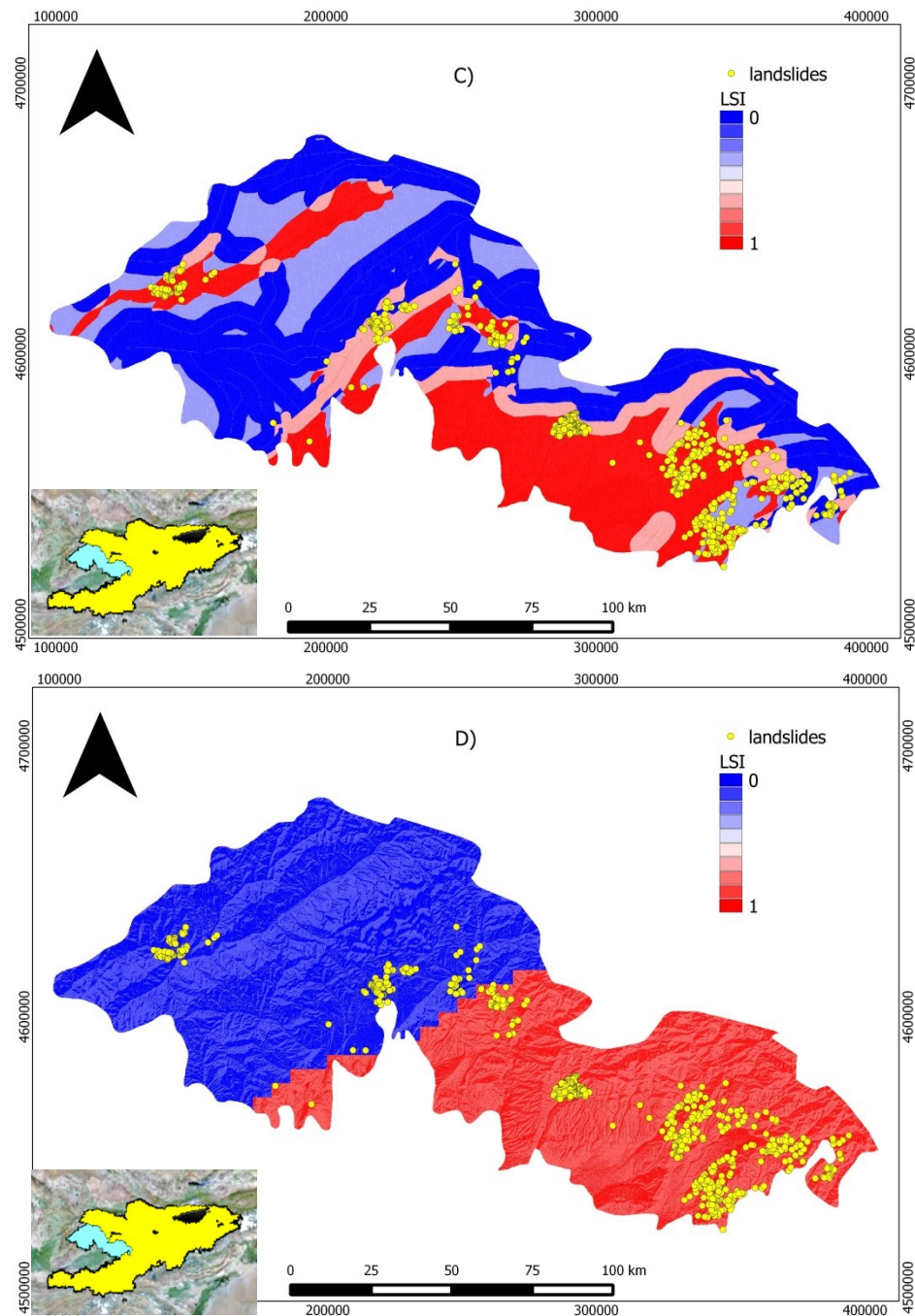


Figure 28 continued. Model C is derived from the combination of profile curvature, geology, and distance from faults factors, while Model D from the combination of aspect, profile curvature, and Seismic Intensity factors.

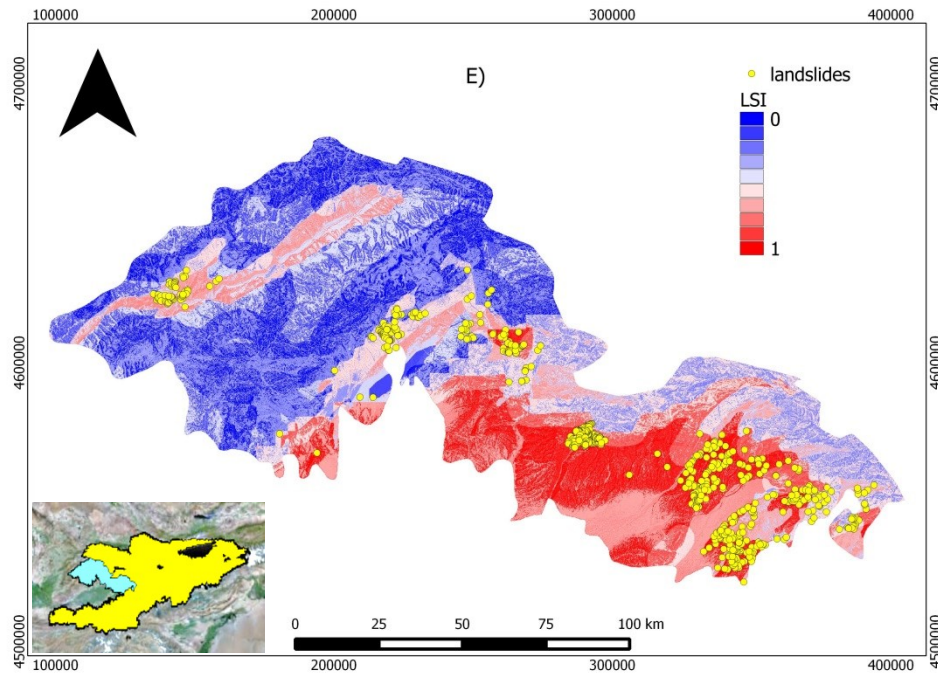


Figure 28 continued. Model E is derived from the combination of all the factors, being slope, aspect, profile curvature, geology, distance from faults, and Seismic Intensity factors.

The result of the summation is a continuous interval of values ranging from -6.720 to 4.531 (Model A), from -3.771 to 3.503 (Model B), from -3.438 to 3.124 (Model C), from -2.848 to 2.011 (Model D), and from -9.062 to 6.021 (Model E), indicative of various degrees of landslide susceptibility. Normalized values are calculated by dividing the difference between a value and the minimum result by the maximum minus the minimum, allowing them to take on values between 0 and 1: from 0.033 to 0.955 (Model A), from 0.060 to 0.945 (Model B), from 0.087 to 0.932 (Model C), from 0.103 to 0.903 (Model D), from 0.016 to 0.971 (Model E). Afterwards, susceptibility values are classified into 10 equal-sized sectors corresponding to different levels of susceptibility (Figure 28).

In particular, it can be observed (Figure 28) that high LSI levels are present in the southern area, precisely along the eastern border of Fergana valley, where slope values mostly range from 0.0° to 16.6° , and the majority of past landslides are also distributed. In addition, high landslide susceptibility are recognized across the Jalal-Abad province region, though the lack of landslide observations. This latter result might indicate the

potential for landslide activation and, therefore, serve as input when estimating landslide risk.

To check the predictive capabilities of any model, an essential requirement is to carry out a validation of the results. Without some kind of validation, such results are useless since they lack knowledge of the degree of confidence in the model, a crucial element for transferring results to end users and stakeholders (Chung & Fabbri, 2003).

Cross-validation is commonly used for assessing the capability of results from a statistical analysis to be generalized to an independent data set. The procedure consists of partitioning a sample of data into complementary subsets. The analysis is, then, performed on one subset – named the “training set”, and the validation carried out on the other subset – named the “test set”.

In the field of landslide hazard assessment, the cross-validation of the results is commonly carried out by partitioning the data in time or in space (Chung & Fabbri, 2003). When the temporal approach is chosen, landslide occurrences are subdivided into two subsets referring to different time periods, typically named “past” and “future” landslides. This approach is meant to construct the prediction model based on “past” occurrences and then to validate the results with respect to “future” ones. When temporal information is missing, spatial robustness validation is commonly applied.

The validity and accuracy of landslide susceptibility maps are typically ascertained with the help of success- and prediction-rate curves in combination with the area under the curves. The curves provide information about the relationship between the proportion of area identified as being landslide susceptible and the actual landslide occurrences. In particular, success-rate curves show how good the susceptibility model is in fitting the already occurred landslides, while prediction-rate curves provide quantitative information about landslides that might occur in the future. The area under the curve provides a measure of the total accuracy based on the rate curves, where a total area equal to one indicates perfect accuracy. The common procedure consists of sorting in descending order the calculated index values that refer to the total number of cells in the study area. Landslide susceptibility results are hence cross-tabulated with landslide locations and presented as a cumulative frequency diagram.

When comparing the landslide training dataset with landslide susceptibility maps, 77.211%, 60.420%, 57.721%, 79.160%, and 68.966% of landslides are found in the 20% of highest susceptibility classes of model A, B, C, D, and E, respectively. Related accuracy values are equal to 0.794, 0.734, 0.723, 0.686, 0.805 (Figure 29a). On the other hand, comparing the landslide test dataset with the five landslide susceptibility models, 75.537%, 60.299%, 58.060%, 79.104%, and 66.119% of landslides are found in the 20% of highest susceptibility classes of model A, B, C, D, and E, respectively. Correspondent accuracy values are equal to 0.788, 0.733, 0.715, 0.691, 0.801 (Figure 29b).

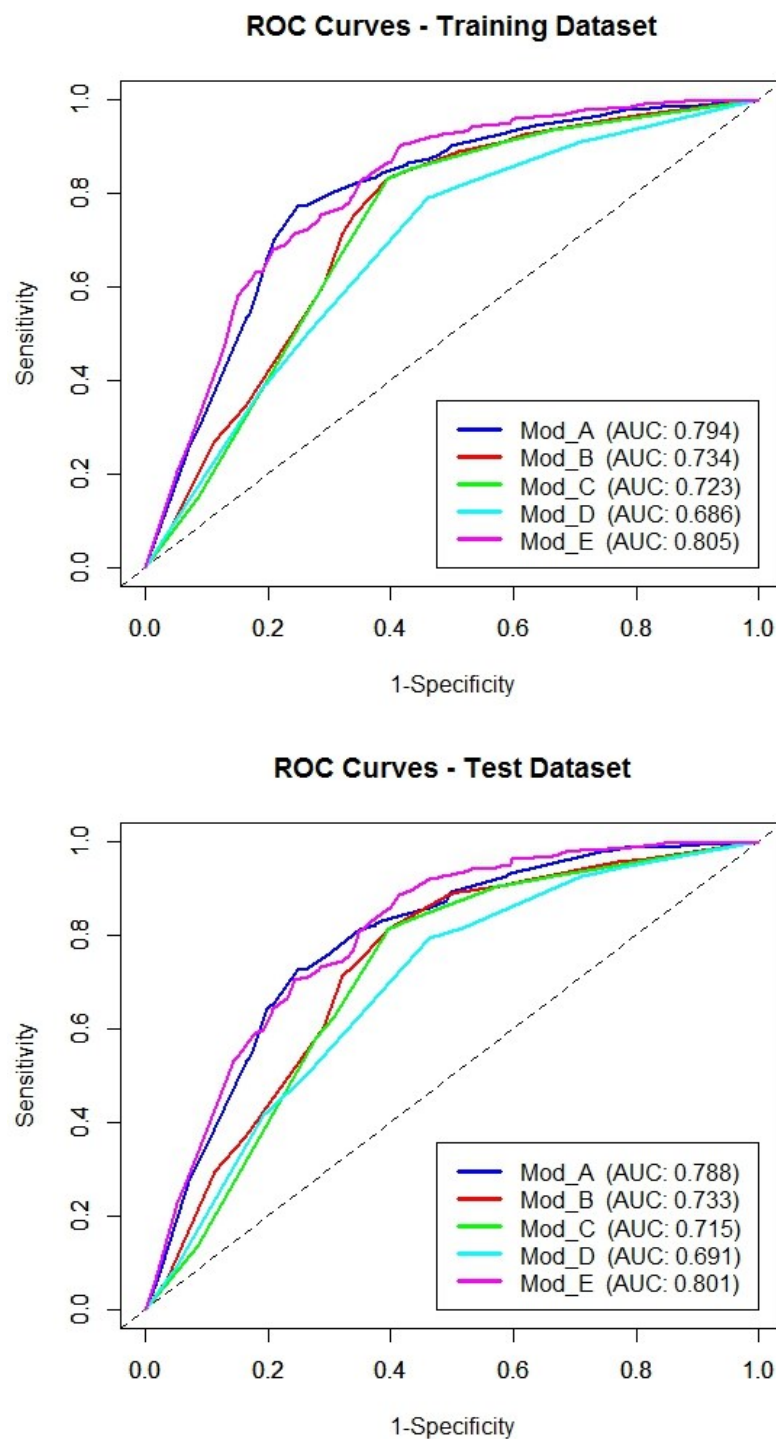


Figure 29: Accuracy assessment of landslide susceptibility models for training (a) and test (b) databases, respectively. Receiving Operating Characteristic Curves (ROC) are used to check the validity and accuracy of landslide susceptibility models.

7.2 Landslide susceptibility map for Central Asia

Based on the accuracy assessment, the landslide susceptibility model calibrated for Jalal-Abad region can be considered reliable as the input landslide factors are good indicators of existing variability conditions. In particular, Model E (Figure 29) shows the highest accuracy ($AUC = 0.800$), and is hence used as the basis for extension to the territories of Kyrgyzstan, Tajikistan and Uzbekistan. For this scope, landslide factors are re-classified and weighted, following the above described procedure. In particular, values are normalized and classified into 10 equal-interval classes, ranging from 0.016 to 0.971.

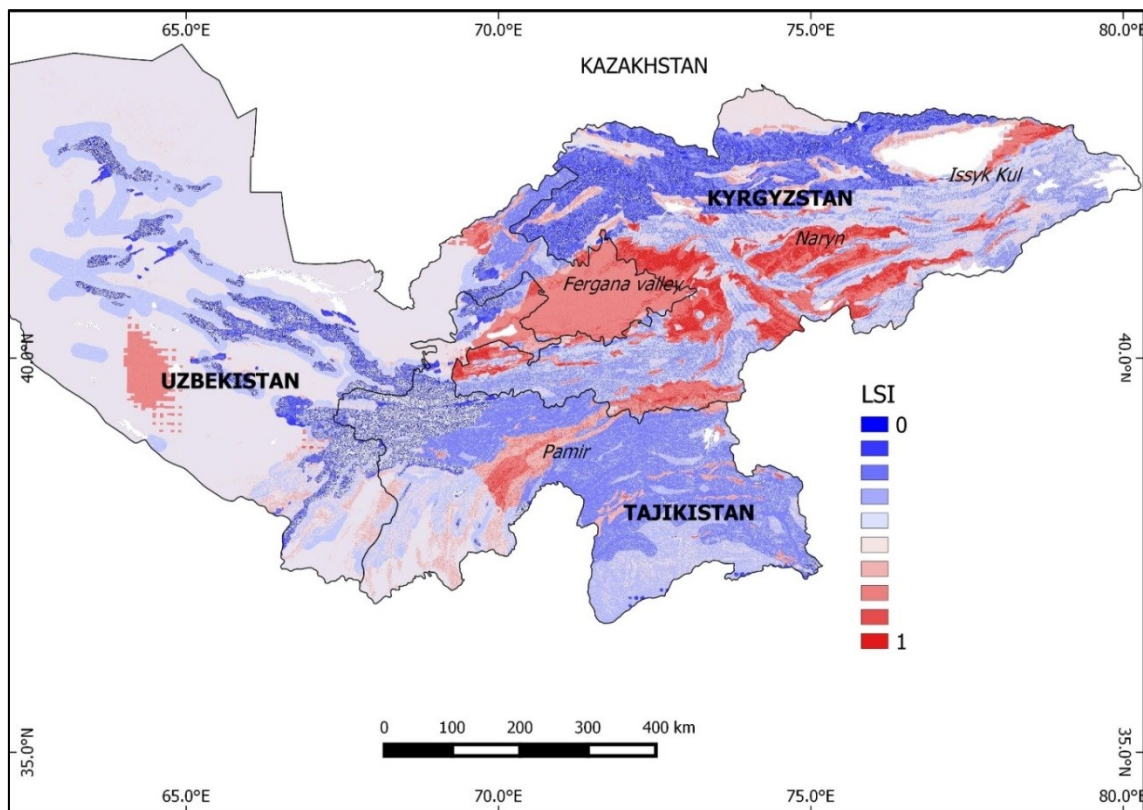


Figure 30: Landslide Susceptibility Index (LSI) map for Kyrgyzstan, Tajikistan and Uzbekistan calculated with respect to (Model E, Table 5) slope gradient, slope aspect, profile curvature, geology, distance from faults, and seismic intensity factors. Normalized susceptibility values are shown.

The resulting cross-border landslide susceptibility map (Figure 30) shows where landslides are preferentially triggered by earthquakes within seismically active Central Asia mountain belts. The map emphasizes the relatively high potential for landslides over the entire territory of Kyrgyzstan, specifically along the eastern boarder of the

Fergana valley, in the South of Talas province, and in the Issyk-kul district. It has to be noted that high levels of susceptibility can be found in the Naryn province where the conditions for slope failures exist though the scarce occurrence of past landslides. A general low level of landslide susceptibility can be observed for almost the entire territory of Uzbekistan. This outcome is plausible given the prominence of flat and desert areas. Exceptions are represented by the Tashkent and Buhkara provinces, which are characterized by high and medium levels of landslide susceptibility, respectively (Figure 30). With regard to the Tajik territory, high levels of landslide susceptibility are expected in the central districts of Tojikobod and Nurobod (Figure 30), in the proximity to the devastating 1949 Khait (Evans et al., 2009).

7.3 Landslide hazard index (LHI) map for Central Asia

This section presents results relative to landslide hazard analysis, obtained by following the procedure described in Chapter Six.

The Landslide Hazard Index (LHI) map (Figure 31) indicates the expected level of hazard due to the activation of slope failures across the Central Asian region. The map shows a relatively high level of hazard where the slope gradient is also relatively high. In particular, highest hazard values are mainly shown along the Alay Range and the Pamir, in Kyrgyzstan and in Tajikistan; relatively high hazard values can also be observed along the North and Central Tien Shan in Kyrgyzstan, in the Pskem Mountains in Uzbekistan.

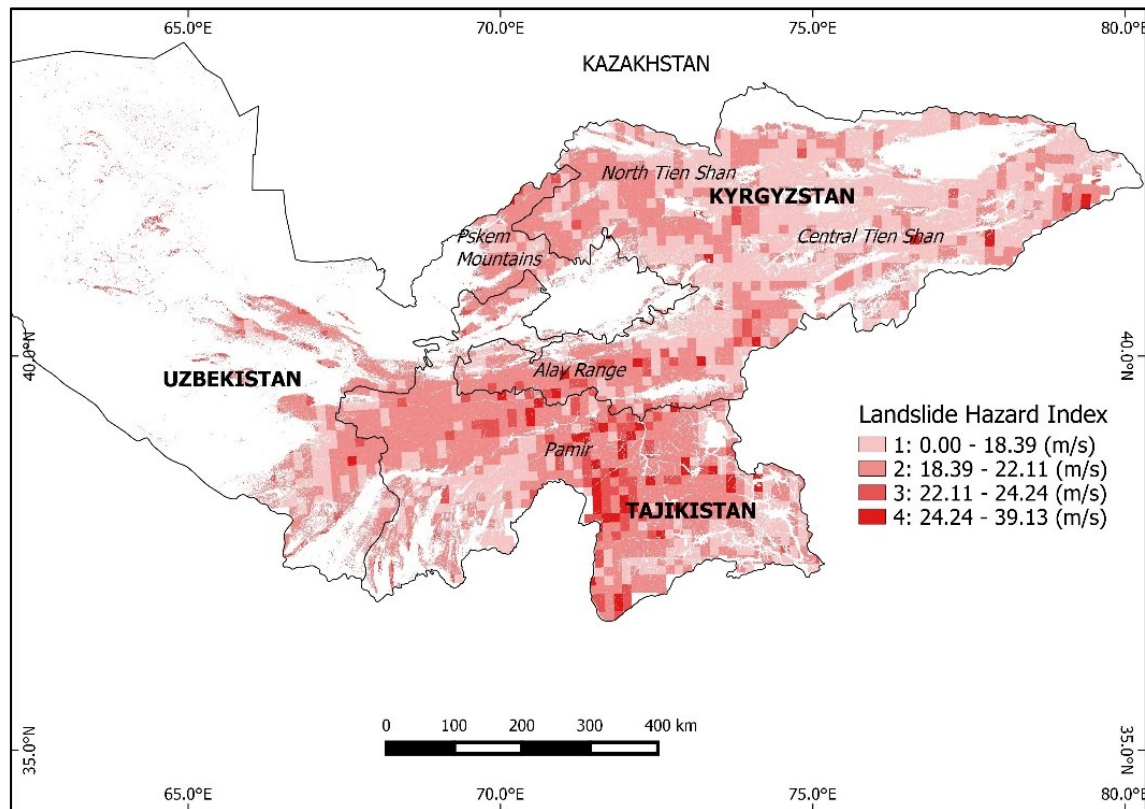


Figure 31: Landslide Hazard Index (LHI) map for the countries of Kyrgyzstan, Tajikistan, and Uzbekistan. The map shows hazard level due to the impact velocity of slope failures across the region. Normalized values are shown.

7.4 Landslide risk map for Central Asia

The risk analysis is achieved by combining the population density map with the landslide hazard index map. As far as the vulnerability component is concerned, a binary function is considered so that vulnerability takes on a value equal to '0', in absence of exposure, and a value equal to '1', in presence of exposure. Both the population density and landslide hazard index maps are initially classified into 4 subcategories, following a quantile classification scheme (Figure 32).

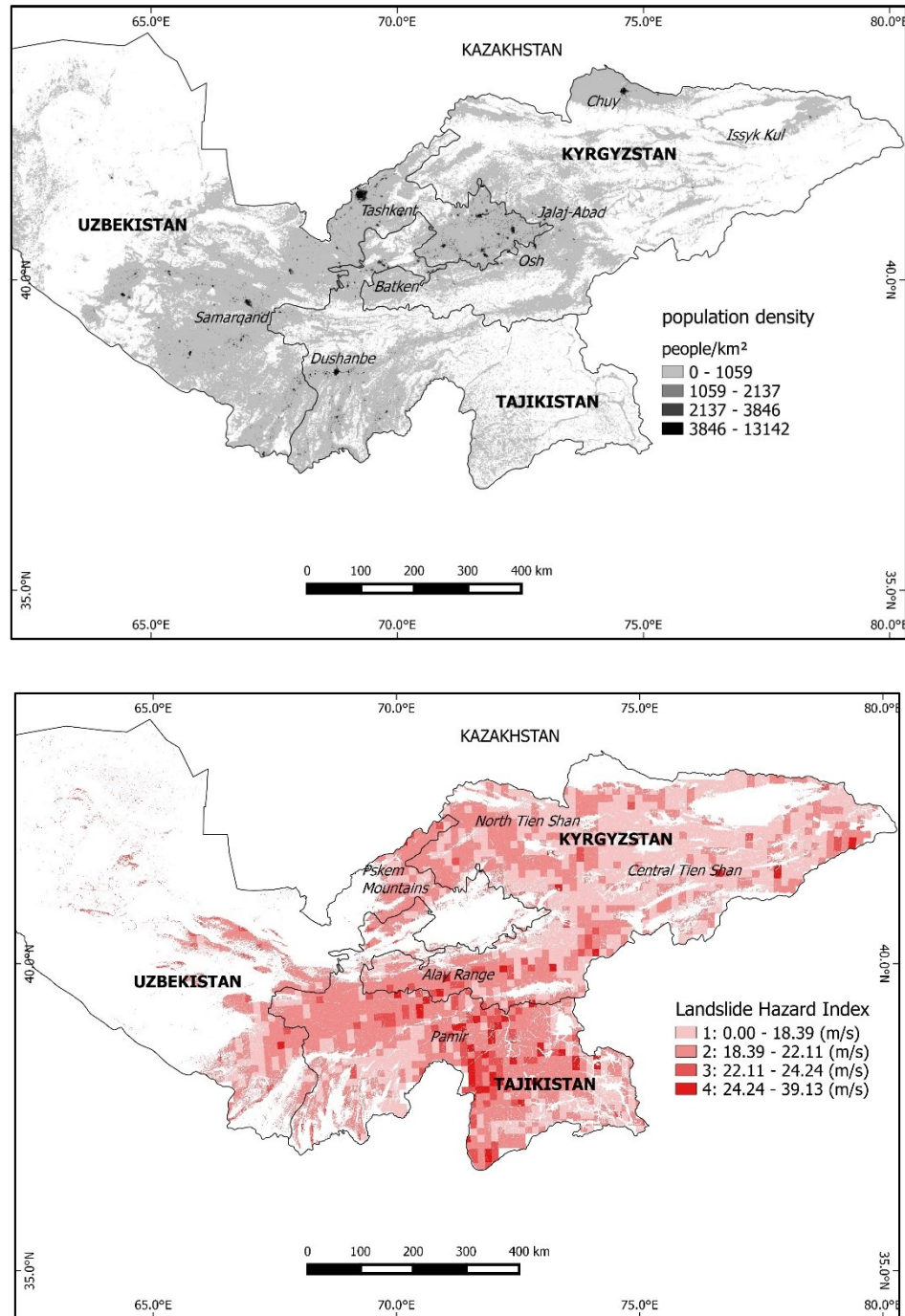


Figure 32: Population density map (top) and landslide hazard index map (bottom) for Kyrgyzstan, Tajikistan and Uzbekistan. A quantile classification scheme has been chosen to categorize values into 4 bins, being 0 – 1059, 1059 – 2137, 2137 – 3846, > 3846 (people/km²), for population density, and 0 – 18.39, 18.39 – 22.11, 22.11 – 24.24, 24.24 – 39.13 (m/s), for landslide hazard index map.

Afterwards, a class-by-class multiplicative method is used to obtain the final landslide risk map. Hence, class 1 of landslide hazard index is multiplied by class 1 of population density returning a value equal to 1, class 1 of landslide hazard index is multiplied by class 2 of population density returning a value equal to 2, and so on. Final values are visualized in form of a matrix, where values ranging between 1 and 2 (shown in yellow) indicate ‘low level’, values ranging between 3 and 6 (shown in light orange) indicate ‘medium level’, values ranging between 8 and 9 (shown in dark orange) indicate ‘high level’, and finally values ranging between 12 and 16 (shown in red) indicate ‘very high level’ (Figure 33). As part of the classification, proportional dependency between population density and expected people vulnerability is assumed, which in turn results in assigning a high level of risk to highly populated areas.

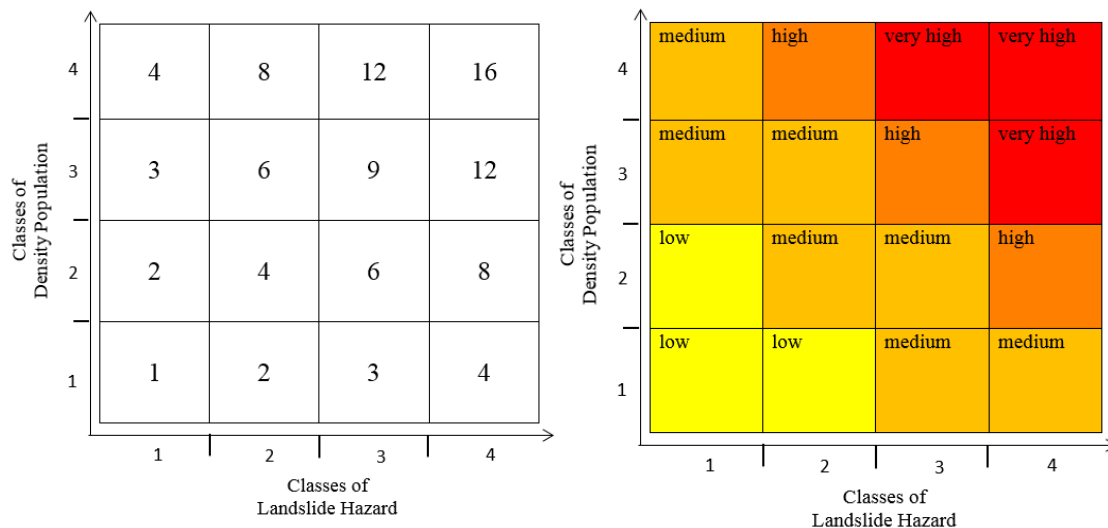


Figure 33: Class-by-class multiplicative approach which has been applied to prepare the landslide risk map. First, each class of Landslide Hazard Map is multiplied by each class of Density Population Map (right); afterwards, values are classified into ‘low’, ‘medium’, ‘high’, and ‘very high’ level (right).

The final outcome is, hence, a map showing 4 different levels of risk due to landslide occurrences across the territory of Kyrgyzstan, Tajikistan and Uzbekistan (Figure 34). As can be seen from the map, a very high level of risk is locally expected in the Jalal-Abad and Osh provinces, Kyrgyzstan, in the Gorno-Badakhshan region near the urban areas of Khorugh and Murghab, Tajikistan, and in the Kashkadarva region, Uzbekistan. Moreover, a high level of risk can be observed for several areas, i.e., those located in the

proximity of Fergana Valley and Jalal-Abad areas in Kyrgyzstan, being highly densely populated areas. A medium level of risk can be identified in the Tashkent province in Uzbekistan. Although the urban area of the city is not at risk, a certain level of risk is expected in the surrounding area proximal to the Pskem Mountains, due to the contribution of vulnerability in the final risk calculation. On the other hand, there is a low-medium level of risk extensively distributed across Kyrgyzstan, Tajikistan, and Uzbekistan, primarily due to the presence of small settlements (having a population density in the order of 1000 persons/km²) exposed to significant landslide hazard. Besides, areas in white correspond to bodies of water and unpopulated areas, mainly the mountain regions of the North and South Tien Shan, the Pamir, and the Kyzylkum desert, for which the risk of having landslide-induced damage is null.

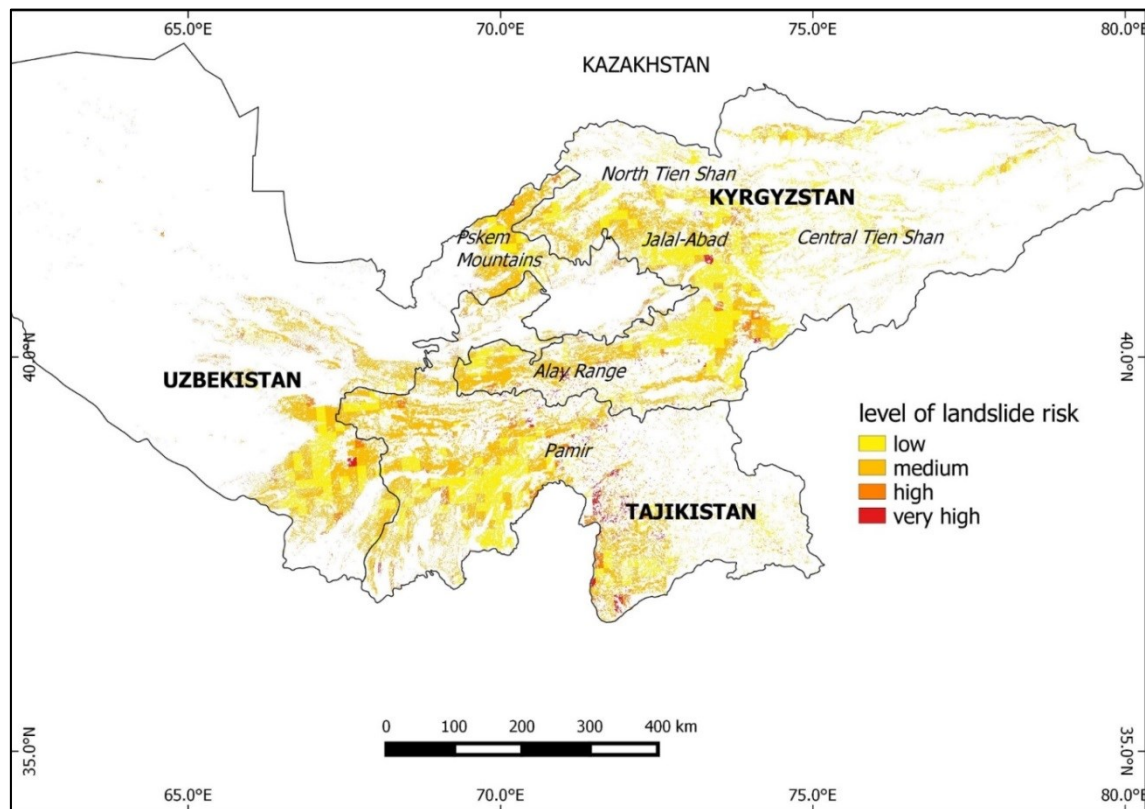


Figure 34: Risk map of earthquake-induced landslides for Kyrgyzstan, Tajikistan and Uzbekistan. The map shows the expected level of damage due to the occurrence of landslides having a certain impact velocity across the region. Specifically, 4 levels of risk are shown: low, medium, high, and very high.

8 DISCUSSION

The analysis of landslide susceptibility results reveals that the most influential factors to slope instability, sorted according to their values of contrast, are: the class of Mesozoic materials, the class IX of seismic intensity, the class $6.6^{\circ} - 16.6^{\circ}$ of slope gradient, distance from faults greater than 10km, the class $292.5^{\circ} - 22.5^{\circ}$ of slope aspect, and the class $-0.00101 - -0.00005$ of profile curvature. In addition, the classes linked to the highest slope stability probabilities are: the class of Paleozoic materials, the class of slope gradient greater than 27.5° , the class VII of seismic intensity, distance from faults less than 1km, the class $157.5^{\circ} - 202.5^{\circ}$ of slope aspect, and the class $-0.00005 - 0.00095$ of profile curvature.

Precisely, relatively high slope values do not imply landslide occurrence, in agreement with the existing evidence (Havenith et al., 2006) that most landslides in Kyrgyzstan occur on relatively low slope angles ($< 20^{\circ}$). Clearly, a relatively low slope angle is associated with the presence of soft materials due to their mechanical properties.

With regard to slope aspect, small contrast values clearly indicate the partial contribution of this factor in the landslide susceptibility analysis. Nevertheless, the presence of southwest monsoon winds, might make south-facing slopes relatively wet and undisturbed, while leaving north-facing slopes drier, less vegetated, and, consequently more exposed to landslide phenomena. In agreement with this statement, similar evidences have already been provided for Central Asia (Strom, 2013).

Most of past landslides are linked to negative values of profile curvature, which correspond to convex-shaped slopes. Although having small contrast values, the control of convex morphologies to slope instability can be explained with local seismic amplification phenomena occurring in topographic ridges.

The influence of geology is also clear, since there is an increase in the contrast values from the older geological units to the more recent ones. This agrees with the fact that, especially in the northern Kyrgyzstan (Kalmetieva et al., 2009), most landslides are found on Quaternary materials. A relatively high degree of rock fracturing might be responsible for the occurrence of slope failures in Mesozoic rocks, as revealed by the high contrast values. On the other hand, it is clear that Palaeozoic materials have no connection with landslide initiation. It has to be remarked that the distribution of geological materials is not uniform throughout Central Asian countries. For example, a relatively lower level of landslide susceptibility is found in Tajikistan with respect to Kyrgyzstan. In fact, the hereby proposed susceptibility model entitles Mesozoic rocks as the most prone to landslides. However, in Tajikistan the majority of rocks are Paleozoic materials (in particular fractured igneous rocks) that, based on the calibrated model, are classified as “not influent”.

Additionally, the widespread presence of loess lithology both in Tajikistan and Uzbekistan should not be underestimated, considering connections to previous slope failures (Evans et al., 2009, Niyazov & Nurtaev, 2013). The fact that both fractured igneous and loess materials are not explicitly addressed in the analysis might reflect the relatively low susceptibility level found in these countries.

At a relatively large distance from the faults ($> 10\text{km}$), an increase of landslide occurrences can be observed. The presence of relatively deep hypocentres might be the reason for a considerable surficial distance between fault lines and landslides, even beyond 10km. This evidence, in line with what has been previously shown (Gemitzi et al., 2011), confirms the influence of neotectonic lineaments and fault density on landsliding phenomena. In addition, a connection between landslide occurrences and focal mechanisms of earthquakes might be speculated. While a relatively high number of landslides are expected in case of strike-slip mechanisms (being rocks materials more

fractured in the proximity of the epicenter), the presence of slope failures at large distances from faults might be connected to reverse focal mechanisms.



Figure 35: Khandiza block slide site (Uzbekistan), occurred in loess and probably caused by an earthquake in the Pamir-Hindu Kush region (April, 2008) (Source: Niyazov & Nurtaev, 2013).

As far as the seismic input is concerned, earthquakes of magnitude around 7 are expected in order to approximate the identified seismic intensity values of VIII and IX. According to observed seismicity, it is possible to find evidence of past earthquakes with magnitude of 6.8 - 7 having an impact on the investigated areas. It has to be underlined that, despite alternative seismic input parameters are possible, in this case, the intensity assigned at the site accounts for all the possible combination of magnitude and distance determining ground shaking at the site. Therefore, for the purpose of the actual landslide susceptibility analysis, seismic intensity is for sure more reliable than other energy-related parameters like PGA.

In reference to landslide hazard results, it must be noted that impact velocities derived from physical modelling turn out to be relatively higher than those typically derived for the same materials (Varnes, 1984). At the first place, this result may be related to the assumption of rapid downhill motion of relatively small masses (Scheidegger, 1973), which is at the root of the physical modeling framework. In addition, the contribution of sudden loading which is typically occurring during an earthquake might be the reason behind extremely rapid velocities, even greater than 5 m/s (Hungr et al., 2005). Such slope failures usually involve loose granular materials overlying stable substrate, and often originate during heavy rain, when the perched saturation condition of the loose layer is reached.

One limitation of the landslide susceptibility model hereby presented is that rockslides and large slope failures are not addressed. This is linked to the choice of developing a susceptibility model by using only landslides occurred in soft materials, due to their majority.

Unfortunately the available information prevents us to clearly distinguish between the trigger mechanisms causing those landslides used to develop the susceptibility model. However, considering the local influence of monsoons, slope failures occurring in the Fergana Area might have been triggered by heavy or prolonged precipitations.

Even though conventional landslide susceptibility analyses do not incorporate triggering information (Fell et al., 2008), the present study considers also the inclusion of the seismic input, in line with susceptibilities analyses previously presented by Schicker & Moon (2012), who included rainfall, and Holec et al. (2013), who included both seismicity and rainfall. Besides, given our focus on investigating the potential for landslide activation over a large territory, only seismicity has been considered as the triggering mechanism. While having an impact on slope instability, the effect due to precipitations might only have a local influence and, therefore, is out of the scope of this study.

Based on the analysis of accuracy values for susceptibility models (Figure 29), it can be seen that most of susceptibility models show AUC values greater than 0.70 and can, therefore, be accepted as significant. Model E has finally been chosen as applicable to

the entire country, being the most accurate one. Given that the condition of total independency among factors is never completely verified in nature (Bonham-Carter, 1994), we have not excluded the combination of those factors known as the most relevant to landslide initiation in Kyrgyzstan, similarly to what has been carried out by Dahal et al. (2008) and Pradhan et al. (2010) in Nepal and Malaysia, respectively.

Moreover, for regional scale analyses of landslide susceptibility, overestimating the number of predicted landslides is a common problem. In order to tackle this problem, the adoption of one single landslide point per unit area is considered in the present study (Neuhäuser & Terhorst, 2007).

An important issue in landslide susceptibility and hazard studies is represented by the influence on the final susceptibility values of transforming continuous variables into discrete variables. In this respect, Remondo et al. (2003) demonstrated how the predictive capability of validation curves obtained from input data, which were classified into only a few intervals, and the outcome from almost continuous variables, is quite similar. Based on this consideration, landslide potential factors have been classified in such a way as not to have many classes in the susceptibility analysis. As a general observation, it can be stated that increasing the number of classes in landslide factors leads to unstable results.

Overall, the operation of classifying susceptibility and hazard values is an ongoing topic of debate within the scientific community, given that there are no reference rules on categorizing data (Ayalew et al., 2004). In this study, susceptibility and hazard values are at first normalised and afterwards classified, following the quantile classification scheme among a number of possible alternatives (i.e., natural breaks, equal size). The reason behind this choice is to have each class approximately equally represented on the final map. Moreover, quantiles are very useful for ordinal data, since the class assignment of quantiles is based on ranked data. Finally, by adopting the same number of classes, a comparison among landslide susceptibility and hazard maps is achievable, together with a statistically reproducible framework.

Moreover, landslide hazard results are clearly linked to slope geometry as well as to landslide susceptibility. In fact, most of expected hazardous areas correspond to areas

either having high slope or high susceptibility. For this reason, landslide hazard index, far from being of site-specific nature, has to be considered as a broad indicator of the expected impact velocity due to mass movements at a national level. Unfortunately, the lack of historical information concerning landslide-related damages over a large area prevents to carry out a validation of both landslide hazard and risk results. Although only sparse, a number of available local landslide datasets allow for a validity check of results, and confirm the potential for landslide activation throughout the region. Besides, historical observations of strongest seismically-induced landslides occurred in Central Asia (Figure 3), are found inside identified most landslide-prone areas. It has to be remarked that, these datasets were not used in the statistical analysis because of their limited nature.

Regarding landslide risk results, it has to be remarked that the physical damage to life lines induced by slope failures is not specifically addressed, and therefore, the total level of risk might be underestimated.

As has already been pointed out (Das, 2011), the validation of risk results is a very difficult task to be achieved, given high uncertain in the estimates. The work hereby presented, by addressing one single landslide type together with expected impact only to exposed population, provides a relatively simple framework allowing results' uncertain to be relatively low. The choice of population density as element at risk has a particular meaning in Central Asian countries, where fatalities due to landslides are more significant than economic losses.

An essential part of any landslide hazard and risk assessment is the prediction of the character of failure and a quantitative estimate of post-failure motion ("runout") including travel distance and velocity (Hungr et al., 2005). In line with this, the computation framework presented in this work allows not only the computation of impact velocity but also to infer information about runout distances of simulated slope failures.

Although various methods to carry out quantitative landslide hazard and risk analyses are available, applications are still rare and mainly dependent on the occurrence of disasters. In order to support this research direction, the hereby proposed method

demonstrate the applicability of a Bayesian-based procedure for detecting landslide-prone areas at the regional scale, and for identifying the most important factors inducing slope failures. Moreover, a quantitative-based landslide hazard and risk framework allowing a prior assessment of the expected destructiveness due to landslide activation is provided. In this way, landslide-prone areas are identified in advance, and the occurrence of disasters might hence be limited. Reinforcing buildings located within the landslide susceptible areas would be high costly, and therefore impracticable on an economic perspective. It is then of vital importance that land planners are provided with appropriate information and tools, which allow the location of people, buildings and main infrastructures being more vulnerable to slope failures.

9 CONCLUSIONS

Central Asia is one of the most challenging places in the world where various natural hazards can heavily injury populations and resources. Among these hazards, landslides pose a serious threat to human life and human facilities. Focusing on landslide-related disasters after they occur is essential from a humanitarian point of view, but unfortunately not sufficient for reducing their tragic consequences to people, infrastructures and the environment. Furthermore, considering remote conditions characterizing Central Asian countries, data are not easily accessible, or limited in nature, or may be affected by different sources of uncertainty. For this reason, collecting of resources and knowledge for identifying areas for future landslide activation and quantifying vulnerability and risk are crucial tasks for long-term risk mitigation.

In order to mitigate landslide risk, this work evaluates its components over the entire Central Asian region. For the first time, a cross-border risk map of earthquake-induced landslides is produced at a transnational level in Central Asia. To this scope, an approach to evaluate the potential of seismically-induced landslides using statistical relationships between past landslides and the most significant seismo-tectonic, geological and morphological factors in Central Asia countries is presented. The Bayesian-based method is initially calibrated and cross-validated with an independent dataset in Kyrgyzstan, providing with a landslide susceptibility model having an accuracy level greater than 70%, which allows considering the model sufficiently reliable for urban planning purposes. Afterwards, due to uniformity in geomorphological and tectonic factors characterizing all Central Asian countries, an

extension of the model to the territories of Uzbekistan and Tajikistan is carried out. At a second stage, the susceptibility analysis is used as prior information for a quantitative hazard analysis and to evaluate expected damage to people due to the sliding process induced by earthquakes, over the entire Central Asian region.

It can be concluded that geology plays a critical role in guarantying slope stability. Mesozoic materials are found to be the most responsible for landslide initiation. The huge variability of these materials (soft and semi-hard rocks, principally deposits of clays, argillites, sandstones, limestones - often covered by Quaternary loess), prevents us to discriminate the influence of specific rock types, which would add more value to the analysis. The contribution of rock structure to instability is also clear given the fact that most of landslides occurred in places with relatively moderate slope gradient values (6-16°). Additionally, due to the presence of neotectonic lineaments all over the country, the strength of rock materials is reduced and slopes are made unstable. It has been observed that, at a certain distance from faults, slope failure phenomena are quite sever. The resulting cross-border landslide susceptibility map emphasizes the relatively high potential for landslides over the entire country of Kyrgyzstan, specifically along the eastern boarder of Fergana valley, in the South of Talas province, and in Issyk-kul district; besides, high levels of susceptibility can be found in the Naryn province where the conditions for slope failures exist though the scarce occurrence of past landslides. A general low level of landslide susceptibility can be observed for almost the entire territory of Uzbekistan, with exceptions of the Tashkent and the Buhkara provinces characterized by high and medium landslide susceptibility, respectively. With regard to the Tajik territory, high levels of landslide susceptibility are expected in central districts of Tojikobod and Nurobod.

Besides, it turns out that impact velocity of earthquake-induced mass movements can be particularly significant along the North and Central Tien Shan, the Pskem Mountains, the Alay Range, and the Pamir. In addition, landslide risk results show that a very high level of risk is locally expected in the Jalal-Abad and Osh provinces, Kyrgyzstan, in the Gorno-Badakhshan region near the urban areas of Khorugh and Murghab, Tajikistan, and in the Kashkadarva region, Uzbekistan. Moreover, a high level of risk can be observed for several areas, i.e., those located in the proximity of Fergana Valley and

Jalal-Abad areas in Kyrgyzstan, being highly densely populated areas. On the other hand, there is a low-medium level of risk extensively distributed across Kyrgyzstan, Tajikistan, and Uzbekistan, primarily due to the presence of small settlements (having a population density in the order of 1000 persons/km²) exposed to significant landslide hazard.

By taking into account limitations and assumptions of the described approach, results hereby presented can be effectively used to model landslide susceptibility, hazard and risk also in neighboring regions as well as in other data-scarce regions of the world, being characterized by the same combination of landslide influential parameters as Central Asia countries.

As part of future work, a more detailed investigation of existing relationships between quaternary rocks (in particular loess) and slope failures is recommended in order to provide specific insight for landslide susceptibility in Tajikistan and Uzbekistan. For this reason, a more detailed inventory of past landslides is under construction, including geological information at the landslide site. Furthermore, a more detailed study of the connections between faults and earthquake source mechanisms would provide a deeper characterization of the seismic ground shaking as input to landsliding phenomena. Finally, collecting information on damages caused by landslides, including not only the number of fatalities but also the number of people affected and injured, would definitely increase the understanding of human vulnerability to landslides. Moreover, the analysis of physical vulnerability to slope failures in Central Asia might be undertaken, provided that information about induced-damages to buildings and life-lines are made available. To this scope, clear dependencies between the impact area of a landslide and the amount of damage to built-up areas and infrastructures can be established.

Although landslide studies have been already started in Central Asia, a sound statistical methodology for susceptibility of earthquake-induced landslides and risk mapping applicable over the entire region at transnational level has never been carried out before. By identifying areas with a potential for future seismically-induced slope instability together with expected impact on population, the present work offers the unique value of presenting first attempts of a cross-border and harmonized landslide analysis, and

Chapter 9: Conclusions

provides national authorities with a regional map which serves as a prelude for landslide risk mitigation activities.

10 REFERENCES

- Abdrakhmatov, K., & Strom, A. (2006). Dissected rockslide and rock avalanche deposits; Tien Shan, Kyrgyzstan. In Evans, Mugnozza, Strom, & Hermanns, *Landslides from massive rock slope failure*, 551-570. Netherlands: Springer.
- AGS. (2007). Guideline for Landslide Susceptibility, Hazard and Risk Zoning. In *Australian Geomechanics* (42, 1), 13-36.
- Akgun, A., Kincal, C., & Pradhan, B. (2012). Application of remote sensing data and GIS for landslide risk assessment as an environmental threat to Izmir city (west Turkey). *Environ. Monit. Assess.* (184), 5453-5470.
- Aleotti, P., & Chowdhury, R. (1999). Landslide hazard assessment: summary review and new perspectives. *Bull. Eng. Geol. Environ.* (58), 21-44.
- Alexander, D. (2005). Vulnerability to Landslides. In Glade, Anderson, & Crozier, *Landslide Hazard and Risk*, 175-198.
- Andersson-Sköld, Y., Falemo, S., & Tremblay, M. (2014). Development of methodology for quantitative landslide risk assessment - Example Göta river valley. *Natural Science* (6,3), p. 14.

Chapter 10: References

- Ayalew, L., Yamagishi, H., & Ugawa, N. (2004). Landslide susceptibility mapping using GIS-based weighted linear combination the case of Tsugawa area of Agano River. Niigata Prefecture Japan. *Landslides* (1), 73-81.
- Bell, J. (1900). General slope stability analysis . *J Soil Mech Found Div* (92 SM5).
- Bell, R., & Glade, T. (2004). Quantitative risk analysis for landslides - Examples from from Bıldudalur, NW-Iceland. *Nat. Hazards Earth Syst. Sci.*(4), 117-131.
- Bindi, D., Abdrakhmaov, K., Parolai, S., Mucciarelli, M., Grüntal, G., Ischuk, A., . . . Zschau, J. (2012). Seismic hazard assessment in Central Asia: outcomes from a site approach. *Soil. Dyn. Earthq. Eng.* (37), 84-91.
- Bindi, D., Parolai, S., Oth, A., Abdrakhmatov, K., Muraliev, A., & Zschau, J. (2011). Intensity prediction equations for Central Asia. *Geophys. J. Int.* (187), 327-337.
- Birkmann, J. (2007). Risk and vulnerability indicators at different scales: Applicability, usefulness and policy implications. *Environmental Hazards* (7), 20-31.
- Bonham-Carter, G. F. (1994). *Geographic Information System for Geoscientists*. Ottawa: Pergamon Press.
- Bonham-Carter, G., Agterberg, F., & Wright, D. (1989). Weights of evidence modelling: A new approach to mapping mineral potential. *Statistical applications in the Earth Sciences, geological survey of Canada*, 171-183.
- Bray, J., & Travarasrou, T. (2009). Pseudostatic coefficient for use in simplified seismic slope stability evaluation. *J. Geotech. Geoenviron. Eng.*(135), 1336-1340.
- Bright, E. A., Coleman, P. R., Rose, A. N., & Laboratory, O. R. (2012). *LandScan Global Population Database*. Oak Ridge National Laboratory, UT-Battelle, LLC.
- Burtman, V., & Molnar, P. (1993). Geological and geophysical evidence for deep subduction of continental crust beneath the Pamir. *Geol. Soc. Am.* (281), 1-76.

Chapter 10: References

- CAC-DRMI. (2009). *Central Asia and Caucasus Disaster Risk Management Initiative*. Desk Study Review.
- Carrara, A., Guzzetti, F., Cardinali, A., & Reichenbach, P. (1999). Use of GIS technology in the prediction and monitoring of landslide hazards. *Nat. Hazards* (20), 117-135.
- Cassidy, M., Uzielli, M., & Lacasse, S. (2008). Probability risk assessment of landslides: A case study at Finneidfjord. *Can. Geotech. J.*(45), 1250-1267.
- Chung, C., & Fabbri, A. (2003). Validation of Spatial Prediction Models for Landslide Hazard Mapping. *Nat. Hazards* (30), 451-472.
- Clough, R., & Chopra, A. (1966). Earthquake stress analysis in earth dams. *J. Eng. Mech-ASCE* (92), 197-211.
- Corominas, J., van Westen, C., Frattini, P., Cascini, L., Malet, J., Fotopoulou, S., . . . Smith, J. (2014). Recommendations for the quantitative analysis of landslide risk. *Bull. Eng. Geol. Environ.* (73), 209-263.
- Cross, J. (2001). Megacities and small towns: different perspectives on hazard vulnerability . *Environmental Hazards* (3), 63-80.
- Crovelli, R., & Coe, J. (2009). Probabilistic estimation of numbers and costs of future landslides in the San Francisco Bay region. *Georisk* (3), 206-223.
- Crozier, M. (2013). '*Landslides - Gravity always wins*', *Te Ara - the Encyclopedia of New Zealand*. Retrieved from <http://www.TeAra.govt.nz/en/diagram/8782/landslide-types>
- Dahal, R. K. (2013). Regional-scale landslide activity and landslide susceptibility zonation in the Nepal Himalaya. *Environ Earth Sci*.
- Dahal, R., Hasegawa, S., Nonoumra, A., Yamanaka, M., Dhakal, S., & Paudyal, P. (2008). Predictive modelling of rainfall-induced landslide hazard in the Lesser

Chapter 10: References

- Himalaya of Nepal based on weights-of-evidence. *Geomorphology* (102), 496-510.
- Dai, F., Lee, C., & Ngai, Y. (2002). Landslide risk assessment and management: an overview. *Eng. Geol.* (64), 65-87.
- Das, I., Kumar, G., & Stein, A. (2011). Stochastic landslide vulnerability modeling in space and time in a part of the northern Himalayas, India. *Environ. Monit. Assess.* (178), 25-37.
- Einstein, H. (1988). Landslide risk assessment procedure. *Proc. Int. Symp. on Landslides*, (pp. 1075-1090). Lausanne.
- Evans, S. G., Roberts, N. J., Ischuk, A., & Delaney, K. B. (109 (2009)). Landslides triggered by the 1949 Khait earthquake, Tajikistan, and associated loss of life. *Eng. Geol.*, 195–212.
- Fell, R., Corominas, J., Bonnard, C., Cascini, L., & Leroi, E. S. (2008). Guidelines for landslide susceptibility, hazard and risk zoning for land-use planning. *Eng. Geol.* (102), 99-111.
- Galli, M., & Guzzetti, F. (2007). Landslide Vulnerability Criteria: A Case Study from Umbria, Central Italy. *Environ. Manage.* (40), 649-664.
- Gaziev, E. (1984). Study of the Usoi landslide in Pamir. *Proc. 4th Int. Symp. on Landslides* (1), 511-514.
- Gemitzi, A., Falalakis, G., Eskioglou, P., & Petalas, C. (2011). Evaluating landslide susceptibility using environmental factors, fuzzy membership functions and GIS. *Global NEST Journal* 13, 28-40.
- Geotechdata.info. (2013). *Angle of Friction*. Retrieved (as of September 14.12.2013), from <http://geotechdata.info/parameter/angle-of-friction.html>
- Gubin, I. (1962). Seismicity and geological structures of Central Asia. *Studia Geophysica et Geodaetica* (6), 410-412.

Chapter 10: References

- Guha-Sapir, D., Below, R., & Hoyois, P. (2015). *EM-DAT: International Disaster Database – Université Catholique de Louvain – Brussels – Belgium*. Retrieved from www.emdat.be
- Guzzetti, F., Carrara, A., Cardinali, M., & Reichenbach, P. (1999). Landslide hazard evaluation: a review of current techniques and their application in a multi-scale study, Central Italy. *Geomorphology* (31), 181–216.
- Guzzetti, F., Reichenbach, P., Cardinali, M., Galli, M., & Ardizzone, F. (2005). Probabilistic landslide hazard assessment at the basin scale. *Geomorphology* (72), 272-299.
- Hasegawa, S., Dahal, R., Nishimura, T., Nonomura, A., & Yamanaka, M. (2009). DEM-Based Analysis of Earthquake-Induced Shallow Landslide Susceptibility. *Geotech. Geol. Eng.* (27), 419-430.
- Havenith, H., & Bourdeau, C. (2010). Earthquake-induced hazards in mountain regions: a review of case histories from Central Asia - an inaugural lecture to the society. *Geologica Belgica* (13), 137-152.
- Havenith, H., Strom, A., Abdrakhmatov, A., Delvaux, D., & Tréfois, P. (1999). Seismic triggering of landslides, Part A: Field evidence from the Northern Tien Shan. *Nat. Haz. Earth Sys. Sc.* (3), 135-149.
- Havenith, H., Strom, A., Caceres, F., & Pirard, E. (2006). Analysis of landslide susceptibility in the Suusamyr region, Tien Shan: statistical and geotechnical approach. *Landslides* (3), 39-50.
- Havenith, H., Strom, A., Torgoev, I., Lamair, L., Ischuk, A., & Abdrakhmatov, K. (online 2015). Tien Shan geohazards database: Earthquakes and landslides. *Geomorphology*, doi:10.1016/j.geomorph.2015.01.037.
- Holec, J., Bednarik, M., Šabo, M., Minár, J., Yilmaz, I., & Marschalko, M. (2013). A small-scale landslide susceptibility assessment for the territory of Western Carpathians. *Nat. Hazards* (69), 1081-1107.

Chapter 10: References

- Hollenstein, K. (2005). Reconsidering the risk assessment concept: Standardizing the impact description as a building block for vulnerability assessment. *Nat. Hazards Earth Syst. Sci.* (5), 301-307.
- Hungr, O., Corominas, J., & Eberhardt, E. (2005). Estimating landslide motion mechanism, travel distance and velocity. In Hungr, Fell, Couture, & Eberhardt, *Landslide risk management* (pp. 99-128). London: Taylor & Francis Group.
- Ishihara, K. (1989). Liquefaction-induced landslide and debris-flow in Tajikistan, USSR. *Landslide News* (3), 6-7.
- Ishihara, K. (2012). Performances of Rockfill Dams and Deep-Seated Landslides During Earthquakes. In Sakr, & Ansal, *Special Topics in Earthquake Geotechnical Engineering* (pp. 273-314). Netherlands: Springer.
- Jaiswal, P., van Westen, C., & Jetten, V. (2011). Quantitative estimation of landslide risk from rapid debris slides on natural slopes in the Nilgiri hills, India. *Nat. Hazards Earth Syst. Sci.* (11), 1723-1743.
- Jibson, R. (2011). Methods for assessing the stability of slopes during earthquakes - A retrospective. *Eng. Geology*, 43-50.
- Kalmetieva, Z., Mikolaichuk, A., Moldobekov, B., Meleshko, A., Janaev, M., & Zubovich, A. (2009). *Atlas of earthquakes in Kyrgyzstan*. Bishkek: Central Asian Institute for Applied Geosciences and United Nations (UNISRD), Springer.
- Kaynia, A., Papathoma-Köhle, M., Neuhäuser, B., Ratzinger, K., Wenzel, H., & Medina-Cetina, Z. (2008). Probabilistic assessment of vulnerability to landslide: Application to the village of Lichtenstein, Baden-Württemberg, Germany. *Eng. Geol.* (101), 33-48.
- Keefer, D. (1984). Landslides caused by earthquakes. *Bull. Geol. Soc. Am.* (95), 406-421.

Chapter 10: References

- Khampilang, N., & Whitworth, M. (2013). Creation of Landslide Inventory Map for the Toktogul Region of Kyrgyzstan, Central Asia. In Margottini, Canuti, & Sassa, *Landslide Science and Practice (1)* (pp. 197-202). Berlin Heidelberg: Springer-Verlag.
- Kramer, S. L. (1996). *Geotechnical Earthquake Engineering*. Prentice-Hall International Series in Civil Engineering and Engineering Mechanics.
- Lee, E., & Jones, D. (2004). *Landslide Risk Assessment*. London: Thomas Telford Publishing.
- Li, W., Huang, R., Tang, C., XU, Q., & van Westen, C. (2013). Co-seismic Landslide Inventory and Susceptibility Mapping in the 2008 Wenchuan Earthquake Disaster Area, China. *J. Mt. Sci.* (10,3), 339-354.
- Li, Z., Nadim, F., Huang, H., Uzielli, M., & Lacasse, S. (2010). Quantitative vulnerability estimation for scenario-based landslide hazards. *Landslides* (7), 125-134.
- Lutz, W. (2010). Emerging population issues in Eastern Europe and Central Asia. Research Gaps on demographic Trends, Human Capital and Climate Change. *UNFPA, New York, USA*.
- Mavrouli, O., Fotopoulou, S., Pitilakis, K., Zuccaro, G., Corominas, J., Santo, A., . . . Ulrich, T. (2014). Vulnerability assessment for reinforced concrete buildings exposed to landslides. *Bull. Eng. Geol. Environ.* (73), 265-289.
- Molnar, P., & Tapponier, P. (1975). Cenozoic tectonics of Asia Effects of a continental collision. *Science* (189), 419-426.
- Mousavi, S., Omidvar, B., Ghazban, F., & Feyzi, R. (2011). Quantitative risk analysis for earthquake-induced landslides - Emamzadeh Ali, Iran. *Engineering Geology* (122), 191-203.

Chapter 10: References

- Nadim, F., Kjekstad, O., Peduzzi, P., Herold, C., & Jaedicke, C. (2006). Global landslide and avalanche hotspots. *Landslides* (3), 159-173.
- Nefeslioglu, H., & Gokceoglu, C. (2011). Probabilistic risk assessment in medium scale for rainfall induced earthflows: Catakli catchment area (Cayeli, Rize, Turkey). *Math. Probl. Eng.*, p. 21.
- Neuhäuser, B., & Terhorst, B. (2007). Landslide susceptibility assessment using "weights-of-evidence" applied to a study area at the Jurassic escarpment (SW-Germany). *Geomorphology* (86), 12-24.
- Newmark, N. (1965). Effects of earthquakes on dams and embankments. *Geotechnique* (15), 139-159.
- Niyazov, R., & Nurtaev, B. (2013). Evaluation of Landslides in Uzbekistan Caused by the Joint Impact of Precipitation and Deep-Focus Pamir-Hindu Kush Earthquakes. In Sassa, Rouhban, Briceno, McSaveney, & He, *Landslides: Global Risk Preparedness* (pp. 255-267). Berlin Heidelberg : Springer-Verlag.
- Niyazov, R., & Nurtaev, B. (2013). Modern Seismogenic Landslides Caused by the Pamir-Hindu Kush Earthquakes and Their Consequences in Central Asia. In Margottini, Canuti, & Sassa, *Landslide Science and Practice* , 343-348. Berlin Heidelberg: Springer-Verlag.
- Oh, H., & Lee, S. (2010). Landslide susceptibility mapping on Panaon Island, Philippines using a geographic information system. *Environ. Earth Sci.* (62), 935-951.
- Papathoma-Köhle, M., Kappes, M., Keiler, M., & Glade, T. (2011). Physical vulnerability assessment for alpine hazards: state of the art and future needs. *Nat. Hazards* (58), 645-680.
- Pascale, S., Sdao, F., & Sole, A. (2010). A model for assessing the systemic vulnerability in landslide prone areas. *Nat. Hazards Earth Syst. Sci.* (10), 1575-1590.

Chapter 10: References

- Pavlis, T., Hamburger, M., & Pavlis, G. (1997). Erosional processes as a control on the structural evolution of an actively deforming fold and thrust belt: An example from the Pamir Tien Shan region, Central Asia. *Tectonics* (16), 810-822.
- Perov, V., & Budarina, O. (2000). Mudflow hazard assessment for the Russian Federation. In Wieczorek, & Naeser, *Debris-flow hazards mitigation: mechanics, prediction, and assessment*, 489-494. Rotterdam, Netherlands: Balkema.
- Petley, D. (2012). Global Patterns of loss of life from landslides. *Geology* 40(10), 927-930.
- Pittore, M. GFZ- Potsdam. (2014). *Focusmapr: computation of Focus Maps from a set of input raster or vector layers. R package version 1.0*.
- Pradhan, B., Oh, H.-J., & Buchroithner, M. (2010). Weights-of-evidence model applied to landslide susceptibility mapping in a tropical hilly area. *Geomatics Nat. Hazards Risk* 1(3), 199-223.
- Quantum GIS Development Team. *Quantum GIS Geographic Information System. Open Source Geospatial Foundation Project*. (2015). Retrieved from <http://qgis.osgeo.org>
- Remondo, J., Bonachea, J., & Cendrero, A. (2005). A statistical approach to landslide risk modelling at basin scale: from landslide susceptibility to quantitative risk assessment. *Landslides* (2), 321-328.
- Remondo, J., Gonzales, A., De Teran, J., Cendrero, A., Fabbri, A., & Chung, C. (2003). Validation of Landslide Susceptibility Maps: Examples and Applications from a Case Study in Northern Spain. *Nat. Hazards* (30), 437-449.
- Rosenfeld, C. (1994). The geomorphological dimensions of natural disasters. *Geomorphology* (10), 27-36.

Chapter 10: References

- Scheidegger, A. E. (1973). On the Prediction of the Reach and Velocity of Catastrophic Landslides. In *Rock Mechanics* (5) (pp. 231-236). Springer-Verlag.
- Scheidegger, A. E. (1975). *Physical Aspects of Natural Catastrophes*. Elsevier Scientific Publishing Company.
- Schicker, R., & Moon, V. (2012). Comparison of bivariate and multivariate statistical approaches in landslide susceptibility mapping at the regional scale. *Geomorphology* (161), 40-57.
- Schlögel, R., Torgoev, I., De Marneffe, C., & Havenith, H. (2011). Evidence of a changing size–frequency distribution of landslides in the Kyrgyz Tien Shan, Central Asia. *Earth Surf. Process. Landforms* (36), 1658–1669.
- Schuster, R. L., & Alford, D. (May 2004). Usoi Landslide Dam and Lake Sarez, Pamir Mountains, Tajikistan. *Environ. Eng. Geosci.* (10,2), 151–168.
- SENSUM. (2014). *Framework to integrate Space-based and in-situ sensing for dynamic vulnerability and recovery monitoring. FP7-SPACE-2012-1. Deliverable 3.4.*
- Sheko, A. (1983). Landslides and Mudflows. *Reports of the Alma-Ata International Seminar, Moscow, Centre of International Projects, GKNT.*
- Sidorova, T. (1997). Potential changes of mudflow phenomena due to global warming. In Rickemann, & Chen, *Debris-flow hazards mitigation: mechanics, prediction, and assessment* , 540-549. Rotterdam, Netherlands: Balkema.
- Soeters, R., & van Westen, C. (1996). Slope stability: recognition, analysis and zonation. In Turner, & Shuster, *Landslides: investigation and mitigation* (pp. 129-177). Transportation Research Board, Special report 247.
- SRTM Shuttle Radar Topography Mission. SRTM digital topographic data US Geological Survey's EROS Data Center.* (2004). Retrieved from <ftp://e0mss21uecsnasagov/srtm/>

Chapter 10: References

- Sterlacchini, S., Frigerio, P., & Giacomelli, M. (2007). Landslide risk analysis: a multi-disciplinary methodological approach. *Nat. Hazards Earth Syst. Sci.*(7), 657-675.
- Stewart, J., Blake, T., & Hollingsworth, R. (2003). A screen analysis procedure for seismic slope stability. *Earthq. Spectra* (19), 697-712.
- Strom, A. (2013). Geological Prerequisites for Landslides' Dams' Disaster Assessment and Mitigation in Central Asia. In Wang, Miyaijma, Li, Shan, & Fathani, *Progress of Disaster Mitigation Technology in Asia* , 17-53.
- Strom, A., & Korup, O. (2006). Extremely large rockslides and rock avalanches in the Tien Shan Mountains Kyrgyzstan. *Landslides* (3), 125-136.
- Terzaghi, K. (1950). Mechanism of landslides. In Paige, *Application of Geology to Engineering Practice (Berkey Volume)* (pp. 83-123). New York: Geological Sosciety of America.
- Terzaghi, L., & Pech, R. (1967). *Soil mechanics in engineering practice*. New York: Wiley, p. 752.
- Thomas, J., Lanza, R., Kazanski, A., Zykin, V., Semakov, N., Mitrokhin, D., & Delvaux, D. (2002). Paleomagnetic study of Cenozoic sediments from the Zaisan basin (SE Kazakhstan) and the Chuya depression (Siberian Altai): tectonic implications for central Asia. *Tecnonophysics* (351), 119-137.
- Tingdong, L., Ujkenov, B., Kim, B., Tomurtogoo, O., Petrov, O., & Strelnikov, S. (2008). Geological map of Central Asia and Adjacent Areas edt by Geological Publishing House. Beijing China.
- Torgoev, A., & Havenith, H.-B. (2013). Landslide Susceptibility, Hazard and Risk Mapping in Mailuu-Suu, Kyrgyzstan. In Margottini, Canuti, & Sassa, *Landslide Science and Practice* (1) , 505-510. Berlin Heidelberg: Springer-Verlag.

Chapter 10: References

- Torgoev, I., Alioshin, Y. G., & Torgoev, A. (2012). Monitoring landslides in Kyrgyzstan. *Freiberg Online Geology* (33), 130-139.
- Trifonov, V., Soboleva, O., Trifonov, R., & Vostrikov, G. (2002). Recent geodynamics of the Alpine-Himalayan collision belt. *Transaction of the Geological Institute RAS* 541, p. 224 (in Russian).
- Uchida, T., Osanai, N., Onoda, S., Takayama, T., & Tomura, K. (2006). A Simple Method for Producing Probabilistic Seismic Shallow Landslide Hazard Maps. In *Disaster Mitigation of Debris Flows, Slope Failures and Landslides* , 529-534. Tokyo, Japan: Universal Academy Press, Inc.
- UNISDR. (2015). *Making Development Sustainable: The Future of Disaster Risk Management. Global Assessment Report on Disaster Risk Reduction*. Geneva, Switzerland: United Nations Office for Disaster Risk Reduction (UNISDR).
- Uzielli, M., Nadim, F., Lacasse, S., & Kaynia, A. (2008). A conceptual framework for quantitative estimation of physical vulnerability to landslides. *Eng. Geol.*(102), 251-256.
- Van Den Eeckhaut, M., Hervás, J., Jaedicke, C., Malet, J., Montanarella, L., & Nadim, F. (2012). Statistical modelling of Europe-wide landslide susceptibility using limited landslide inventory data. *Landslides* (9), 357-369.
- Van Westen, C., Rengers, N., & Soeters, R. (2003). Use of geomorphological information in indirect landslide susceptibility assessment. *Nat. Hazards* (30), 399-419.
- Van Westen, C., Van Asch, T., & Soeters, R. (2006). Landslide hazard and risk zonation - why is it still so difficult? *Bull. Eng. Geol. Environ.*, 297-306.
- Varnes, D. (1978). *Slope Movement Types and Processes*.

Chapter 10: References

- Varnes, J., & IAEG. (1984). *IAEG International Association of Engineering Geology Commission on Landslides and Other Mass Movements, Landslide hazard zonation: a review of principles and practice*. Paris, 63p: The UNESCO Press.
- Wieczorek, G. F. (1996). Landslide triggering mechanisms. In Turner, & Schuster, *Landslide investigation and mitigation. Special report 247* (p. 673). Washington, D. C.: National Academic Press.
- Yang, S., He, S., Du, J., & Sun, X. (2015). Screening of social vulnerability to natural hazards. *Nat. Hazards*, 1-18.
- Yilmaz, I. (2010). The effect of the sampling strategies on the landslide susceptibility mapping by conditional probability and artificial neural networks. *Environ. Earth Sci.* (60), 505-519.
- Zezere, J., Oliveira, S., Garcia, R., & Reis, E. (2007). Landslide risk analysis in the area North of Lisbon (Portugal): evaluation of direct and indirect costs resulting from a motorway disruption by slope movements. *Landslides* (4), 123-136.

11 LIST OF PUBLICATIONS

Journals and report

Pilz, M., Roessner, S., Janssen, C., Behling, R., Parolai, S., **Saponaro, A.**, Schäbitz, M. (2013). *Massenbewegungen in Zentralasien: Lawinen aus Boden und Gestein*. System Erde 3, 2. doi: 10.2312/GFZ.syserde.03.02.

Pilz, M., Parolai, S., Bindi, D., **Saponaro, A.**, Abdybachaev, U. (2014): *Combining seismic noise techniques for landslide characterization*. Pure and Applied Geophysics 171, 1729-1745, doi: 10.1007/s00024-013-0733-3.

Saponaro, A., Pilz, M., Wieland, M., Bindi, D., Moldobekov, B., & Parolai, S. (online 2014). *Landslide susceptibility analysis in data-scarce regions: the case of Kyrgyzstan*. Bull. Eng. Geol. Environ., doi: 10.1007/s10064-014-0709-2.

Saponaro, A., Pilz, M., Bindi, D., & Parolai, S. (2015). *The contribution of EMCA to landslide susceptibility mapping in Central Asia*. Annals of Geophysics (58, 1), doi: 10.4401/ag-6668.

Conferences and presentations

Saponaro, A. (2013). *An innovative tool for landslide susceptibility mapping in Kyrgyzstan, Central Asia*. 8th PhD Day of the GeoForschungsZentrum, Potsdam, March 2013

Saponaro, A. (2013). *An innovative tool for landslide susceptibility mapping in Kyrgyzstan, Central Asia*. Poster presentation at the General Assembly of the European Geosciences Union (EGU), Vienna, Austria, April 2013

Saponaro, A. (2013). *Earthquake-induced Landslides and Site-effects*. Workshop in the frame of TIPTIMON capacity-building activities in Central Asian countries. Bishkek, Kyrgyzstan, 18th – 22nd November 2013

Fleming, K.M., **Saponaro, A.** (2014). *Use of TRMM rainfall products and other remote sensing missions for hazard and vulnerability assessment in Central Asia*. Symposium on earthquake and landslide risk in Central Asia and Caucasus: exploiting remote sensing and geo-spatial information management Bishkek, Kyrgyzstan, 29th – 30th January 2014

Saponaro, A., Bindi, D. and Parolai S. (2014). *A statistical approach for earthquake-induced landslide susceptibility mapping in Kyrgyzstan*. 9th PhD Day of the GeoForschungsZentrum, Potsdam, March 2014

Saponaro, A., Pilz, M., Parolai, S. (2014). *A statistical approach for landslide susceptibility mapping in Kyrgyzstan, Central Asia*. TIPTIMON Midterm Meeting in the framework of joint activities between CAIAG and GFZ, Potsdam, April 2014

Saponaro, A. (2014). *Use of GIS for Landslide Susceptibility Mapping*. Talk presented at the GIS DAY at GFZ 2014, Potsdam, November 2014

Saponaro, A., Pilz, M., Wieland, M., Pittore, M., Bindi, D., Parolai, S. (2014). *Towards Cross-Border Landslide Hazard and Risk Assessment in Central Asia*. Oral presentation at the American Geophysical Union (AGU)'s 47th annual Fall Meeting, San Francisco, US, December 2014

Chapter 11: List of Publications

Saponaro, A., Pilz, M., Wieland, M., Pittore, M., Bindi, D., Parolai (2015). *Towards cross-border landslide hazard and risk assessment in Central Asia*, 10th PhD Day of the GeoForschungsZentrum, Potsdam, March 2015